AD-A105 861 ARMY ENGINEER WATERWAYS EXPERIMENT STATION VICKSBURG--ETC F/G 13/13
FLOOD CONTROL AND IRRIGATION OUTLET WORKS AND TAILRACE CHANNEL --ETC(U)
SEP 81 S T MAYNORD

UNCLASSIFIED WES/TR/HL-81-6 NL

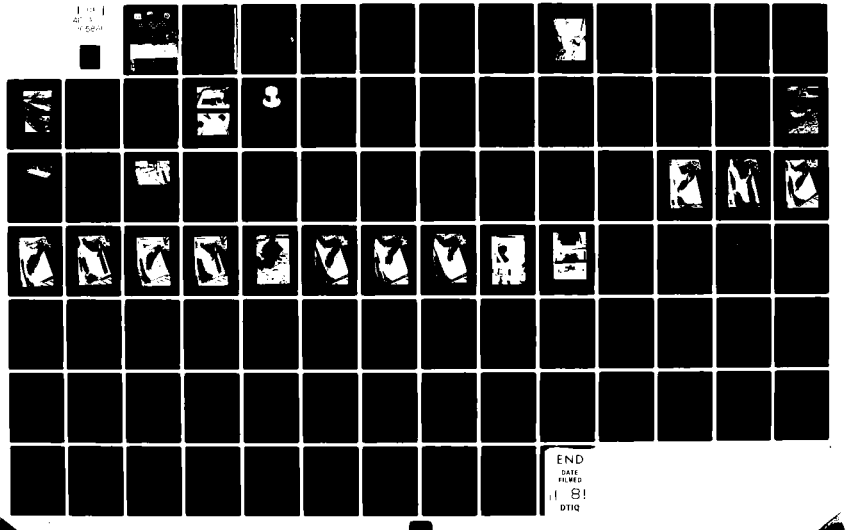

END
DATE FILMED
1 81
DTIC

LEVEL II

FLOOD CONTROL AND IRRIGATION OUTLET WORKS AND TAILRACE CHANNEL FOR NEW MELONES DAM, STANISLAUS RIVER CALIFORNIA

Hydraulic Model Investigation

by

Stephen T. Maynord
Hydraulic Laboratory
U. S. Army Engineer Waterways Experiment Station
P. O. Box 631, Vicksburg, Miss. 39180

Technical Report HL-81-1
Final Report

Approved For Public Release; Distribution Unlimited

Prepared for U. S. Army Engineer District, Sacramento
Sacramento, California 95814

Destroy this report when no longer needed. Do not return it to the originator.

The findings in this report are not to be construed as an official Department of the Army position unless so designated by other authorized documents.

The contents of this report are not to be used for advertising, publication, or promotional purposes. Citation of trade names does not constitute an official endorsement or approval of the use of such commercial products.

Unclassified

SECURITY CLASSIFICATION OF THIS PAGE (When Data Entered)

WES/TR/HL-81-6

REPORT DOCUMENTATION PAGE

READ INSTRUCTIONS BEFORE COMPLETING FORM

1. REPORT NUMBER: Technical Report HL-81-6
2. GOVT ACCESSION NO.: AD A105861
3. RECIPIENT'S CATALOG NUMBER:
4. TITLE (and Subtitle): FLOOD CONTROL AND IRRIGATION OUTLET WORKS AND TAILRACE CHANNEL FOR NEW MELONES DAM, STANISLAUS RIVER, CALIFORNIA, Hydraulic Model Investigation
5. TYPE OF REPORT & PERIOD COVERED: Final report. Oct 71-Aug
6. PERFORMING ORG. REPORT NUMBER:
7. AUTHOR(s): Stephen T. Maynord
8. CONTRACT OR GRANT NUMBER(s):
9. PERFORMING ORGANIZATION NAME AND ADDRESS: U. S. Army Engineer Waterways Experiment Station, Hydraulics Laboratory, P. O. Box 631, Vicksburg, Miss. 39180
10. PROGRAM ELEMENT, PROJECT, TASK AREA & WORK UNIT NUMBERS:
11. CONTROLLING OFFICE NAME AND ADDRESS: U. S. Army Engineer District, Sacramento, 650 Capitol Mall, Sacramento, Calif. 95814
12. REPORT DATE: September 1981
13. NUMBER OF PAGES: 86
14. MONITORING AGENCY NAME & ADDRESS (if different from Controlling Office):
15. SECURITY CLASS. (of this report): Unclassified
15a. DECLASSIFICATION/DOWNGRADING SCHEDULE:
16. DISTRIBUTION STATEMENT (of this Report): Approved for public release; distribution unlimited.
17. DISTRIBUTION STATEMENT (of the abstract entered in Block 20, if different from Report):
18. SUPPLEMENTARY NOTES: Available from National Technical Information Service, 5285 Port Royal Road, Springfield, Va. 22151
19. KEY WORDS (Continue on reverse side if necessary and identify by block number):
Flood control
Hydraulic models
Irrigation
Outlet works
New Melones Dam
Tailraces
20. ABSTRACT (Continue on reverse side if necessary and identify by block number):

A model study of the flood control and irrigation (FC&I) outlet works and tailrace channel for New Melones Dam was conducted to develop measures to stabilize the tailrace channel. During the initial operation of the prototype FC&I outlet works, flows at a relatively low pool elevation resulted in failure of the 4-ft-diam derrick stone on the opposite bank.

Several alternatives were tested in the 1:24-scale model. In the first

(Continued)

DD FORM 1 JAN 73 1473 EDITION OF 1 NOV 65 IS OBSOLETE

Unclassified

SECURITY CLASSIFICATION OF THIS PAGE (When Data Entered)

411389

20. ABSTRACT (Continued).

alternative the existing concrete chute and impingement pad located downstream of the two 78-in.-diam fixed-cone valves were modified to form a basin similar in concept to an impact basin. This design resulted in adequate energy dissipation but concern for the structural integrity and the cost of this basin eliminated this alternative. The second alternative evaluated in the model was a plunge pool or preformed scour hole concept. The plunge pool was not effective because the length available was too short for adequate energy dissipation, and the angle at which the jet entered the pool caused the jet to ride along the surface rather than plunge and dissipate energy throughout the depth of the pool. The third design tested in the model involved increasing the tailwater by means of an inflatable dam located downstream in the tailrace channel. An inflatable or removable dam would be required so that it could be lowered during power generation and raised during FC&I outlet works operation. Increased tailwater together with a partial plunge pool resulted in adequate energy dissipation but possible operation problems and the cost of the inflatable dam excluded this alternative.

The recommended design consisted of the addition of deflector plates to the 18-ft-diam hoods and baffle blocks and an end sill added to the existing concrete chute and impingement pad. This design resulted in good energy dissipation at all flows. The loadings exerted on the baffle blocks and end sill were measured in the 1:24-scale model. The loadings and pressures exerted on the deflector plates were measured in a 1:12-scale model. These loadings were used in the structural design of the elements of the recommended design. Although low-pressure zones were found in the deflector plate design, the high level of aeration that occurs when fixed-cone valves discharge into freely aerated hoods should reduce the potential for cavitation damage. Aeration of flow within the hoods was supplemented by air vents located between the deflector plates.

PREFACE

The model investigation reported herein was authorized by the U. S. Army Engineer Division, South Pacific, on 10 October 1979 at the request of the U. S. Army Engineer District, Sacramento. The studies were conducted by personnel of the Hydraulics Laboratory, U. S. Army Engineer Waterways Experiment Station (WES) during the period October 1979 to August 1980 under the general supervision of Messrs. H. B. Simmons, Chief of the Hydraulics Laboratory, and J. L. Grace, Jr., Chief of the Hydraulic Structures Division. Tests were conducted by Messrs. S. T. Maynord and H. R. Smith, under the supervision of Mr. N. R. Oswalt, Chief of the Spillways and Channels Branch. Instrumentation support was obtained from Mr. Homer Greer. This report was prepared by Mr. Maynord.

During the course of the model investigation, Messrs. Sam Powell of the Office, Chief of Engineers; Ted Albrecht and Jim Tanouye of the South Pacific Division; and Herman H. C. (Bud) Pahl III and John White of the Sacramento District visited WES to discuss test results and decide on further modification and/or alternatives to be tried. Because the basic structure was already constructed and the project was in operation, Messrs. White and Pahl provided significant input regarding types of modifications that would be hydraulically and structurally feasible.

Commanders and Directors of WES during this testing program and the preparation and publication of this report were COL Nelson P. Conover, CE, and COL Tilford C. Creel, CE. Technical Director was Mr. F. R. Brown.

CONTENTS

CONVERSION FACTORS, U. S. CUSTOMARY TO METRIC (SI)
UNITS OF MEASUREMENT

U. S. customary units of measurement used in this report can be converted to metric (SI) units as follows:

Multiply	By	To Obtain
cubic feet per second	0.02831685	cubic metres per second
feet	0.3048	metres
feet per second	0.3048	metres per second
feet per second per second	0.3048	metres per second per second
inches	25.4	millimetres
miles (U. S. statute)	1.609344	kilometres
pounds (mass)	0.4535924	kilograms
tons (2000 lb, mass)	907.1847	kilograms

Figure 1. New Melones project

FLOOD CONTROL AND IRRIGATION OUTLET WORKS AND TAILRACE CHANNEL FOR NEW MELONES DAM STANISLAUS RIVER, CALIFORNIA

Hydraulic Model Investigation

PART I: INTRODUCTION

Pertinent Features of the Prototype

1. New Melones Dam (Figure 1) is located on the Stanislaus River near Sacramento, California; vicinity and locality maps are shown in Figure 2. Details of the project, shown in Plate 1, consist of a rock-fill dam; a multiple-purpose tunnel with outlet facilities for diversion, hydropower, flood control, and irrigation releases; a powerhouse; and an ungated detached spillway.

2. The dam, a rolled rock-fill section with a central impervious core inclined upstream of the axis, is located about 3/4 of a mile* downstream from the old Melones Dam. The embankment has a maximum height above streambed of about 625 ft and a crest length of about 1560 ft. The rock-fill dam is arched upstream on a 2000-ft radius. Crest elevation of the embankment is 1135,** providing 11.0 ft of freeboard above spillway design flood pool to allow for possible settlement due to earthquake. The crest width is 40 ft and the upstream and downstream slopes, down to el 1113.3, are 1V on 2H and 1V on 1.9H, respectively.

3. A multipurpose outlet works for diversion, flood control, irrigation and hydropower, and other purposes is located in the right abutment of the dam. The outlet works consist of a 23-ft-diam multipurpose tunnel with a low-level intake for diversion; a multipurpose high-level intake for flood control, hydropower, and irrigation; a 55-ft-diam surge

---

* A table of factors for converting U. S. customary units of measurement to metric (SI) units is presented on page 3.

** All elevations (el) cited herein are in feet referred to mean sea level.

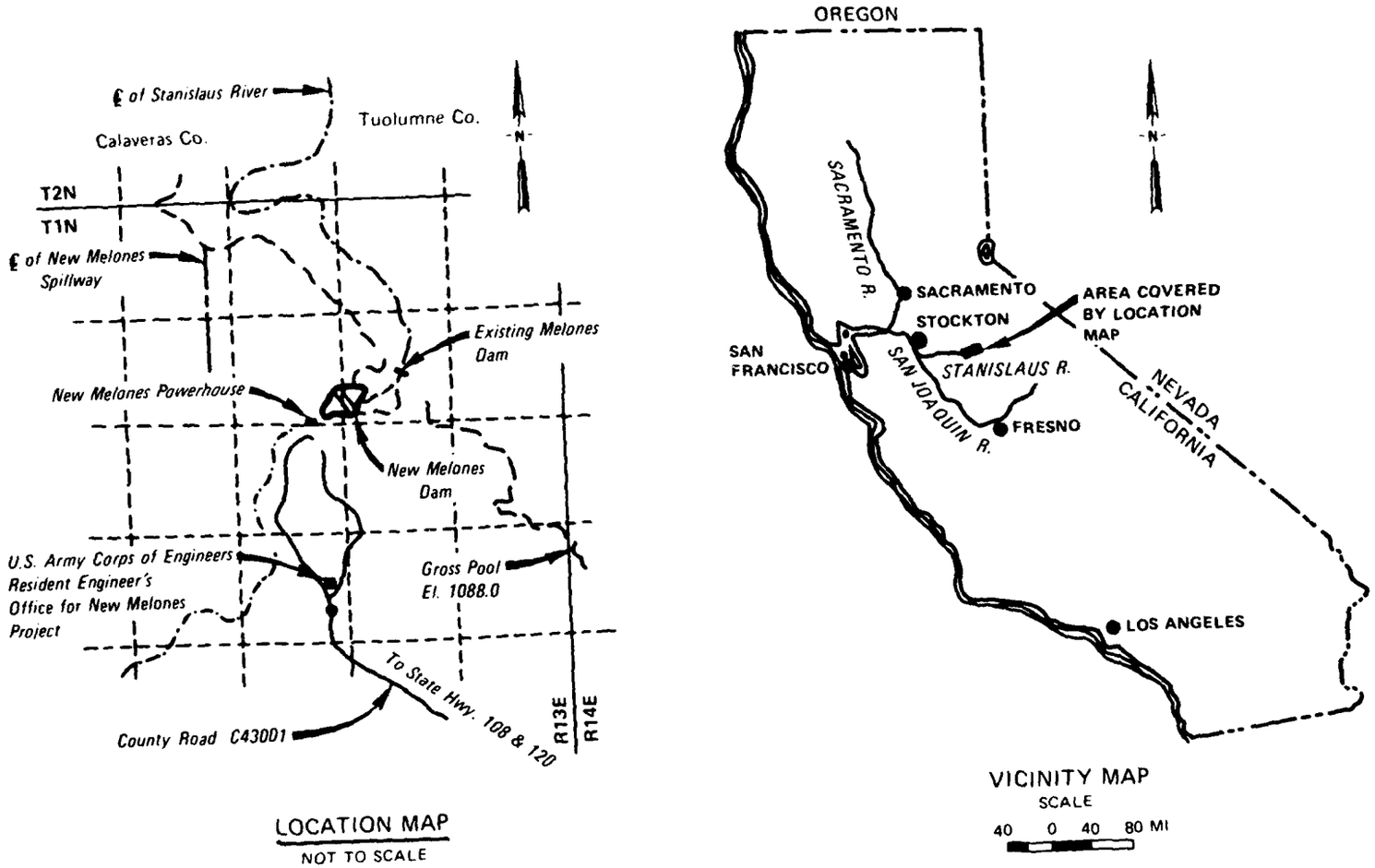

Figure 2. Vicinity and location maps

tank for pressure relief due to water hammer action; two 17-ft-diam power tunnels and steel penstocks branched into two 174-in.-diam butterfly valves and two 14.5-ft-diam steel penstocks to serve turbines in the powerhouse; a 13-ft-diam tunnel and steel penstock equipped with a bifurcation at its downstream end to accommodate two 96-in.-diam ring follower gates, two 78-in.-diam fixed-cone valves and two 18-ft-diam hoods for control of flood and irrigation releases; two 6-ft-diam low-level outlet works equipped with two 72-in.-diam ring follower gates, two 66-in.-diam fixed-cone valves and two 15.5-ft-diam hoods for control of diversion releases; and a tailrace channel. Tunnel plugs were installed in the diversion tunnel inlet and outlet after completion of diversion and before the outlet works operated as a pressure tunnel. The fixed-cone valves at New Melones are 8-vane designs having 1.75-in.-thick and 2.25-in.-thick vanes in the low-level outlet works and the flood control and irrigation outlet system (FC&I), respectively.

4. The new powerhouse is located about 700 ft downstream from the toe of the rock-fill dam on the right bank of the Stanislaus River, opposite the old Melones powerhouse. Two 14.5-ft-diam penstocks from the multipurpose tunnel serve the two turbines. Maximum gross head, at pool el 1088, will be about 585 ft. Minimum gross head, at pool el 808, will be about 303 ft; and design head, at pool el 971, will be about 466 ft. The new powerhouse consists of two generating units and an erection bay, all complete with superstructure. Two 166,667-kva generators, at 0.9 power factor, will produce the rated 300,000-kw capacity. One 375-ton overhead traveling bridge crane will be used to handle generator and turbine components and other powerhouse equipment during maintenance. A 230-kv switchyard is located about 2000 ft downstream from the powerhouse and switchyard. A 90-ft-wide tailrace channel for the powerhouse was excavated in the streambed for a distance of approximately 2150 ft.

5. An ungated detached spillway was excavated through the saddle, approximately 2 miles northwest of the damsite to Bowman Gulch, to carry spillway flows to Bean Gulch, a tributary entering the Stanislaus River about 2000 ft downstream of the powerhouse. This spillway channel is about 6000 ft long with a maximum depth of cut of approximately 250 ft

on the center line. Spillway flows will be controlled by a broad-crested sill set at gross pool el 1088 and at a distance of about 2190 ft downstream of the channel entrance. The control sill extends across the channel and up both banks to the top of the spillway flood pool, el 1124. The channel has a bottom width of 200 ft and side slopes of 1.0V on 0.5H in rock and 1.0V on 1.5H in overburden, with 20-ft-wide berms at 40-ft intervals in elevation. The approach channel was excavated to invert el 1086.5 and the return channel downstream of the crest was excavated to a slope of 0.03 ft/ft beginning at the crest.

Purpose of Model Studies

6. During the initial operation of the FC&I, flow from the two 78-in.-diam fixed-cone valves severely eroded the bank opposite the FC&I and powerhouse (Figure 3). These flows were at pool el 804 which is considerably less than the maximum operating pool el 1088. Velocities exiting the FC&I hoods in the original design are approximated by the empirical equation:

$$V = 0.84 \sqrt{2g\ H_{net}}$$

where

V = velocity, fps

g = acceleration due to gravity, ft/sec^2

H_{net} = total head on valve, ft

These velocities would approach 155 fps at maximum operating conditions. The derrick stone was washed off the opposite bank and deposited in the tailrace channel. A scour hole approximately 15 ft deep developed downstream of the impingement pad. The access road to the powerhouse was in danger of being washed out if operation of the valves had been continued.

7. The purpose of the model study was to develop remedial measures that would stabilize the tailrace channel and prevent deposition of material that could affect powerhouse operation.

8. Since the project was already completed and in operation, only

a. Closeup of failure of opposite bank

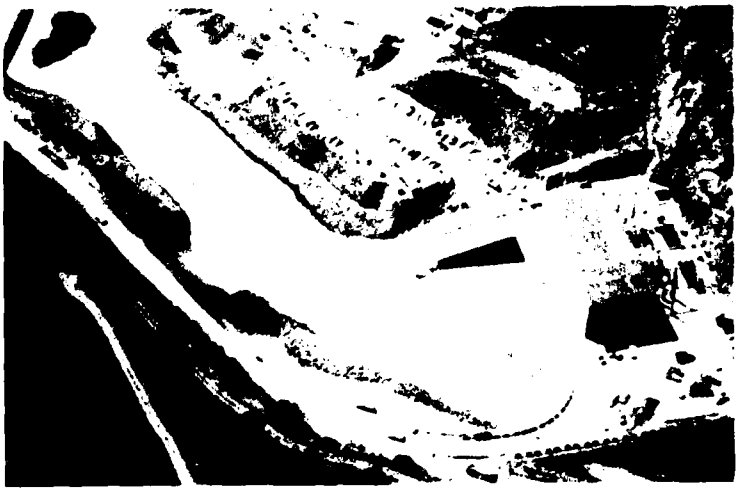

b. Aerial view of failure of opposite bank

Figure 3. Initial prototype operation

a short time frame was available for construction of any remedial works if project operation was not to be compromised. This necessitated that the design of these works be kept as simple and constructible as possible, utilizing conventional techniques. It also required an accelerated modeling program with close coordination between the design team, U. S. Army Engineer Waterways Experiment Station (WES); U. S. Army Engineer Division, South Pacific; and U. S. Army Engineer District, Sacramento (SPK). In fact, plans and specifications were prepared simultaneously with the model study. Some structural elements were designed using the best estimates of loads which were later verified by modeling.

PART II: THE MODEL

Description

9. The model of the New Melones FC&I tailrace, constructed to a scale of 1:24, included the two 78-in.-diam fixed-cone valves, the 18-ft-diam hoods, the concrete chute and impingement pad, the area downstream of the powerhouse, and the tailrace channel down to the vicinity of the island (Figure 4).

10. The fractured rock present in the bed of the prototype tailrace channel was simulated by using loose rock in the model. The size of the loose rock used in the model was determined by subjecting various sizes of model stone to the flows that were released in the prototype and comparing scour in the model relative to that experienced in the prototype. Initially rock representing a prototype size of 9- to 12-in. diam was used in the model. The resulting scour in the model was relatively greater than that measured in the prototype. The model rock was changed to simulate 12- to 18-in.-diam prototype rock and the resulting scour was similar to that measured in the prototype. This rock was used throughout the remainder of the study.

11. The discharge characteristics of the model FC&I valves (Figure 5) were determined on a calibration test stand at WES. Knowing the relationship of the head, valve opening, and discharge allowed reproduction of the proper flow conditions in the 1:24-scale model. Flow in the model was provided by pumps, and water-surface elevations were measured by point and staff gages. Velocities were measured by a pitot tube and pressures were measured with a dial-faced-Bourdon-type pressure gage.

12. Testing was also conducted in the 1:12-scale model used for study of the FC&I fixed-cone valve study.* Load cells, pressure transducers, and piezometers were used to measure forces, instantaneous

---

* S. T. Maynord and J. L. Grace, Jr. 1981 (Apr). "Fixed-Cone Valves, New Melones Dam, California; Hydraulic Model Investigation, U. S. Army Engineer Waterways Experiment Station, CE, Vicksburg, Miss.

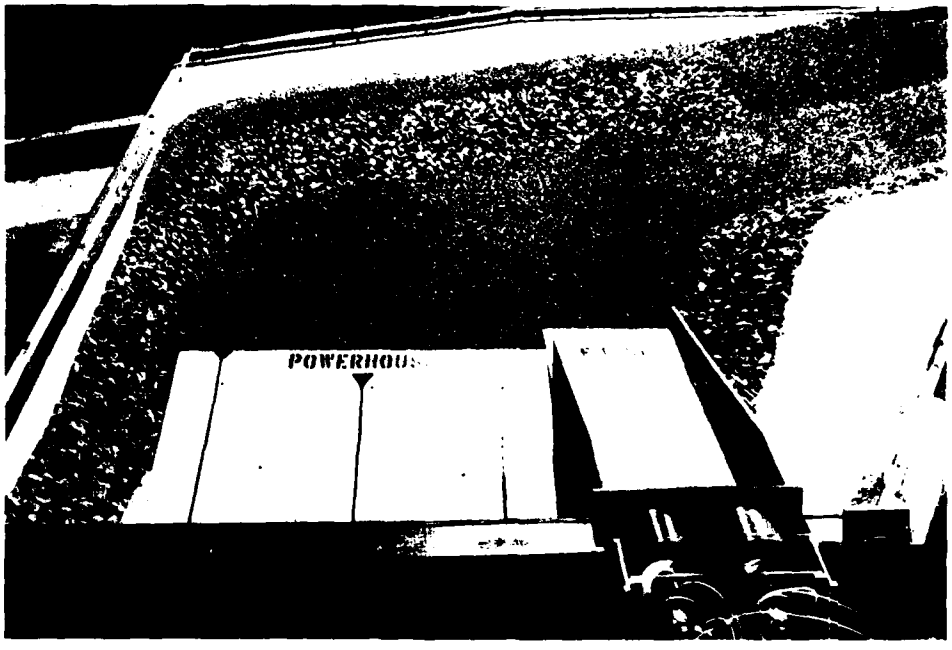

a. Looking downstream

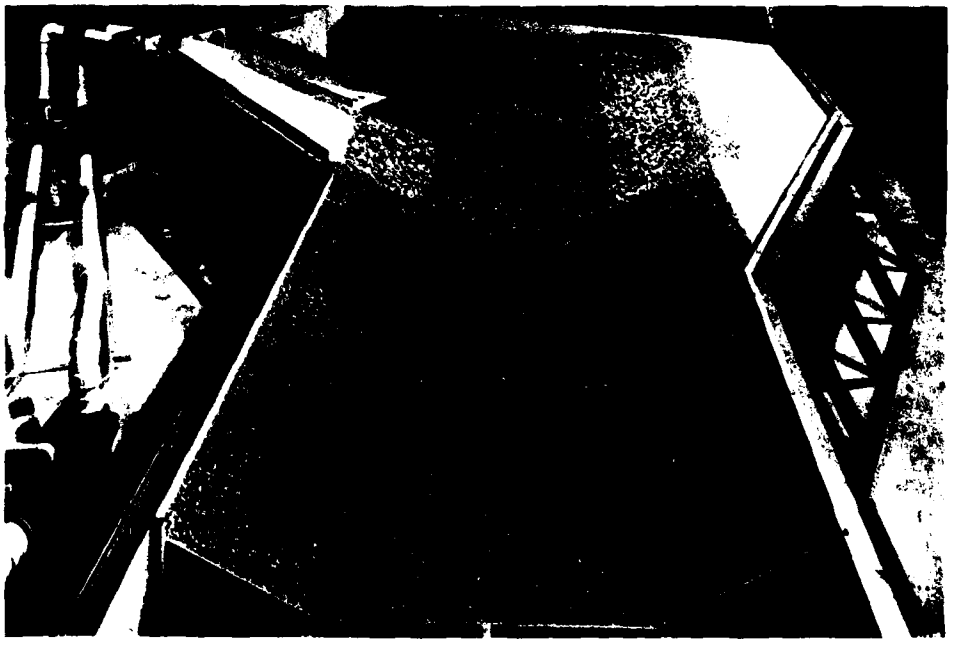

b. Looking upstream

Figure 4. Original design FC&I valve tailrace model

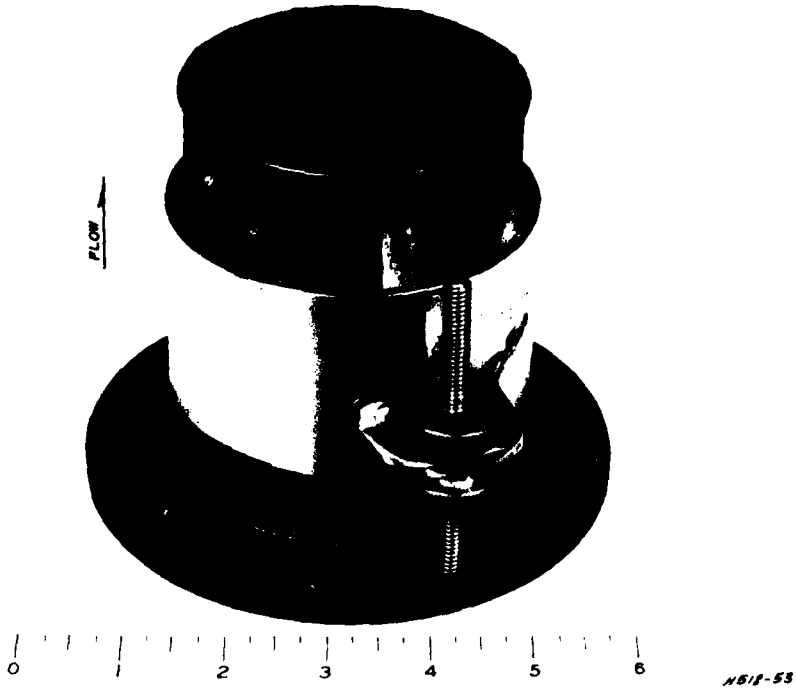

Figure 5. Model FC&I valve

pressures, and static pressures on various components of the recommended design.

Scaling Relations

13. The flow patterns in the New Melones tailrace study are affected by two dominant forces, gravity and inertia. This required duplication of prototype Froude numbers in the model for preserving similarity between the model and prototype. The following relations are valid for transferring model results to the prototype equivalents with similitude based on Froude number criteria:

Dimension	Ratio	Model to Prototype Scale Relations	
		Tailrace	Hood
Length	L_r	1:24	1:12
Area	$A_r = L_r^2$	1:576	1:144

(Continued)

Dimension	Ratio	Model to Prototype Scale Relations	
		Tailrace	Hood
Velocity	$V_r = L_r^{1/2}$	1:4.90	1:3.46
Discharge	$Q_r = L_r^{5/2}$	1:2,822	1:498.8
Weight	$W_r = L_r^3$	1:13,824	1:1,728

PART III: TESTS AND RESULTS

Original Design

14. Details of the original design of the FC&I tailrace channel are shown in Plates 2 and 3, respectively. The discharge rating curve for the valves is shown in Plate 4. Details of the valve dimensions and how valve openings were measured are shown in Plate 5. Tailwaters, upper pools, and net heads tested are shown in the following tabulation.

Pool Elevation ft msl	Net Head on Valve ft*	Sleeve Travel in.	Tailwater** Elevation ft msl
1088	533	28.1	511.0†
1088	544	23.6	502.5††
1088	558	16.6	501.2††
1088	565	11.3	499.9††
1048	495	28.1	503.2††
1048	505	23.6	502.3††
1048	517	16.6	501.0††
1048	525	11.3	499.7††

* Based on maximum losses through upstream piping.
** All tailwaters can be affected by level of downstream Tullock Reservoir.
† Tailwater based on Tullock Reservoir level.
†† Minimum tailwater resulting from free overfall at downstream end of model.

Operation of the FC&I system is to be limited to a maximum pool elevation of 1088. Sleeve travel is to be limited to 28.1 in. which was determined from prototype test results and analysis of data from the 1:12-scale model of the fixed-cone valves. The initial operation of the prototype at pool el 804 revealed that modifications to the original design were required. Resulting scour patterns in the prototype tailrace channel are shown in Plate 6.

15. Testing of the original design in the 1:24-scale model was

conducted to obtain model-prototype conformity relative to scour experienced in the tailrace. Initially the opposite bank was grouted and tests were conducted to determine the proper size of bed material for use in the model. The grouted stone was then replaced with loose rock simulating the 4-ft-diam derrick stone that was placed on the opposite bank. Flow conditions simulating the initial prototype operation resulting from a pool elevation of 804 and a sleeve travel of 16.6 in. were established in the model (Photo 1); note that the flow overtopped the derrick stone. The opposite bank failed (Photo 2), and as in the prototype, the derrick stone was moved down into the tailrace channel. Contour lines of 495, 490, and 485 are depicted with string in the resulting scour hole shown in Photo 2.

Alternate Designs

16. It was evident from the beginning of the studies that a considerable number of alternative designs would be required to develop an energy dissipator that would be both effective and economical. It was not possible to analytically design an energy dissipator that would be sure to work because of the combined effect of extremely high velocities (up to 155 fps) exiting the two valves, the aeration and spreading provided by the 18-ft-diam hoods, the flat trajectory of the jet leaving the hoods, the short distance to the opposite bank, the sharp angle which the flow would have to turn at the opposite bank, and the variable tailwater conditions that could occur caused by the fluctuating pool level in the downstream Tullock Reservoir. Therefore, it was decided to narrow the number of alternatives by taking a quick look at the following basic alternatives and to look at combining alternatives as needed.

a. Revet opposite bank to withstand velocities.

b. Artificially provide higher tailwater.

c. Provide plunge pool or preformed scour hole to reduce attack on opposite bank.

d. Modifications to the hoods.

e. Modifications to the chute and splash pad.

The following tabulations shows a summary of the alternatives modeled in chronological sequence:

Alternative	Description	Reference
Type 2 design basin	Existing chute and impingement pad with hood deflectors and 5-ft-high vertical end sill at downstream end of chute	Paragraph 17, Plate 7
Type 3 design basin	Same except end sill has 1V-on-1H face and roof added to direct flow downstream	Paragraph 18, Plate 7
Type 7 design basin	Same except hanging end sill added to roof	Paragraph 19, Plate 7
Type 10 design basin	Same except impingement pad lowered to el 480 and extended 24 ft in length with end sill at downstream end.	Paragraph 20, Plate 7
Plunge pool design (1)	Impingement pad removed, bottom excavated to el 466	Paragraph 21, Plate 8
Plunge pool design (2)	Same except 5-ft-high baffle blocks at downstream end of concrete chute	Paragraph 21, Plate 8, Photo 3
Plunge pool design (3)	Same except opposite bank slope changed to 1V on 1H	Paragraph 21, Plate 8
Plunge pool design (4)	Same except without baffle blocks	Paragraph 21, Plate 8
Plunge pool design (5)	Same except without hood deflectors	Paragraph 21, Plate 8
Increased tailwater (1)	Original design with tailwater raised to el 518	Paragraph 22
Increased tailwater (2)	Impingement pad removed, hood deflector added, tailwater el 518	Paragraph 22, Photo 4 and 5
Increased tailwater (3) with type 11 basin	Hood deflectors added. 7-ft baffle blocks at downstream end of impingement pad, tailwater el 518	Paragraph 23, Plate 9, Photo 6 and 7
Conical deflector rings	Conical deflector rings placed inside 18-ft-diam hoods	Paragraph 24, Plate 10

17. Attention was directed at reducing the energy entering the exit channel by installing some type of structural device in the hoods and within the concrete chute. The type 2 design basin (Plate 7)

consisted of a hood deflector and a 5-ft-high vertical end sill at the downstream end of the concrete chute. The 5-ft-long hood deflectors were placed around the top half of each hood at a 15-deg angle with the horizontal axis of the hood. This design was unacceptable because flow impinged on the end sill and was deflected vertically (90 deg) upward.

18. This led to the type 3 design basin (Plate 7) which consisted of the hood deflector with a 5-ft-high end sill with an upstream face slope of 1V on 1H and a 30-ft-long roof to redirect the flow near the toe of the chute. This design resulted in substantial energy dissipation, but attack on the opposite bank remained severe at the higher pool elevations. Types 4-6 design basins were variations of the type 3 design basin which did not increase energy dissipation.

19. To further dissipate energy, a hanging end sill was added in the type 7 design basin (Plate 7). This design resulted in greater energy dissipation than the type 3, but attack on the opposite bank was severe at the highest pool elevations.

20. The impingement pad was lowered to el 480 and lengthened 24 ft. A 3-ft-high end sill having a 1V-on-1H upstream face slope was placed at the downstream end of the impingement pad. This type 10 design basin (Plate 7) resulted in good energy dissipation at all flows. However, SPK engineers expressed concern for the structural integrity of the roof and the cost of the type 10 design basin.

21. The plunge pool or preformed scour hole concept with the bottom excavated to el 466 was modeled as a possible means of reducing attack on the opposite bank (see Plate 8). This plan included moving the access road on the opposite bank back into the hill a distance of about 25 ft. Performance with the hood deflectors added for pool el 804 and a 32.4-in. sleeve travel was investigated in the model. The derrick stone on the opposite bank failed. The hood deflectors were then tested with 5-ft-high baffle blocks placed at the downstream end of the concrete chute. This design was tested with pool el 804 and a 32.4-in. sleeve travel (Photo 3) and again the derrick stone on the opposite bank failed. The opposite bank slope was changed from the 1V-on-1.5H to a milder 1V-on-2H slope and tested using hood deflectors

with baffle blocks and hood deflectors only. The derrick stone failed at pool el 804 for both cases. Finally, the plunge pool without hood deflectors or baffle blocks was tested in the model. The derrick stone remained stable for conditions with pool el 804 and a 32.4-in. sleeve travel. However, the derrick stone failed when the pool elevation was raised to 935 with a 28.1-in. sleeve travel. This series of tests shows that the plunge pool concept alone would not provide adequate energy dissipation downstream of the valves.

22. Increased tailwater was proposed as a means of reducing attack on the opposite bank. The tailwater could be increased by means of an inflatable dam which would be lowered during power generation. The original design was simulated in the model and tested with tailwater el 518, pool el 850, and a 28.1-in. sleeve travel. After a test duration of 2 hr (prototype time), a substantial scour hole resulted but the derrick stone on the opposite bank remained stable. All of the scoured material in the channel bottom above el 495 was removed and flow at pool el 935 was tested in the model for a duration of 2 hr. The scour hole was enlarged and the derrick stone on the opposite bank failed. Next, the impingement pad was removed and the hood deflectors were installed. Flow conditions resulting from pool el 850, a 28.1-in. sleeve travel, and tailwater el 518 induced a substantial scour hole within a duration of 2 hr (prototype) but the derrick stone on the opposite bank remained stable. The bed material deposited above el 495 was removed and after testing for 2 hr with pool el 935 the scour hole was enlarged and the opposite bank experienced minor derrick stone failure. Again, the bed material deposited above el 495 was removed and after testing for 2 hr with pool el 1008, the scour hole was only slightly enlarged but the opposite bank suffered failure of the derrick stone. This flow condition after failure is shown in Photo 5.

23. The last concept tested with the increased tailwater was the type 11 design basin shown in Plate 9, which consisted of the addition of hood deflectors, baffle blocks, and a sidewall on the east side of the impingement pad to the original design. This design was tested for conditions up to pool el 1088, a 28.1-in. sleeve travel, and tailwater

el 518 (Photo 6). The dry bed condition after testing is shown in Photo 7; note the rather limited extent of bottom scour and stable opposite bank.

24. Efforts were directed at reducing energy within the 18-ft-diam hoods. Conical deflector rings were placed inside the hoods as shown in Plate 10. These rings concentrated the flow leaving the hoods into a solid jet approximately 6 ft in diameter and resulted in failure of the opposite bank.

Recommended Design

25. Deflector plates (a modification of the conical deflector rings) resulted in a significant reduction in energy leaving the 18-ft-diam hoods. Each hood was extended 10 ft in length to accommodate the upstream and downstream deflector plates. Numerous deflector plate sizes and locations were tested in the 1:24-scale model until the optimum combination was found (Plate 11). This design resulted in exit velocities leaving the hoods of approximately 60 percent of the velocity leaving the original design hoods. At pool el 1088 and a 28.1-in. sleeve travel, velocities exiting the hood were reduced from 155 fps to approximately 95 fps with the deflector plates.

26. Although exit velocities were significantly reduced, additional measures were needed to reduce energy in the downstream area to an acceptable level. Many combinations of baffle blocks and end sills were tested in the 1:24-scale model. The optimum design and performance data are shown in Plate 12. Many factors were involved in selecting this configuration. The height of the spray "rooster tail" became excessive with larger baffle blocks. However, more energy was dissipated by the larger blocks. Flow overtopped the concrete chute walls with the larger blocks or with blocks having vertical upstream faces. This would require some type of lip on the right sidewall. The baffle blocks with 1V-on-1H upstream face slopes were subjected to lower drag forces than the vertical-faced blocks. The 2-ft-high baffle blocks

with 1V-on-1H upstream face slope provided in the recommended plan were particularly desirable because flow did not overtop the concrete walls which eliminated the need for some type of deflector lip on the top of the wall. The energy dissipation obtained with these relatively small blocks was enough to provide stable conditions on the opposite bank.

27. The recommended deflector plate design is shown in Figure 6. Flow conditions resulting from pool el 1048, minimum tailwater el 503, and a 28.1-in. sleeve travel are shown in Photo 8; note the significant attack on the bank adjacent to the impingement pad. This slope should be grouted in the prototype as was done in the model or cut back to stable rock. The slope protection should extend up to a minimum elevation of 515. In addition, the area adjacent to the concrete chute on the right bank should be protected with a concrete slab or grouted rock from 20 ft upstream of the impingement pad to the downstream end of the impingement pad. Photo 9 is the same flow condition as Photo 8 showing flow conditions in the tailrace channel and on the opposite bank. Photo 10 depicts the maximum flow condition to be experienced with the FC&I outlet works, pool el 1088, maximum tailwater el 511, and a 28.1-in. sleeve travel. Photo 11 shows flow condition with pool el 800, maximum tailwater el 511, and a 28.1-in. sleeve travel.

28. The configuration of the scour hole that developed in the 1:24-scale model for the deflector plate design is shown in Plate 13. This scour hole was developed in the model by running a full range of discharges until the size of the scour hole remained constant.

29. Tests were conducted in the 1:24-scale model to determine the loading on the recommended baffle blocks and end sill. These tests were conducted because analytical means of determining the forces on the blocks and end sill would not be reliable. The approach velocity, depth, and fluid/air concentration cannot be adequately defined. The force measuring apparatus shown in Figure 7 was used in both the baffle block and end sill loading tests. This device was developed to measure only the drag force exerted on the baffle blocks and end sill. The vertical component was not determined in these tests. In the baffle block

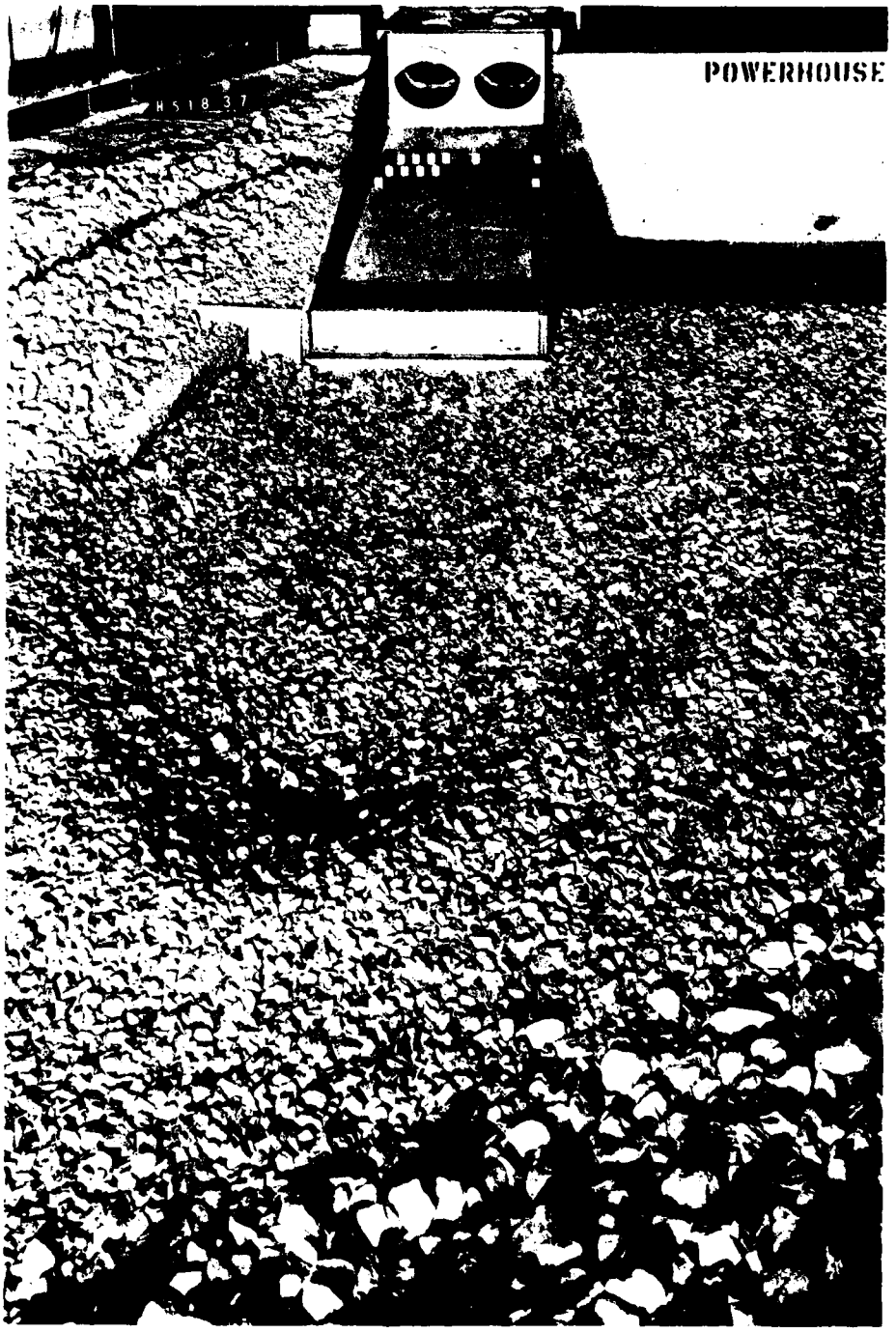

Figure 6. Recommended deflector plate design

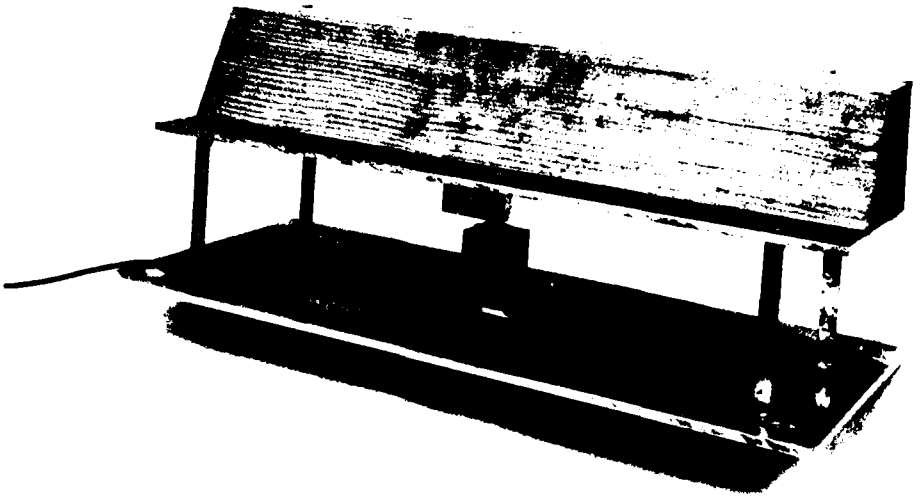

Figure 7. Baffle block and end sill force measuring apparatus

loading tests the force was measured on only the upstream row of blocks. The design loading was determined by measuring the load exerted on the three blocks centered on each hood (Plate 14). These six blocks were subjected to slightly greater loads than the blocks located farther away from the center line of the hoods. The drag force acting on the plate which represents the concrete chute floor was measured without baffle blocks. This drag force acting on the floor alone was subtracted from the total load with baffle blocks to obtain loadings on the blocks. Results of the loading tests are shown in Table 1. The maximum loading occurred with the maximum pool el 1088, a 28.1-in. sleeve travel, and was equal to 12 kips per block with a fluctuation of +7 kips.

30. The end sill loading tests were conducted by measuring the load on the entire end sill. The drag force acting on the exposed portion of the plate representing the basin floor was small relative to the load on the end sill and was not included in the analysis. Results of the end sill loading tests are shown in Table 2. The maximum loading occurred with pool el 1048, a 28.1-in. sleeve travel, and the minimum tailwater. With the maximum pool el 1088, and a 28.1-in. sleeve travel,

the resulting higher tailwater elevation causes dissipation of energy upstream of the end sill and consequently loads on the end sill are reduced.

31. Although none of the 18- to 48-in.-diam derrick stone on the opposite bank failed under any of the FC&I outlet works operating conditions, some method was needed to determine the approximate stability of the derrick stone during the most adverse flow conditions. A blanket of model rock representing 12- to 18-in.-diam prototype rock was placed over the derrick stone. This rock was subjected to maximum flow conditions at varying tailwater elevations and none of the 12- to 18-in.-diam rock was moved off the opposite bank. Tests with varying tailwater elevations showed that protection of the opposite bank should be carried up to el 520.

32. Problems with spray over the concrete chute wall occur when only one of the 78-in.-diam fixed-cone valves is operated. When the right valve (looking downstream) is operated, the spray goes over the wall into the area in front of the powerhouse and should cause no problems. However, when the left fixed-cone valve is operated, the spray goes over the right wall and onto the right bank. This spray may damage the rock slope protection on the right bank and would likely be injurious to any person or property in this area. A divider wall was tested in the FC&I tailrace model which eliminated the spray going over the concrete chute walls when either of the fixed-cone valves was operated. Details of the wall are shown in Plate 15.

33. Testing of several aspects of the deflector plate design was conducted in the 1:12-scale model used in the New Melones fixed-cone valve study (Figure 8). Flow conditions in the 1:12-scale model of the 18-ft-diam hoods are shown in Photos 12 and 13 for pool el 1088 and a 28.1-in. sleeve travel. Flow arrows are shown on the photographs because dye injections did not photograph well in the model. Note the extensive bracing used to stiffen the model test stand.

34. The 1:12-scale model was used to determine the forces acting on the deflector plates. A schematic of the test stand showing the

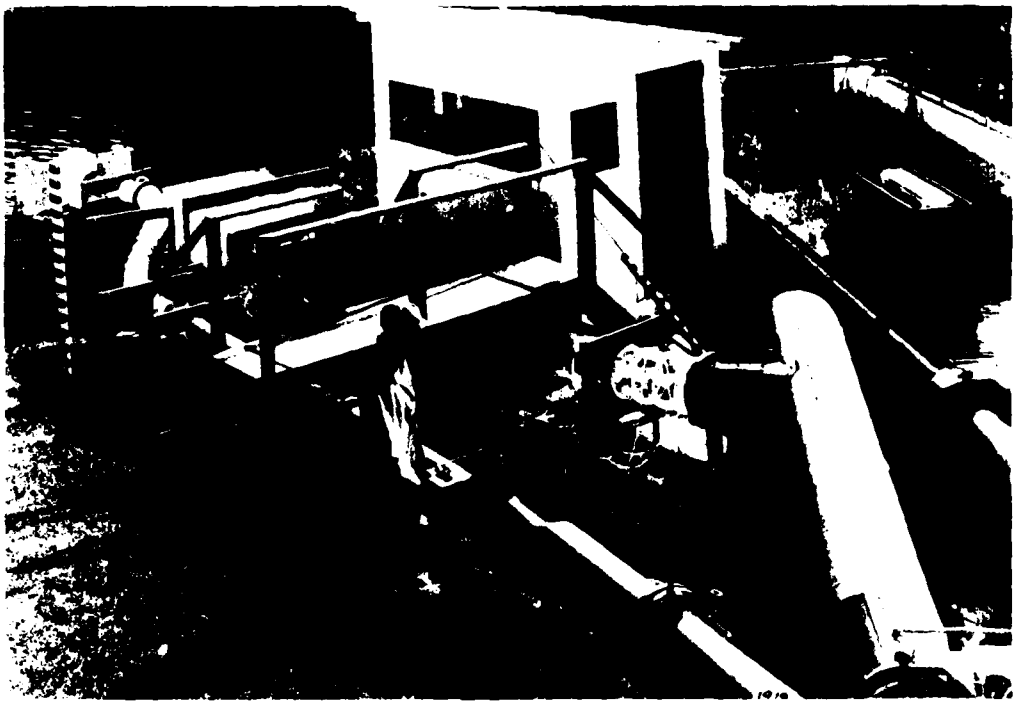

Figure 8. 1:12-scale model of New Melones fixed-cone valve

locations at which forces were measured is shown in Plate 16. The bottom vertical load cell (No. 5) was positioned near the center of gravity of the plastic hood and set to support the entire weight of the model hood (83 lb). This ensured that little vertical load was placed on the four horizontal load cells (Nos. 1-4). Rollers were provided with both vertical load cells (Nos. 5-6) to ensure freedom of movement in the horizontal direction.

35. Initial tests were conducted without the deflector plates to determine the force exerted upstream by the flow deflected by the backsplash cone. Load cell 6 was not used because no net upward force was anticipated. Time-histories of loading and the amplitude spectrum of loads measured with the maximum flow, pool el 1088, and a 28.1-in. sleeve travel are shown in Plates 17-21 for load cells 1-5, respectively. The left figure on each plate is the time-history of loading with the mean loading subtracted out. The right figure is the amplitude spectrum

for frequencies up to 200 Hz. Summing mean horizontal loads from cells 1-4 yielded an average upstream horizontal force of 56 kips due to flow deflected by the backsplash cone.

36. The second series of loading tests were conducted with only the upstream deflector plate. Load cell 6 was used in these tests because a net upward force was expected. Time-histories and amplitude spectrum of loads measured with pool el 1088 and a 28.1-in. sleeve travel are shown in Plates 22-27 for load cells 1-6, respectively. Summing mean horizontal loads from cells 1-4 yields an average downstream force of 369 kips. Adding 369 kips to the upstream force of 56 kips exerted on the backsplash cone yields an average horizontal force of 425 kips acting on the upstream deflector plate.

37. The third series of loading tests were conducted with both deflector plates. Time-histories and amplitude spectrum of loads measured with pool el 1088 and a 28.1-in. sleeve travel are shown in Plates 28-33 for load cells 1-6, respectively. Summing mean horizontal loads from cells 1-4 yields an average downstream force of 507 kips. Taking the difference between this value and the average horizontal force of 369 kips with only the upstream deflector plate yields an average horizontal loading of 138 kips on the downstream deflector plate.

38. Resonant vibration of the model test stand was a problem throughout the hood deflector plate loading tests. Stiffening of both the plastic hood and the support frame was undertaken in an attempt to raise the natural frequency of the model test stand above the range of interest in the prototype. This was found to be difficult to accomplish. During prototype testing predominant frequencies up to 160 Hz were observed in the FC&I hood accelerometers and pressure cells. Model test stand natural frequencies would have to be 500-600 Hz to be above this range in the prototype. The stiffened model test stand had predominant natural frequencies beginning at about 100 Hz and up. Therefore, observed model load fluctuations may have been amplified by test stand resonance. Load fluctuations at these resonant frequencies cannot be filtered out or ignored because they are in the range of interest in

the prototype. Average values of loads measured in the model are correct and only the load fluctuations may be conservative.

39. Pressures on the face of the deflector plates in the 1:12-scale model were measured to detect low-pressure zones, check total loading as measured by the load cells, and determine distribution of loading for use in the structural analysis of the deflector plate. Pressures were measured by simple piezometers at the locations shown in Plate 34. Lines of equal pressure were plotted as shown in Plates 35 and 36 for flow conditions with pool el 1088 and a 28.1-in. sleeve travel. The total load perpendicular to the plate was determined by planimetering areas of equal pressure and summing the product of those areas and the respective pressure. The total load perpendicular to the upstream plate determined in this manner was 466 kips. The horizontal component of the force estimated by pressures measured on the upstream deflector plate was 417 kips and acted downstream. This compares well with the 425 kips measured by the load cells. The total load perpendicular to the downstream plate based on pressure measurements was 150 kips. The horizontal component of the force estimated by pressures measured on the downstream deflector plate was 134 kips. This also compares favorably with the 138 kips measured by the load cells.

40. Additional pressures were measured throughout the hoods to locate any low-pressure zones. Two zones designated A and B (Plate 37) were found that exhibited low pressures. In zone A, pressures of -11 ft of water (prototype) were measured with pool el 1088 and a 28.1-in. sleeve travel. This low pressure (zone A) is created because the jet coming off the downstream deflector plate closes off the end of the hood at the higher discharges. One 12-in.-diam air vent was added to the side of the hood at the location shown in Plate 38. However, the pressure remained at -11 ft of water. A second air vent was added at the same location but on the other side of the hood and the pressure inside the downstream cavity fell to -7 ft of water for the same flow condition. The air vents were increased to 18-in. in diameter but the pressure remained at -7 ft of water. Model-prototype comparisons of air demand for fixed-cone valves have shown that air demand may be higher in the

prototype than indicated by models that are constructed to large-scale ratios. The 1:12-scale model should be an accurate simulation of the prototype. To ensure adequate aeration, the 18-in.-diam air vents (Plate 38) are recommended for the prototype. These air vents should provide greater aeration of both the flow within the hood and the flow entering the concrete chute and possibly reduce the potential for cavitation. Instantaneous pressure measurements show that the air vents increase pressure on the face of the deflector plate. These results will be discussed in paragraph 41.

41. A low pressure, zone B (Plate 37), was found in the area just downstream of the fixed-cone valve. In this upstream cavity, static pressures were -6 ft of water with or without the 18-in.-diam air vents for pool el 1088 and a 28.1-in. sleeve travel. For comparison, both deflector plates were removed from the hoods to simulate a typical fixed-cone valve discharging into a circular hood. The resulting pressure in the zone B cavity downstream of the fixed-cone valve was -4 to -5 ft of water for the flow condition with pool el 1088 and a 28.1-in. sleeve travel. The deflector plates were installed in the model and various methods of introducing air into the upstream cavity were evaluated. Aeration of these low-pressure zones might reduce the potential for cavitation damage. A splitter pier and wedge (Plate 39) were attached to the upstream deflector plate to induce separation of flow leaving the upstream plate and aeration of the upstream cavity. The splitter pier was effective but the static pressure in the upstream cavity, zone B, remained at -6 ft of water. Instantaneous pressures measured on both the upstream and downstream deflector plates were not affected. Since typical fixed-cone valve installations have experienced similar low-pressure zones in the area immediately downstream of the valve without severe cavitation damage, no aeration device for the upstream low pressure, zone B, was proposed for the prototype.

42. Instantaneous pressures were measured on the deflector plates at the locations shown in Plate 40. These locations correspond to the locations of minimum static pressures observed with piezometers on each of the deflector plates. The resulting minimum and average pressures

measured with and without air vents and splitter piers are shown in Table 3 for both deflector plates. These results show the increase in pressures that results from having the two 18-in.-diam air vents for each hood. No significant increase in pressures was seen when the splitter pier was added. The measured pressures show that the potential exists for severe cavitation. However, the large air concentration present within the flow reduces the potential for cavitation damage. In addition, no reports of cavitation damage were found in the literature where fixed-cone valves discharge into freely aerated hoods.

PART IV: SUMMARY AND CONCLUSIONS

43. The severe problems experienced in the tailrace channel of the original design prototype were simulated in the model. Of the alternatives tested in the model, only the design consisting of deflector plates within the hoods, with baffle blocks, and an end sill on the impingement pad met all the constraints of the system. The first alternate design tested that consisted of an end sill and roof at the downstream end of the concrete chute (type 10 basin) was effective in reducing the energy leaving the basin; however, doubts about the structural feasibility of the roof and the estimated prototype cost eliminated this alternative.

44. The preformed scour hole alternative was not effective in reducing the energy entering the tailrace channel. The length available for the scour hole was too short and the flow would not plunge and dissipate energy as desired. Increased tailwater by means of an inflatable dam located downstream was effective in reducing energy in the tailrace channel. However, the cost and possible operation problems eliminated adoption of this alternative.

45. The deflector plate design had several areas that were studied in detail to ensure the adequacy of this design. Velocities exiting the fixed-cone valves approached 155 fps which is more than sufficient for severe cavitation damage. Significant loadings on both deflector plates were measured in the model. These loadings were provided to the Sacramento District for use in the structural design of the deflector plates. The distribution of the loading was determined by static pressure measurements made with piezometers on the face of each deflector plate. Good agreement was found between the measured averaged loadings on the deflector plates and the estimated loading computed from the pressure measurements.

46. Techniques for computing loadings on both the baffle blocks and end sill for stilling basins cannot be relied upon for the flow conditions in New Melones. Velocity, depth, and air-water concentrations were impossible to define downstream of the deflector plates. For this

reason, loadings were measured on both the baffle blocks and the end sill and these data were provided to the sponsor for use in the structural design of the elements.

47. The scour hole that developed downstream of the impingement pad with the recommended design was similar in depth to and larger in lateral extent than the scour hole that developed in the prototype during initial operations of the original design. With the deflector plate design, the 4-ft-diam derrick stone on the opposite bank was shown to be stable.

48. At no time during testing of the deflector plate design did any material build up in the area immediately downstream of the powerhouse.

49. The area on the right bank adjacent to the concrete chute and impingement pad receives severe attack from flow with the deflector plate design. This area might be cut back or excavated away from the zone of attack or grouted for stabilization.

50. A divider wall was developed that solves the problem of spray created by single valve operation. However, this should never be a concern because single valve operation will not be permitted by the Sacramento District.

51. The possibility of cavitation cannot be fully addressed with the model. Under normal conditions velocities of 155 fps almost certainly indicate the likelihood of severe cavitation damage. Velocities of 90-100 fps impinging on the baffle blocks also have the potential for severe cavitation damage. However, when fixed-cone valves discharge into freely aerated hoods considerable aeration of the flow takes place. This aeration will limit the potential for cavitation damage. Aeration of flow within the hoods for the deflector plate design was supplemented by 18-in.-diam air vents located between the deflector plates. In addition, no reports of cavitation damage were found in the literature where fixed-cone valves discharge into freely aerated hoods. The operation of the FC&I valves is to be infrequent because most flows will be stored temporarily and subsequently released through the powerhouse.

Table 1

Baffle Block Loading Tests

Final Deflector Plate Design

Test No.	Pool Elevation ft msl	Sleeve Travel in.	Load on 6 Blocks Minus Drag kips	Fluctuation on 6 Blocks kips ±	Load Block kips	Fluctuation* Block kips ±
510	850	28.1	39.4	20.9	6.6	3.5
511	935	28.1	48.3	27.9	8.1	4.7
512	1008	28.1	62	34.9	10.3	5.8
513	1048	28.1	62	38.3	10.3	6.4
515	1088	28.1	72	42.0	12.0	7.0

* Assumes each block receives 1/6 of the total fluctuation.

Table 2

End Sill Loading Tests

Final Deflector Plate Design

Test No.	Pool Elevation ft msl	Tailwater Elevation fl msl	Sleeve Travel in.	Load on End Sill kips	Fluctuation kips
600	850	Minimum	28.1	247	±29
601	435	Minimum	28.1	326	±43
602	1008	Minimum	28.1	372	±70
603	1048	Minimum	28.1	382	±89
604	1088	511	28.1	254	±48

Table 3

Instantaneous Deflector Plate Pressures

Final Deflector Plate Design

Condition	Deflector Plate	Sleeve Travel in.	Pool Elevation ft msl	Pressure Feet of Water	
				Minimum	Average
Without vents	Upstream	28.1	1088	-41	9
Without splitter pier	Upstream	23.6	1088	-32	1
With vents	Upstream	28.1	1088	-23	12
Without splitter pier	Upstream	23.6	1088	-22	5
With vents	Upstream	28.1	1088	-29	20
With splitter pier	Upstream	23.6	1088	-21	18
Without vents	Downstream	28.1	1088	-52	0
	Downstream	23.6	1088	-43	0
With vents	Downstream	28.1	1088	-35	3
	Downstream	23.6	1088	-32	2

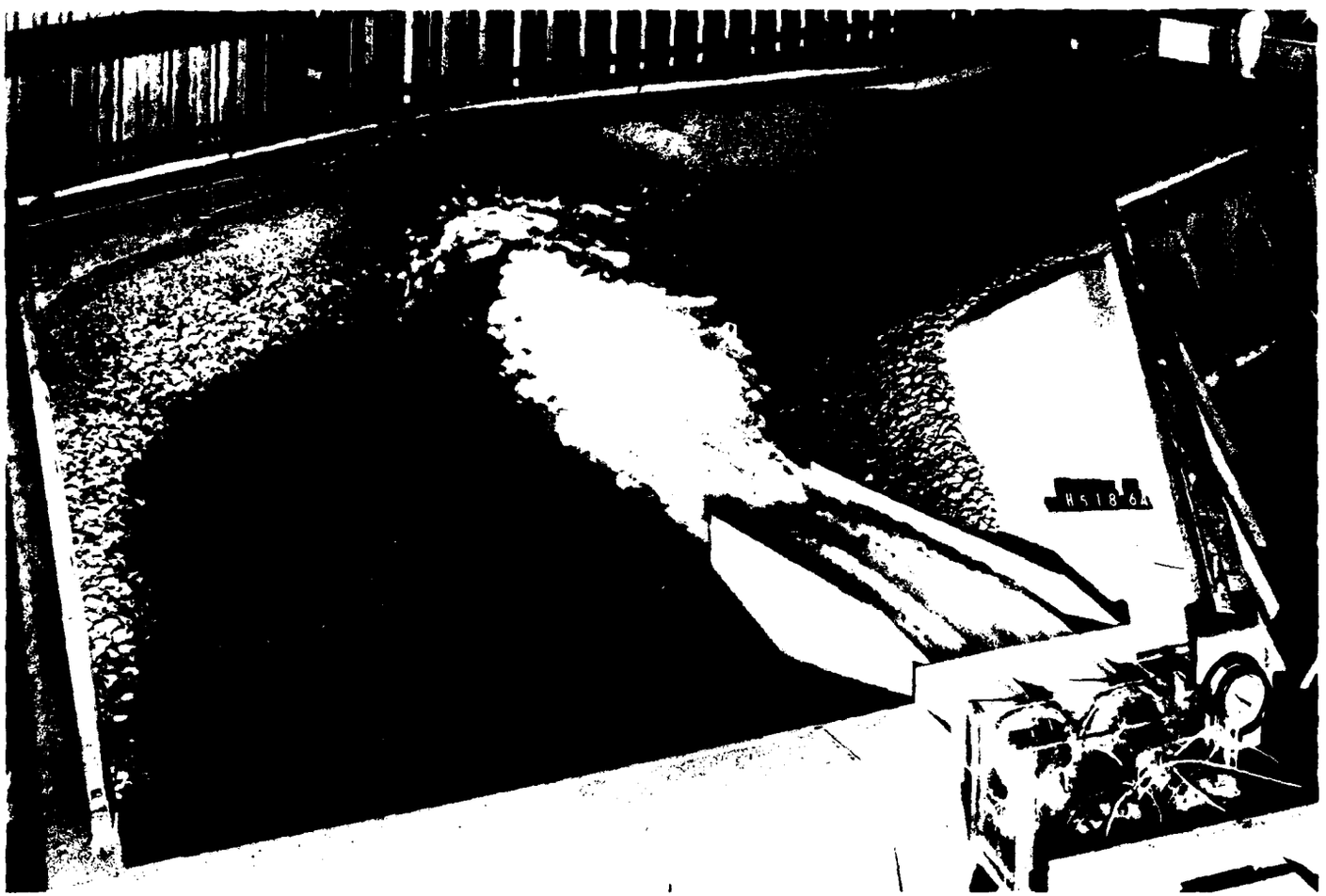

Photo 1. Original design, pool el 804, 16.6-in. sleeve travel, minimum tailwater

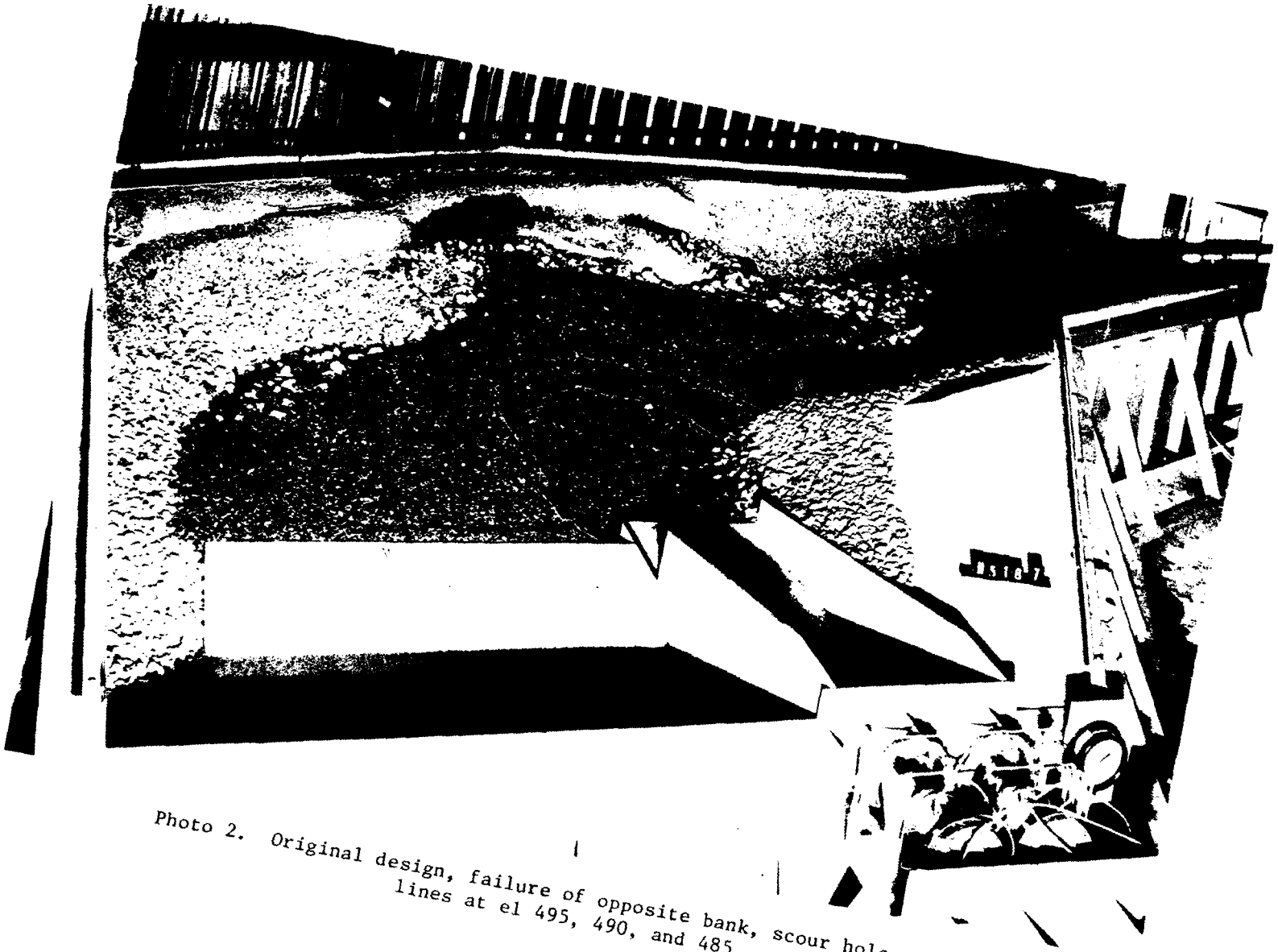

Photo 2. Original design, failure of opposite bank, scour hole contour lines at el 495, 490, and 485

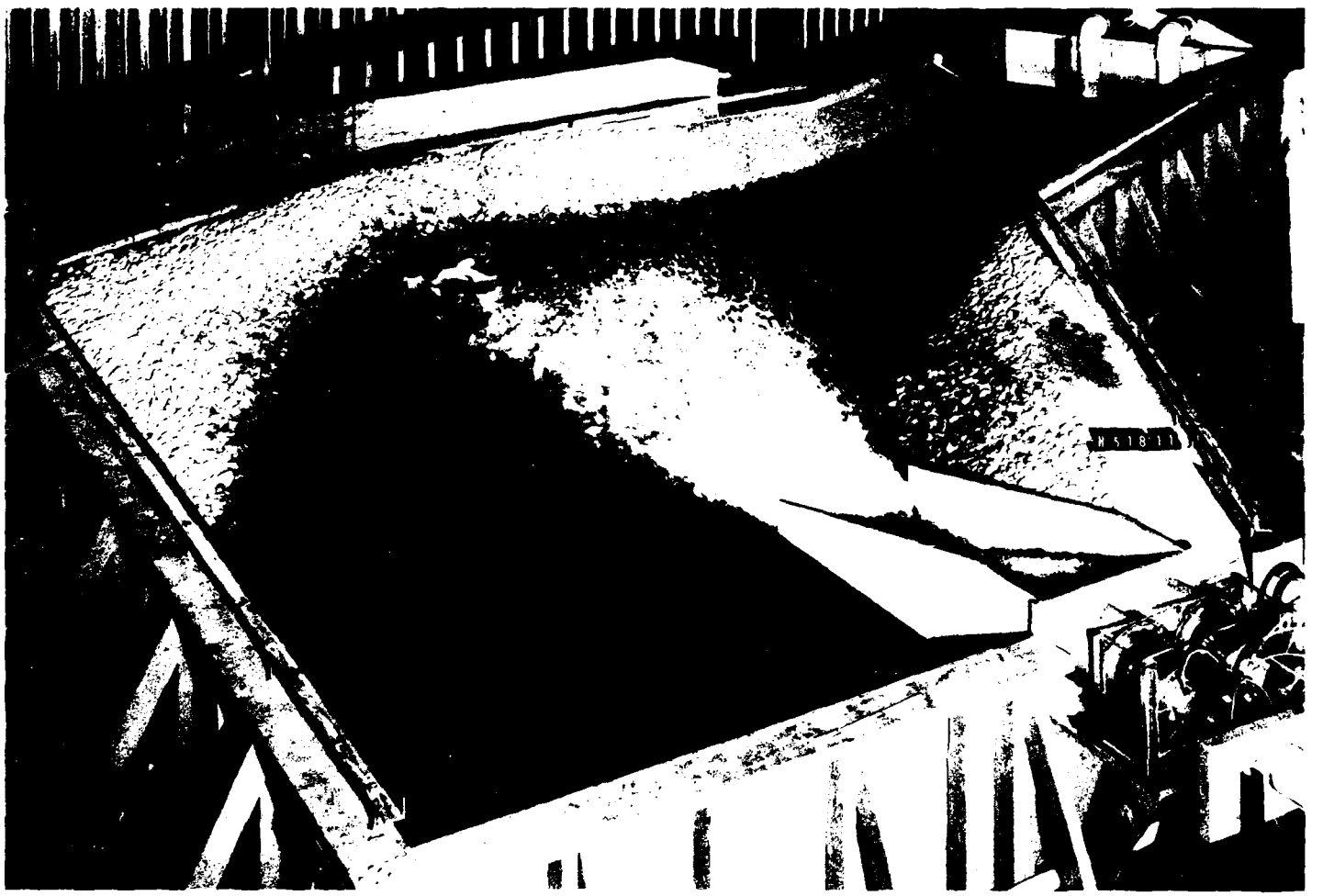

Photo 3. Plunge pool design, impingement pad removed, hood deflector and baffle blocks added; pool el 804, 32.4-in. sleeve travel, minimum tailwater

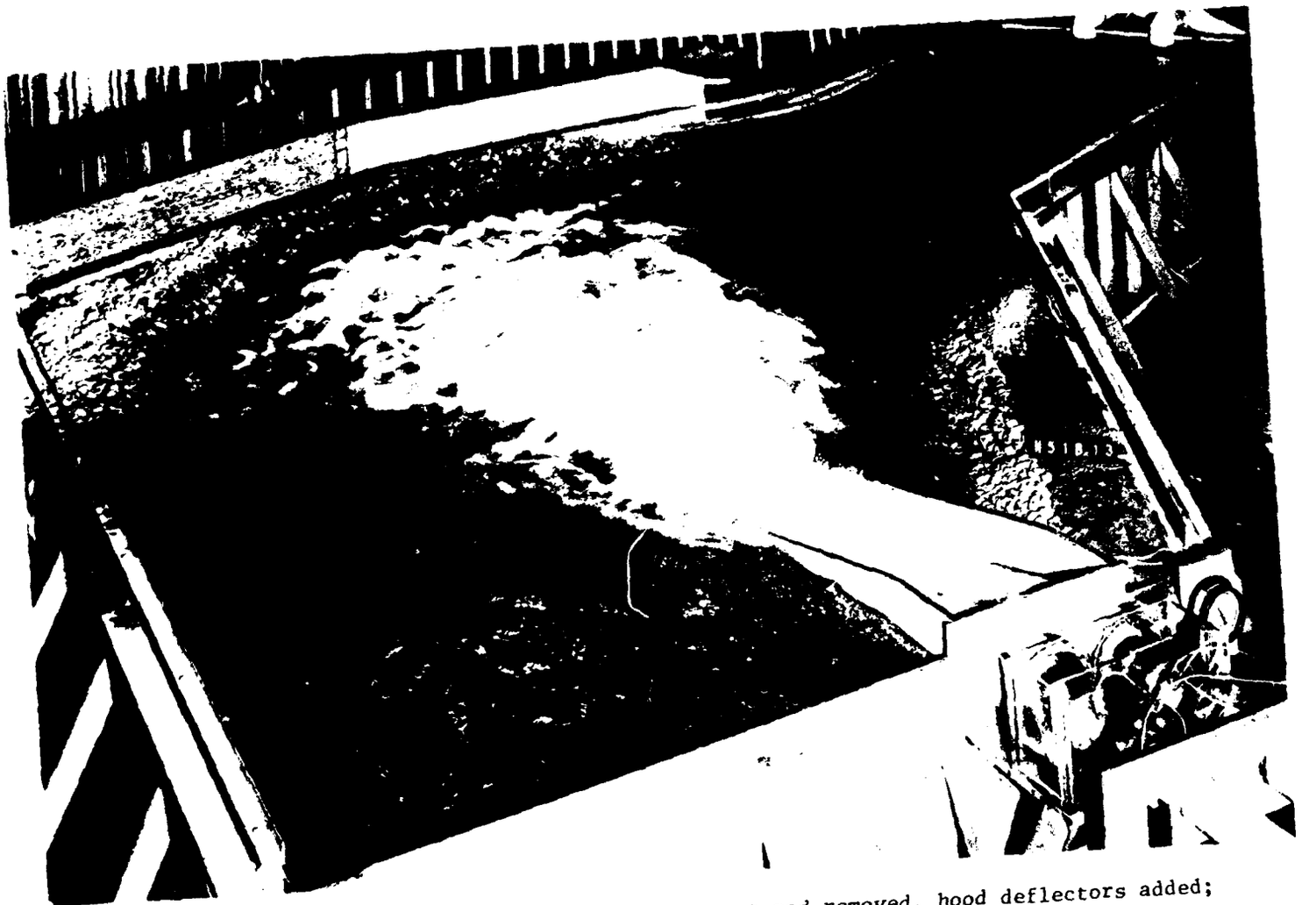

Photo 4. Increased tailwater design, impingement pad removed, hood deflectors added; pool el 1008, 28.1-in. sleeve travel, tailwater el 518

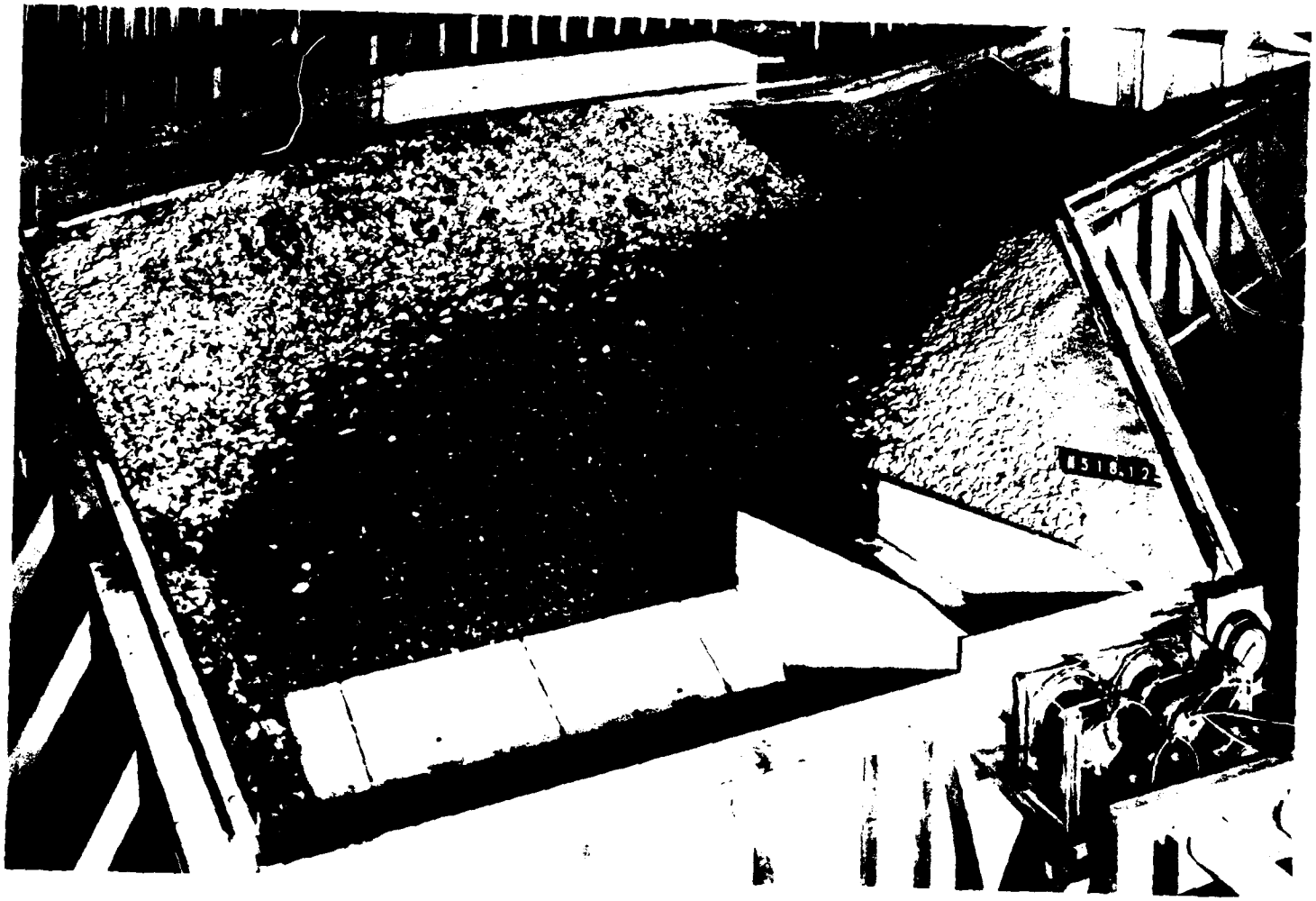

Photo 5. Increased tailwater design, failure of derrick stone on opposite bank after flow conditions shown in Photo 4

Photo 6. Increased tailwater design, type 11 basin. Flow conditions at pool el 1088, 28.1-in. sleeve travel, tailwater el 518

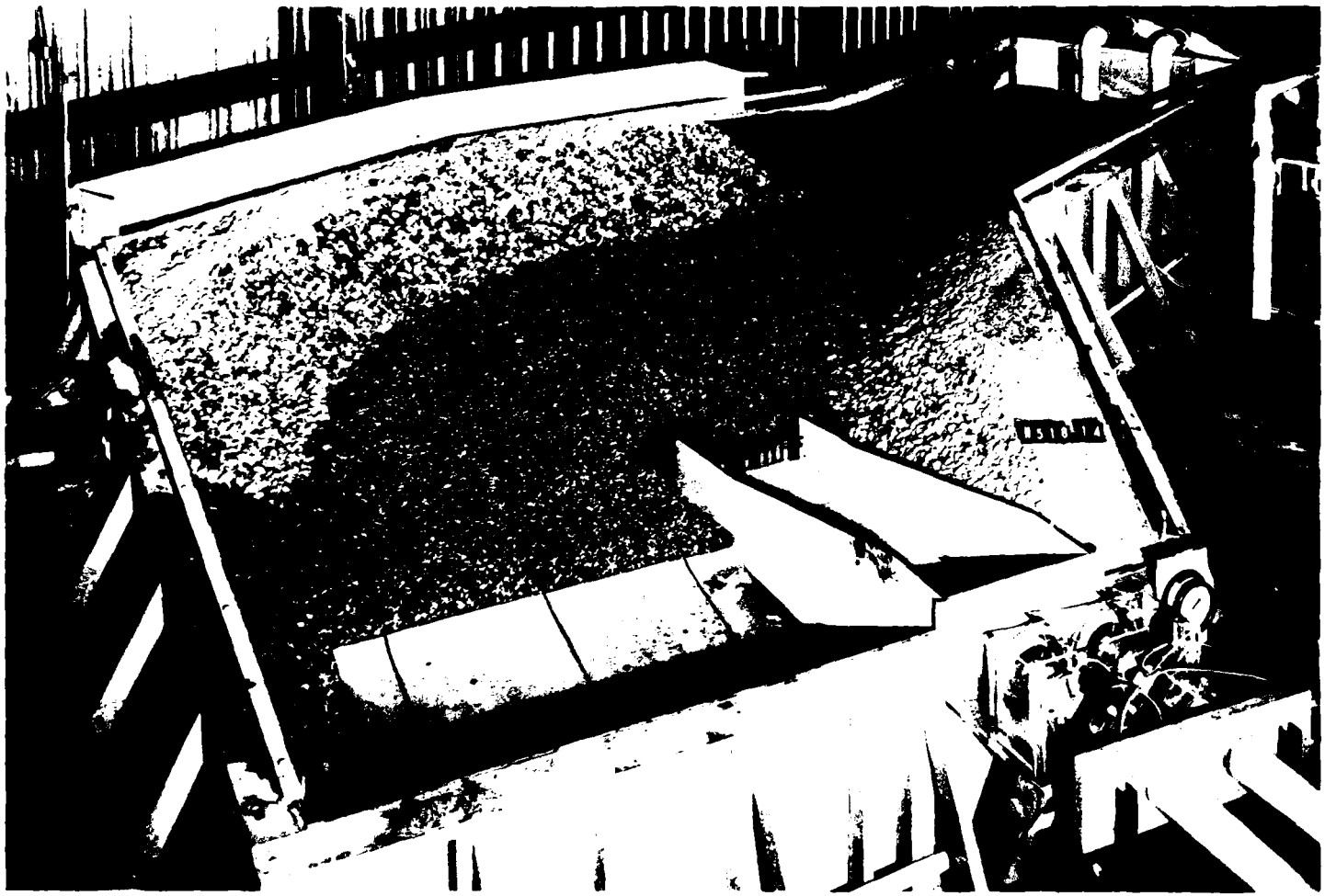

Photo 7. Increased tailwater design, dry bed after flow shown in Photo 6

Photo 8. Recommended deflector plate design. Flow at pool el 1048, 28.1-in. sleeve travel, tailwater el 503, view from opposite bank showing attack on bank adjacent to tailrace

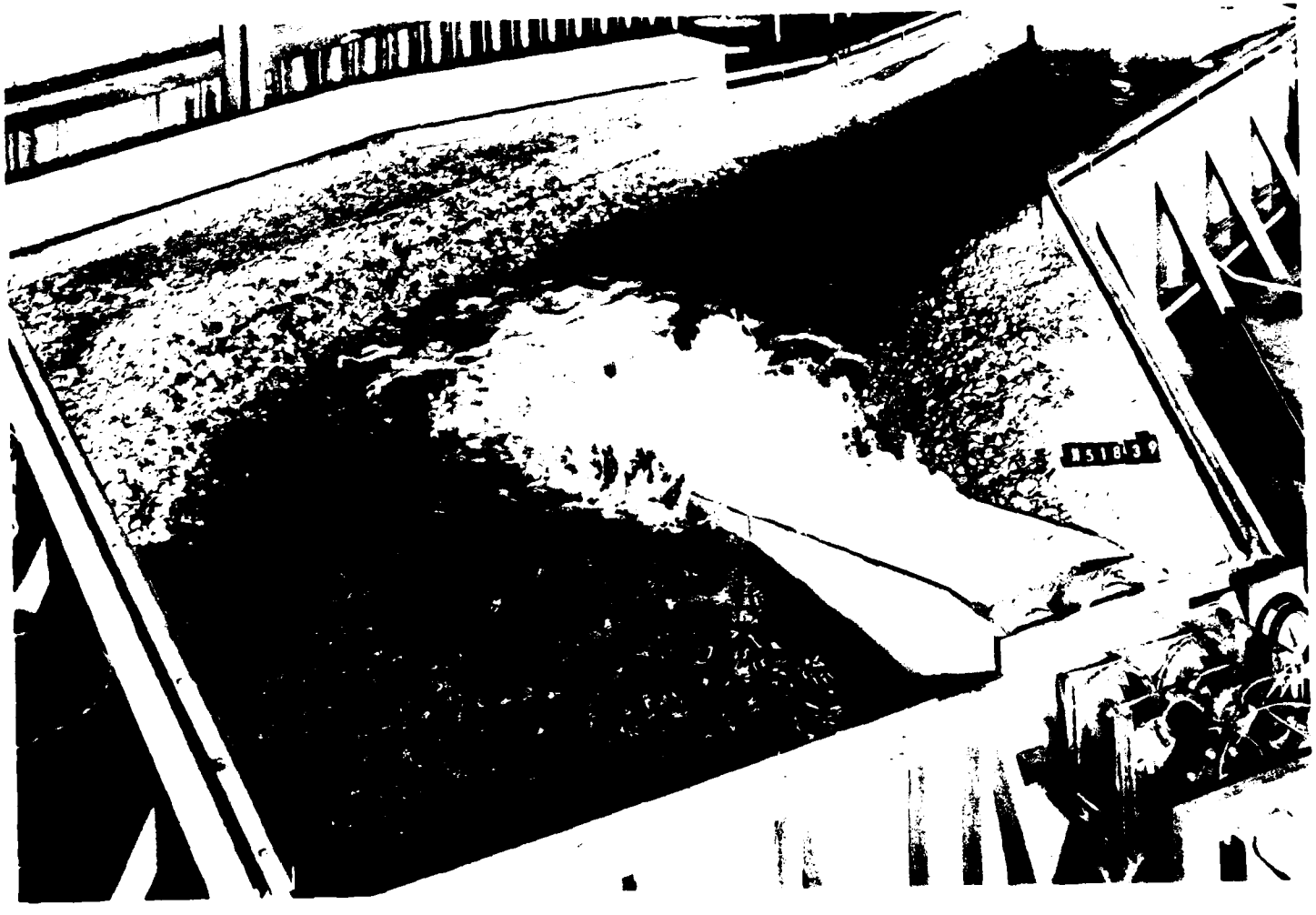

Photo 9. Recommended deflector plate design. Same flow as in Photo 9, showing attack on opposite bank

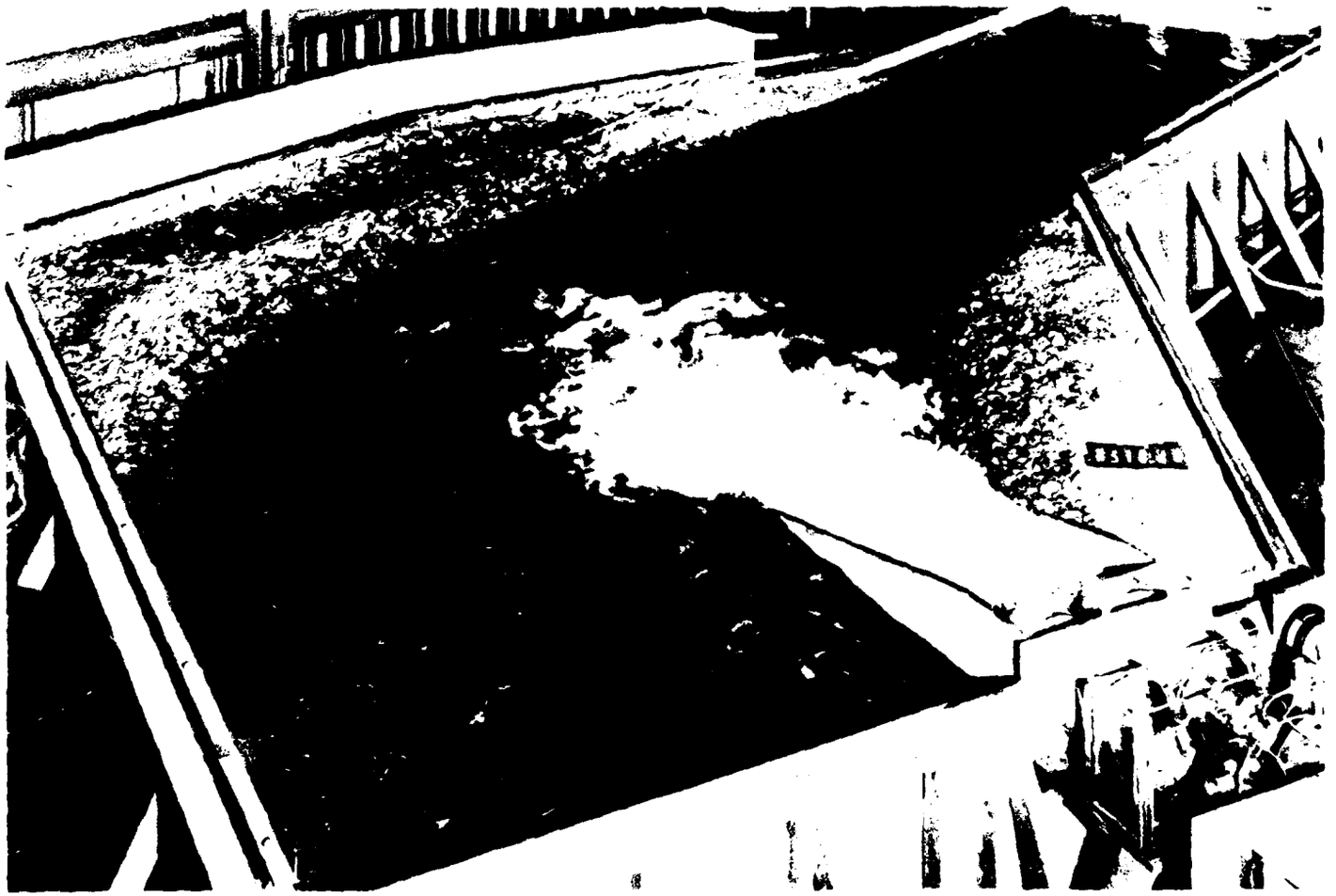

Photo 10. Recommended deflector plate design. Flow at pool el 1088, 28.1-in. sleeve travel, tailwater el 511

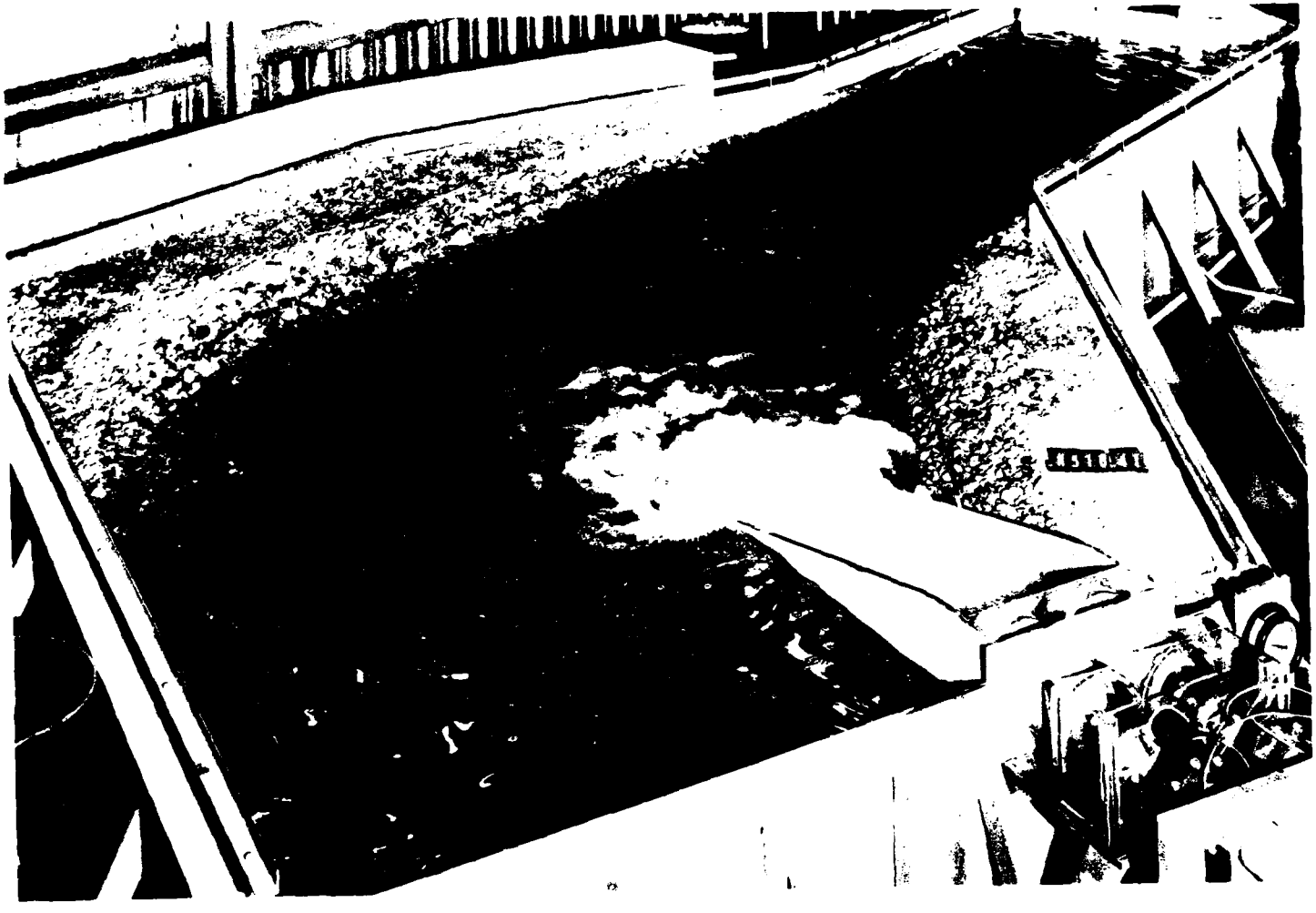

Photo 11. Recommended deflector plate design. Flow at pool el 800, 28.1-in. sleeve travel, tailwater el 511

Photo 12. Recommended deflector plate design. Side view of flow conditions in 1:12-scale model

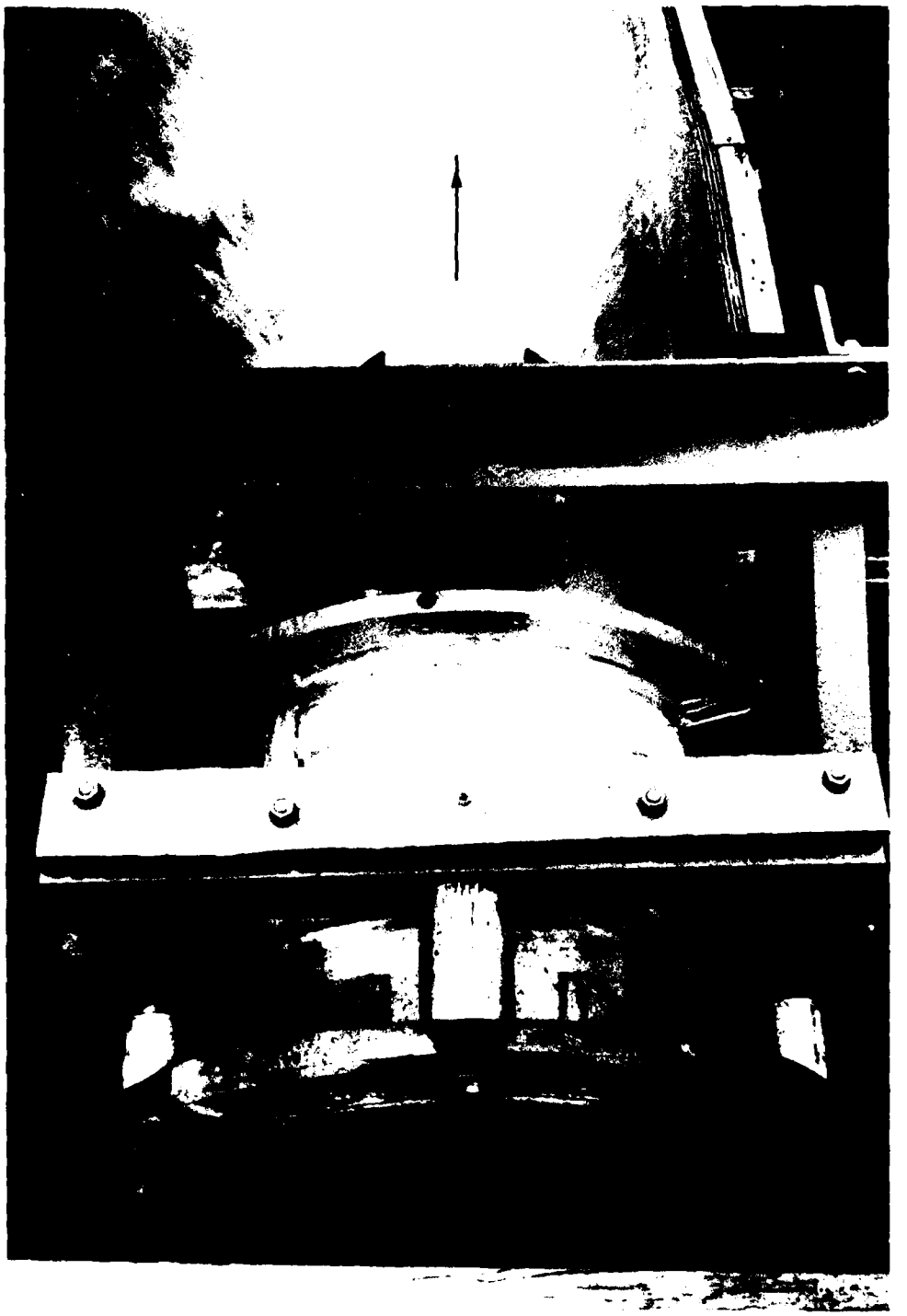

Photo 13. Recommended deflector plate design. Top view of flow conditions in 1:12-scale model

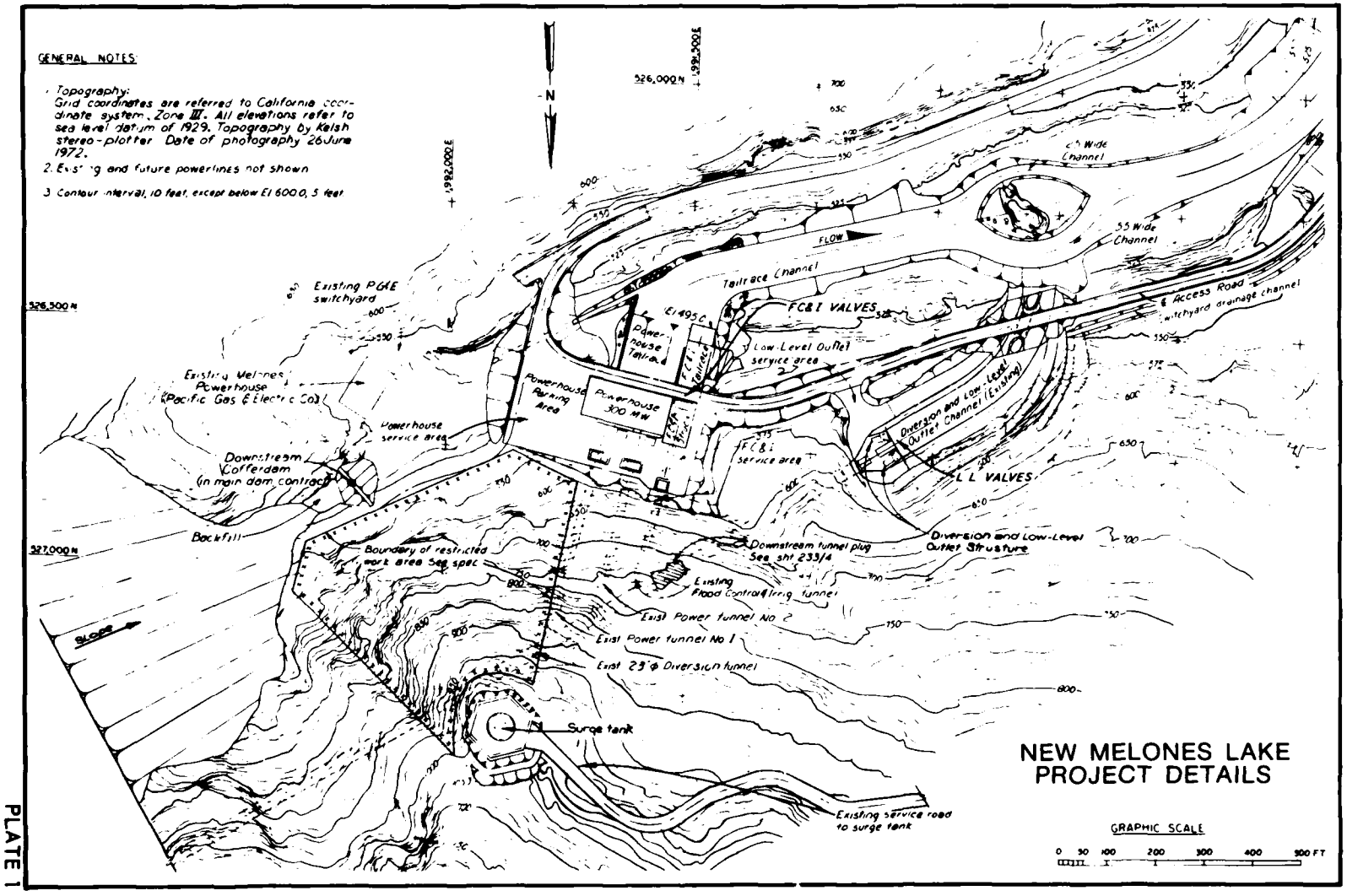
GENERAL NOTES
1. Topography:
Grid coordinates are referred to California coordinate system, Zone III. All elevations refer to sea level datum of 1929. Topography by Kelsh stereo-plotter. Date of photography 26 June 1972.
2. Existing and future powerlines not shown
3. Contour interval, 10 feet, except below El 600.0, 5 feet
N
526,000 N
1982,500 E
1982,000 E
526,500 N
527,000 N
Existing PG&E switchyard
Existing Melones Powerhouse (Pacific Gas & Electric Co.)
Powerhouse service area
Downstream Cofferdam (in main dam contract)
Backfill
Boundary of restricted work area See spec
Powerhouse Parking Area
Powerhouse 300 MW
F.C.B.I. service area
Tailrace Channel
El 495.0
Powerhouse Tailrace
F.C.B.I. Tailrace
F.C.B.I. VALVES
Low-Level Outlet service area
Diversion and Low-Level Outlet Channel (Existing)
L.L.V. VALVES
Diversion and Low-Level Outlet Structure
Downstream tunnel plug See sht 233/4
Existing Flood Control Irrig. tunnel
Exist Power tunnel No. 2
Exist Power tunnel No. 1
Exist 23'-0" Diversion tunnel
Surge tank
Existing service road to surge tank
FLOW
55 Wide Channel
& Access Road
switchyard drainage channel
NEW MELONES LAKE
PROJECT DETAILS
GRAPHIC SCALE
0 50 100 200 300 400 500 FT

PLATE 1

PLATE 2

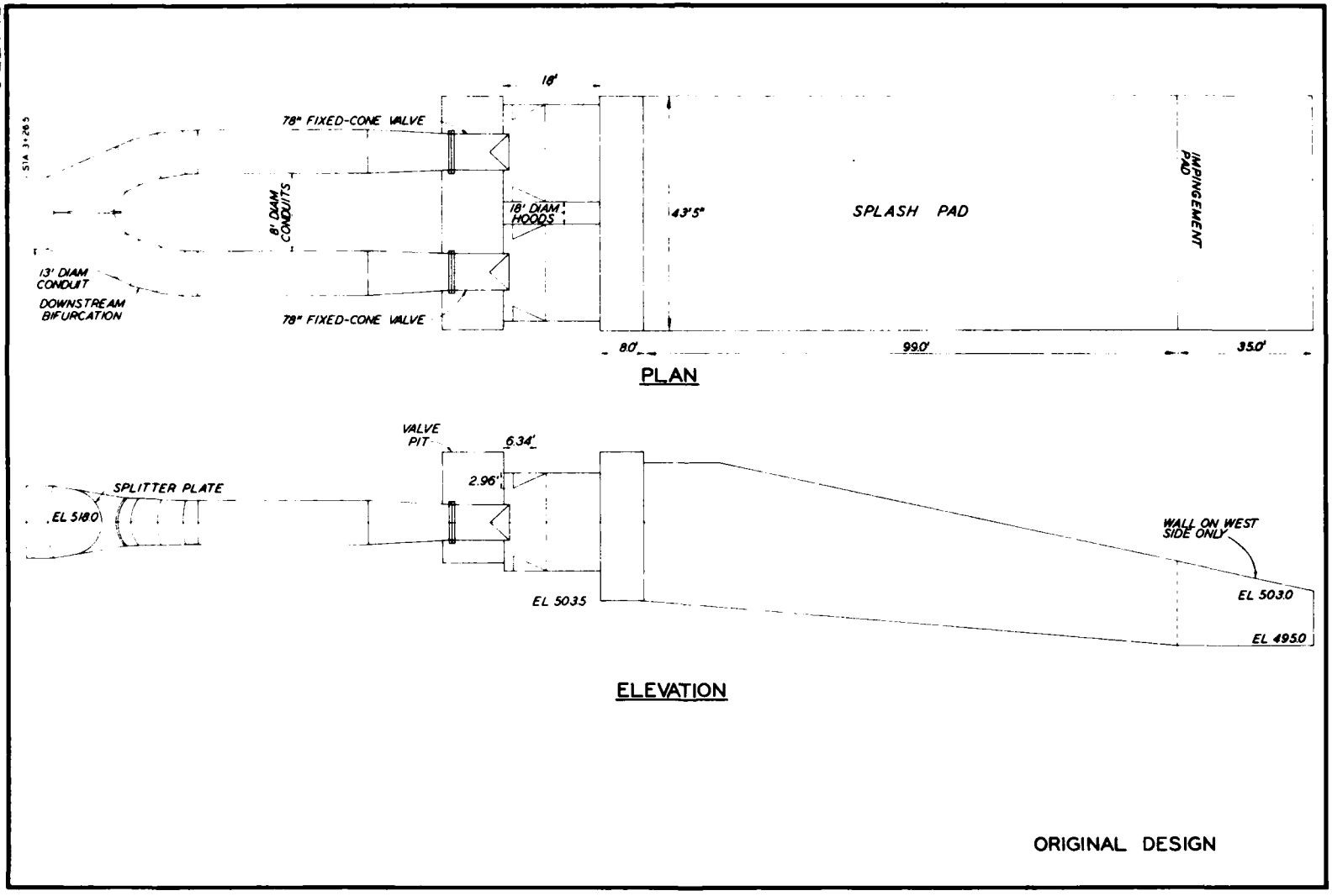
STA 3+28.5
78" FIXED-CONE VALVE
8' DIAM CONDUITS
18' DIAM HOODS
18'
43'5"
SPLASH PAD
IMPINGEMENT PAD
13' DIAM CONDUIT
DOWNSTREAM BIFURCATION
78" FIXED-CONE VALVE
8.0'
99.0'
35.0'
PLAN
VALVE PIT
6.34'
2.96'
SPLITTER PLATE
EL 5180
EL 5035
WALL ON WEST SIDE ONLY
EL 503.0
EL 495.0
ELEVATION
ORIGINAL DESIGN

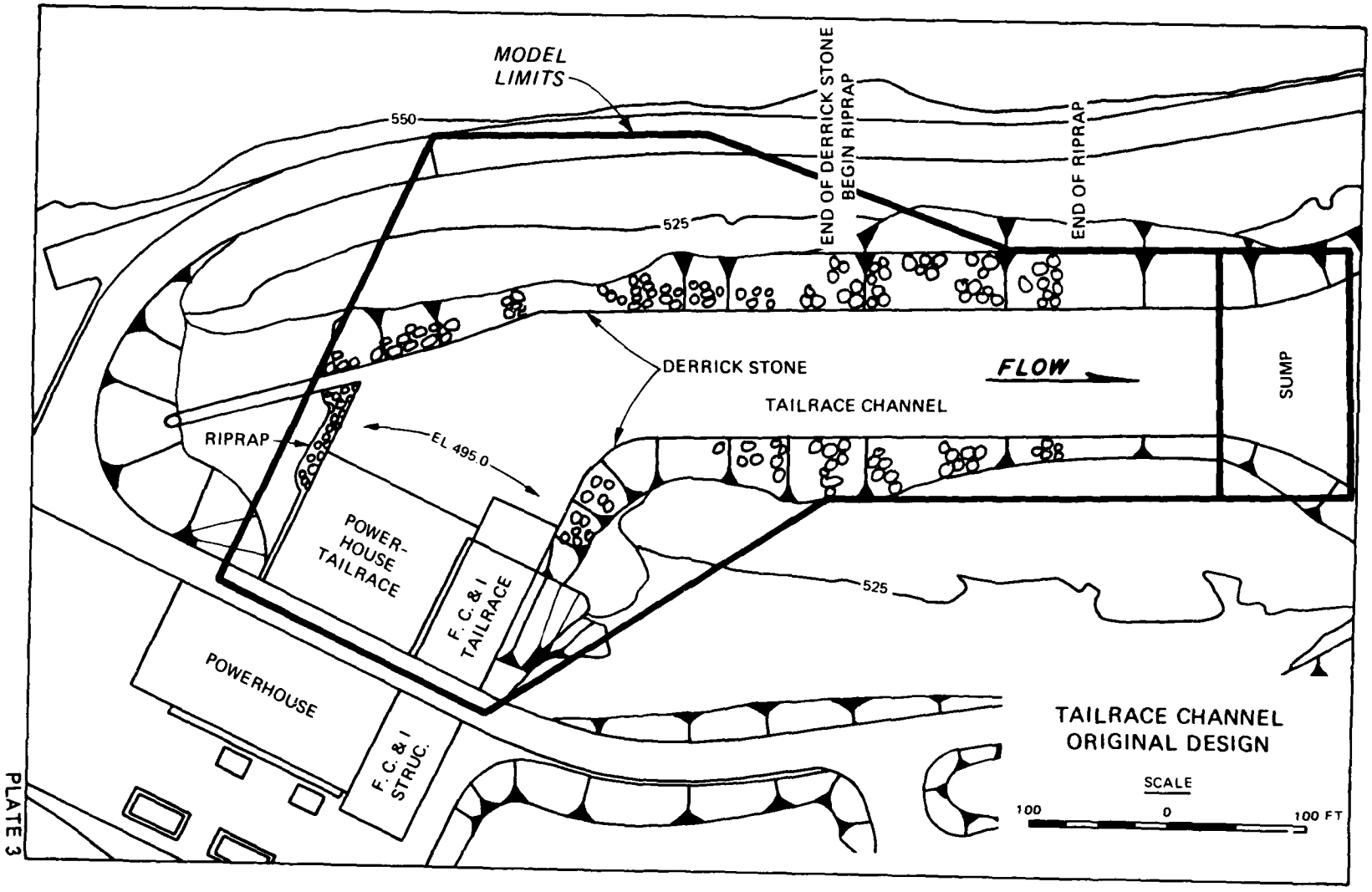
MODEL LIMITS
550
525
END OF DERRICK STONE
BEGIN RIPRAP
END OF RIPRAP
DERRICK STONE
FLOW
TAILRACE CHANNEL
SUMP
RIPRAP
EL 495.0
POWER-HOUSE TAILRACE
F.C.&I TAILRACE
525
POWERHOUSE
F.C.&I STRUC.
TAILRACE CHANNEL
ORIGINAL DESIGN
SCALE
100
0
100 FT
PLATE 3

PLATE 4

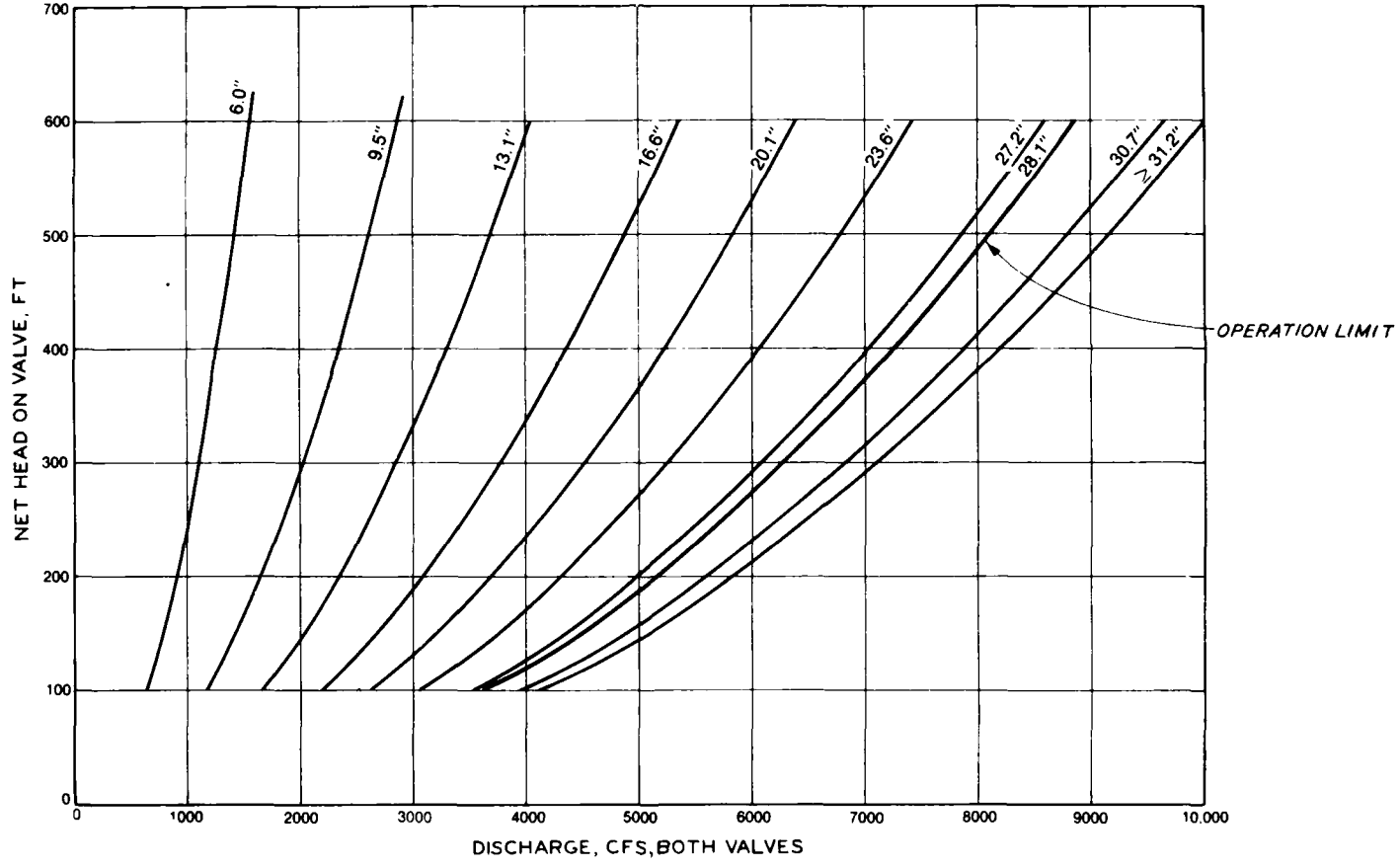

LEGEND

16.6-IN. SLEEVE TRAVEL

DISCHARGE RATING CURVE

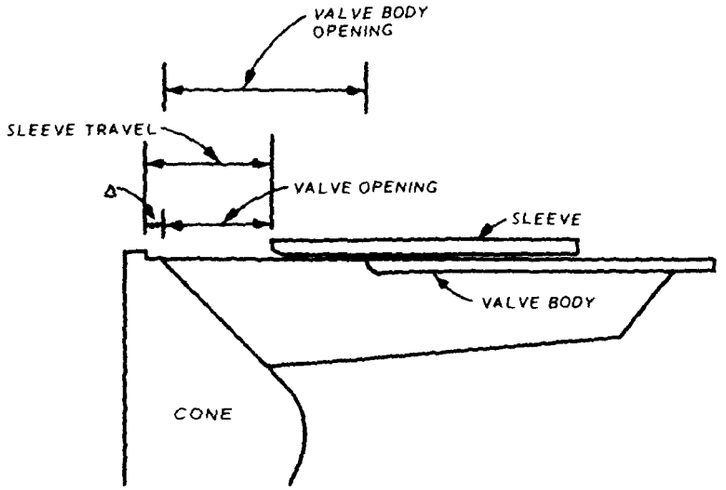

VALVE DIMENSIONS, IN.

VALVE DIAMETER	78
VALVE BODY OPENING	39.62
Δ	2.48

NOTE: DIMENSIONS FOR SLEEVE TRAVEL AND VALVE OPENING ARE VARIABLE.

PLATE 5

FIXED-CONE VALVE DIMENSIONS

PLATE 6

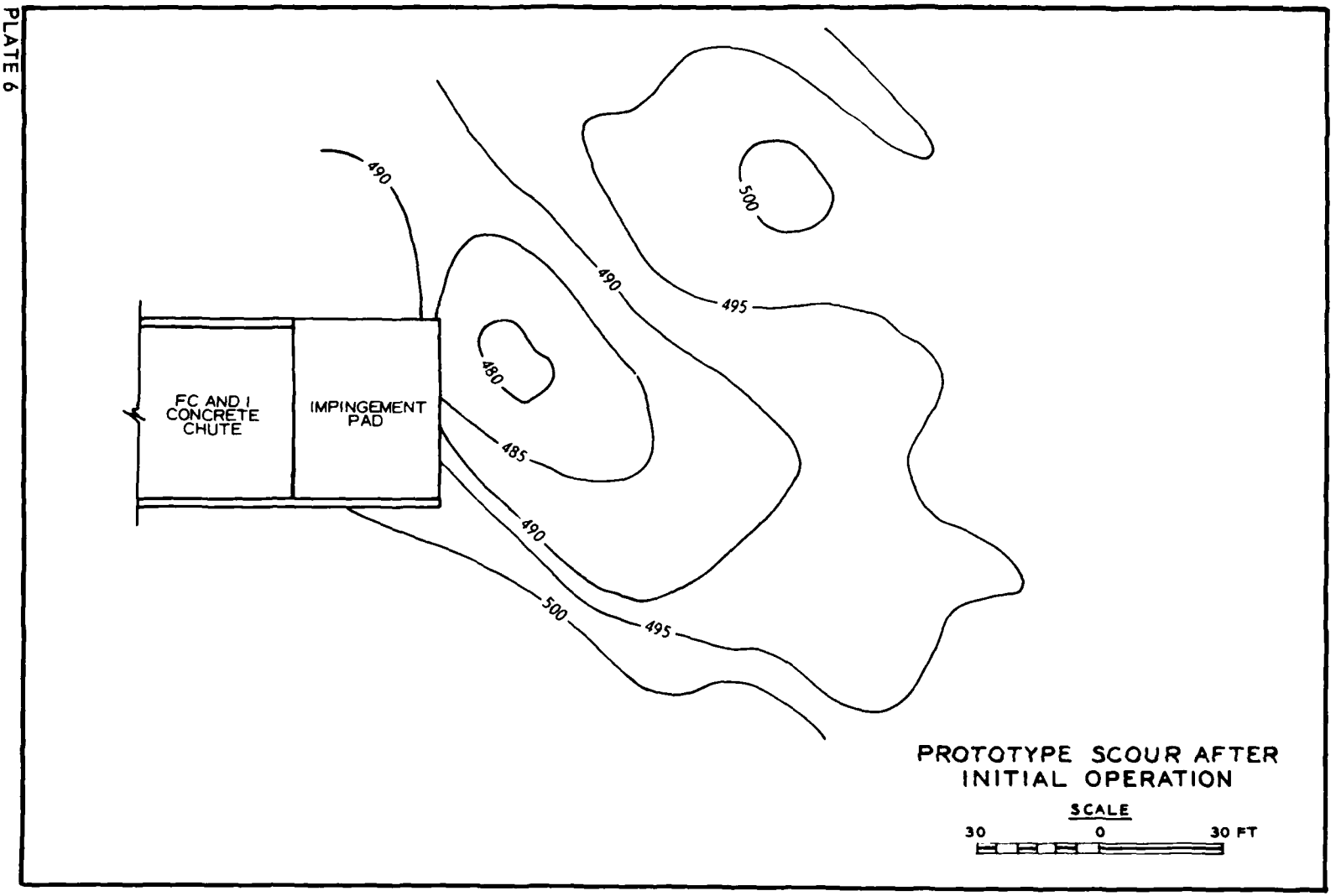
FC AND I CONCRETE CHUTE
IMPINGEMENT PAD
490
480
485
490
495
500
490
495
500
PROTOTYPE SCOUR AFTER INITIAL OPERATION
SCALE
30
0
30 FT

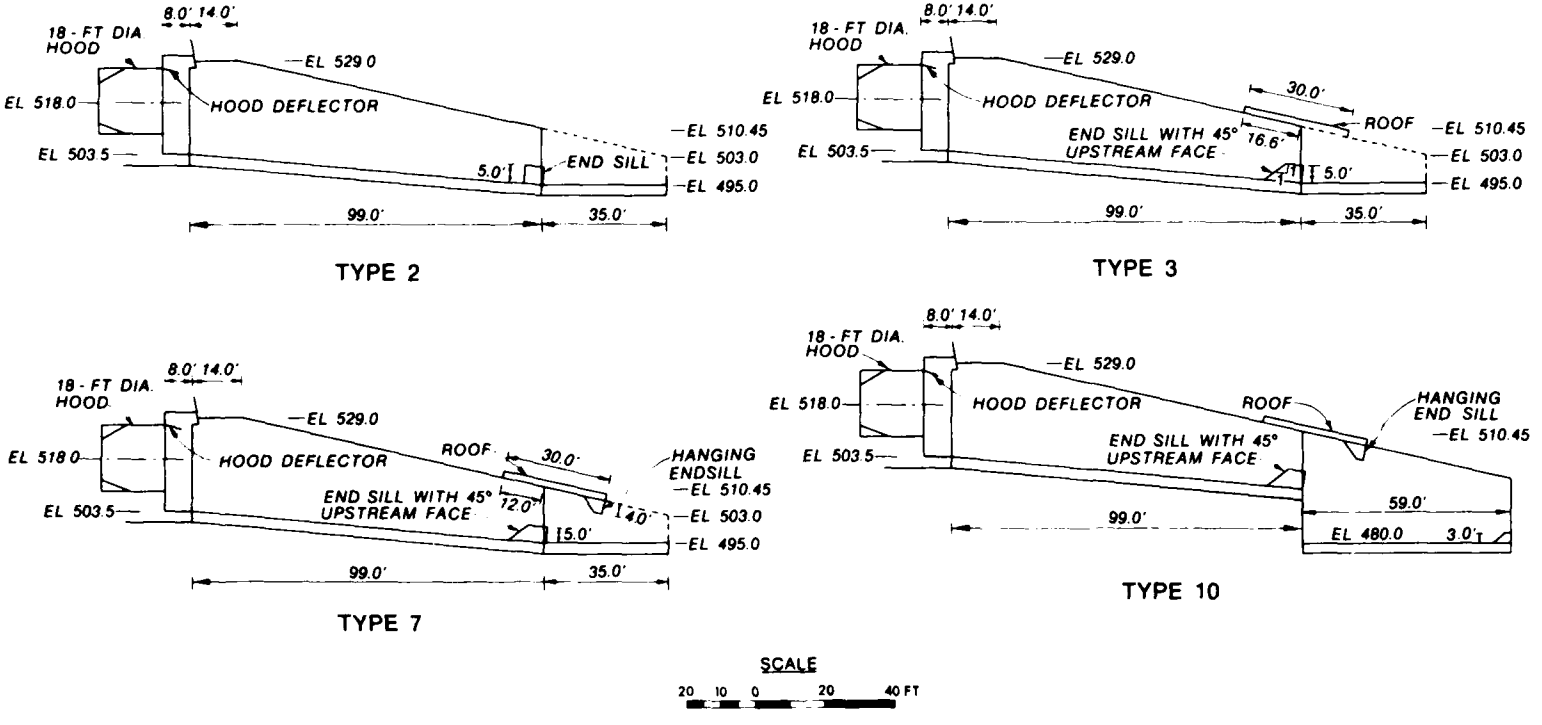

PLATE 7

TAILRACE AND IMPINGEMENT PAD
BASIN TYPES 2, 3, 7, AND 10

PLATE 8

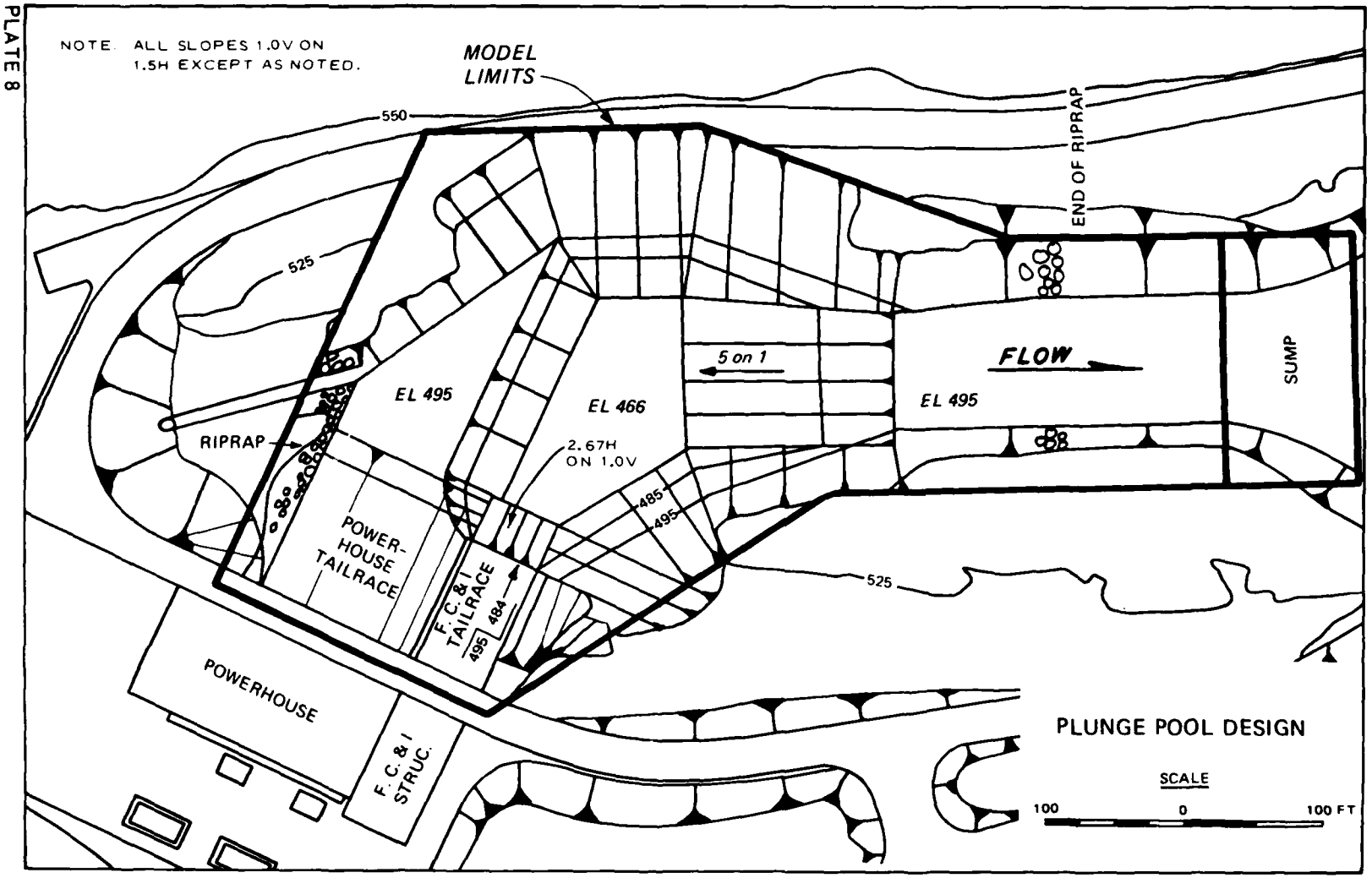
NOTE. ALL SLOPES 1.0V ON 1.5H EXCEPT AS NOTED.
MODEL LIMITS
550
END OF RIPRAP
525
5 on 1
FLOW
SUMP
EL 495
EL 466
EL 495
RIPRAP
2.67H ON 1.0V
485
495
POWER-HOUSE TAILRACE
F.C.&I TAILRACE
484
495
525
POWERHOUSE
F.C.&I STRUC.
PLUNGE POOL DESIGN
SCALE
100
0
100 FT

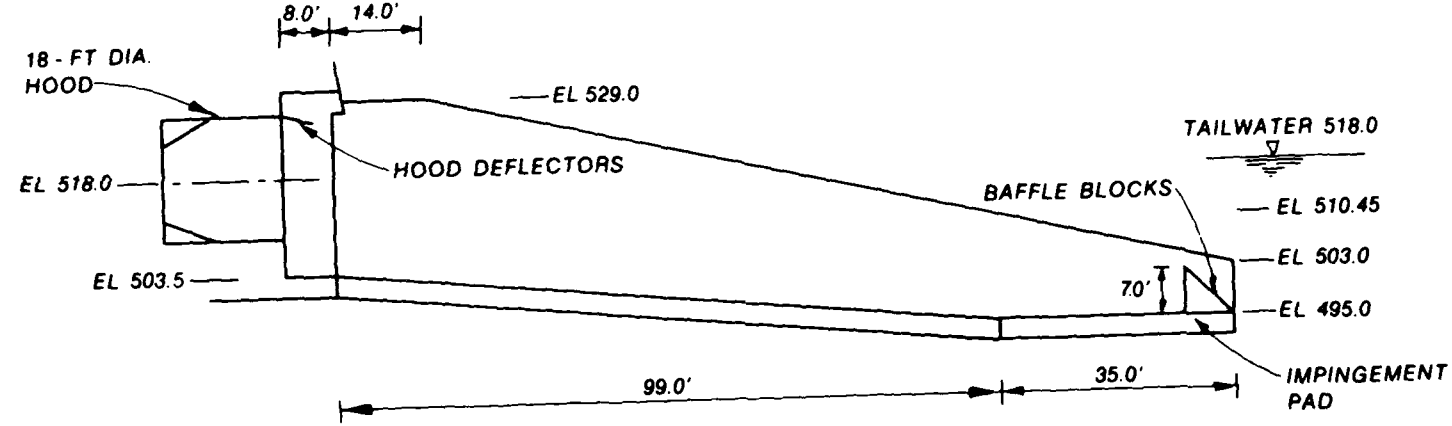

NOTE BAFFLE BLOCK 2' WIDE 1' SPACING
SIDEWALL ON BOTH SIDES OF
IMPINGEMENT PAD

SCALE

20 0 10 20 FT

TAILRACE AND IMPINGEMENT PAD TYPE 11 BASIN

PLATE 9

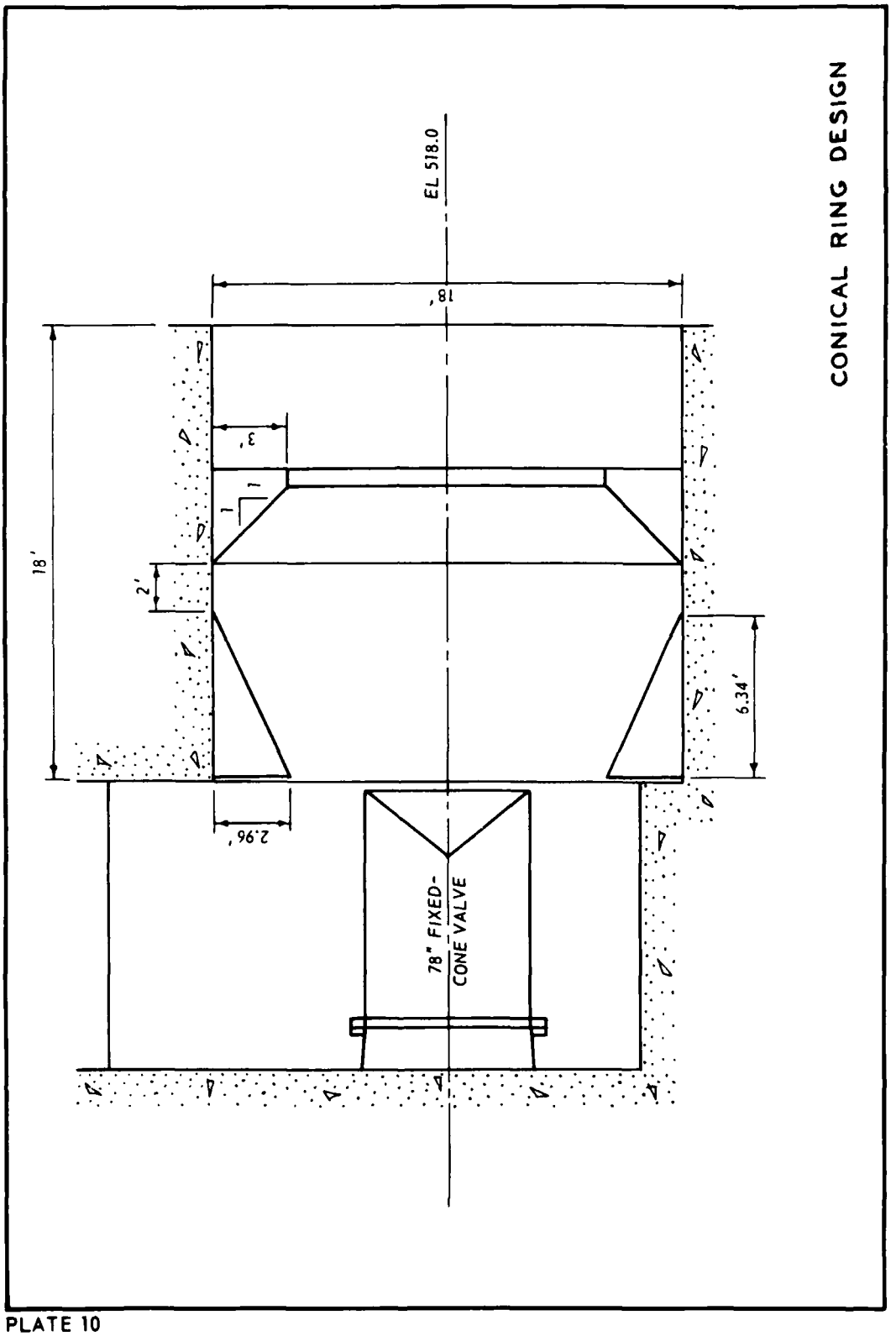
CONICAL RING DESIGN
EL 518.0
18'
3'
1
1
18'
2'
6.34'
2.96'
78" FIXED-
CONE VALVE

PLATE 10

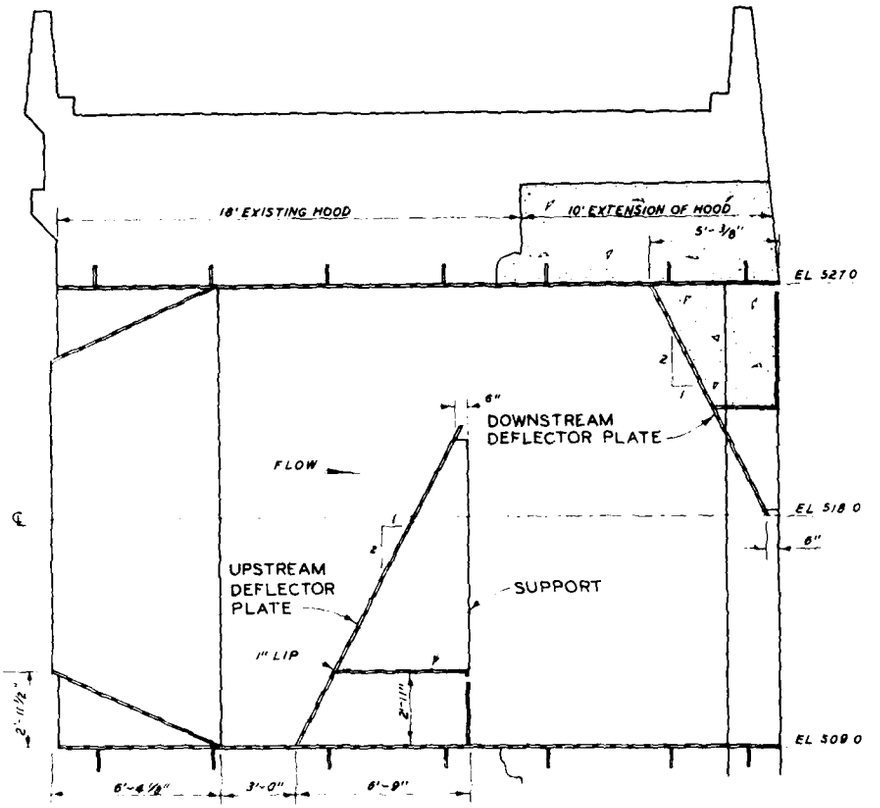

SECTION THROUGH CENTER OF HOOD

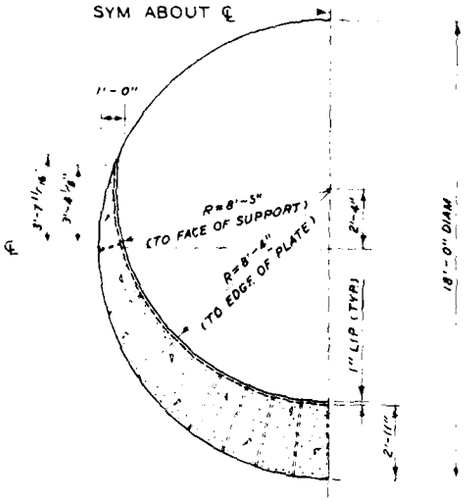

HALF SECTION
UPSTREAM PLATE

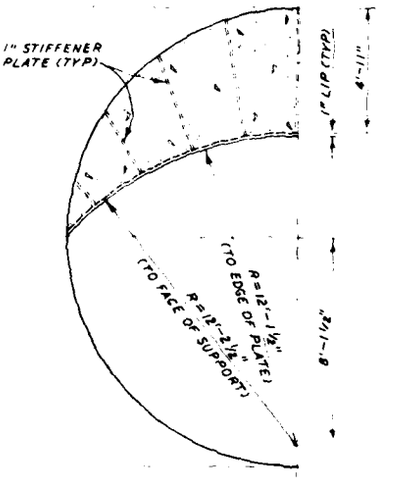

HALF SECTION
DOWNSTREAM PLATE

FINAL DEFLECTOR PLATE DETAILS

PLATE 11

PLATE 12

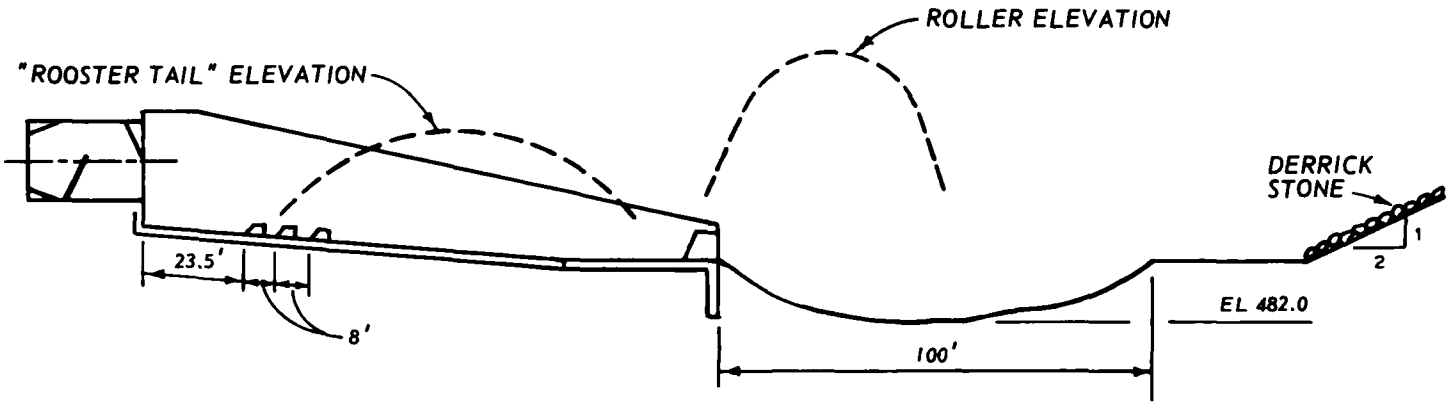

BAFFLE BLOCKS: 3 ROWS (11 BLOCKS – 1ST ROW, 10 BLOCKS – 2ND ROW, 11 BLOCKS – 3RD ROW)
1ST ROW 23.5' DOWNSTREAM OF HOOD
2' WIDE × 2' HIGH × 2' SPACING – 45° UPSTREAM FACE

SIDEWALL: SIDEWALL ADDED TO EAST SIDE OF IMPINGEMENT PAD

END SILL: 7' HIGH, 8' WIDE AT BOTTOM, 5' WIDE AT TOP

ROOSTER TAIL ELEVATION: 528 AT POOL EL 1088, 28.1-IN. SLEEVE TRAVEL
525 AT POOL EL 1048, 28.1-IN. SLEEVE TRAVEL

ROLLER ELEVATION: 528 AT POOL EL 1088, 28.1-IN. SLEEVE TRAVEL
542 AT POOL EL 1048, 28.1-IN. SLEEVE TRAVEL (HIGHER THAN AT POOL EL 1088 BECAUSE TAILWATER AT POOL EL 1048 IS LOWER AND DOES NOT AFFECT HEIGHT OF ROLLER)

SCOUR HOLE: BOTTOM EL 482.0, LENGTH 100', WIDTH 80'

TAILRACE DESIGN DETAILS
DEFLECTOR PLATE DESIGN

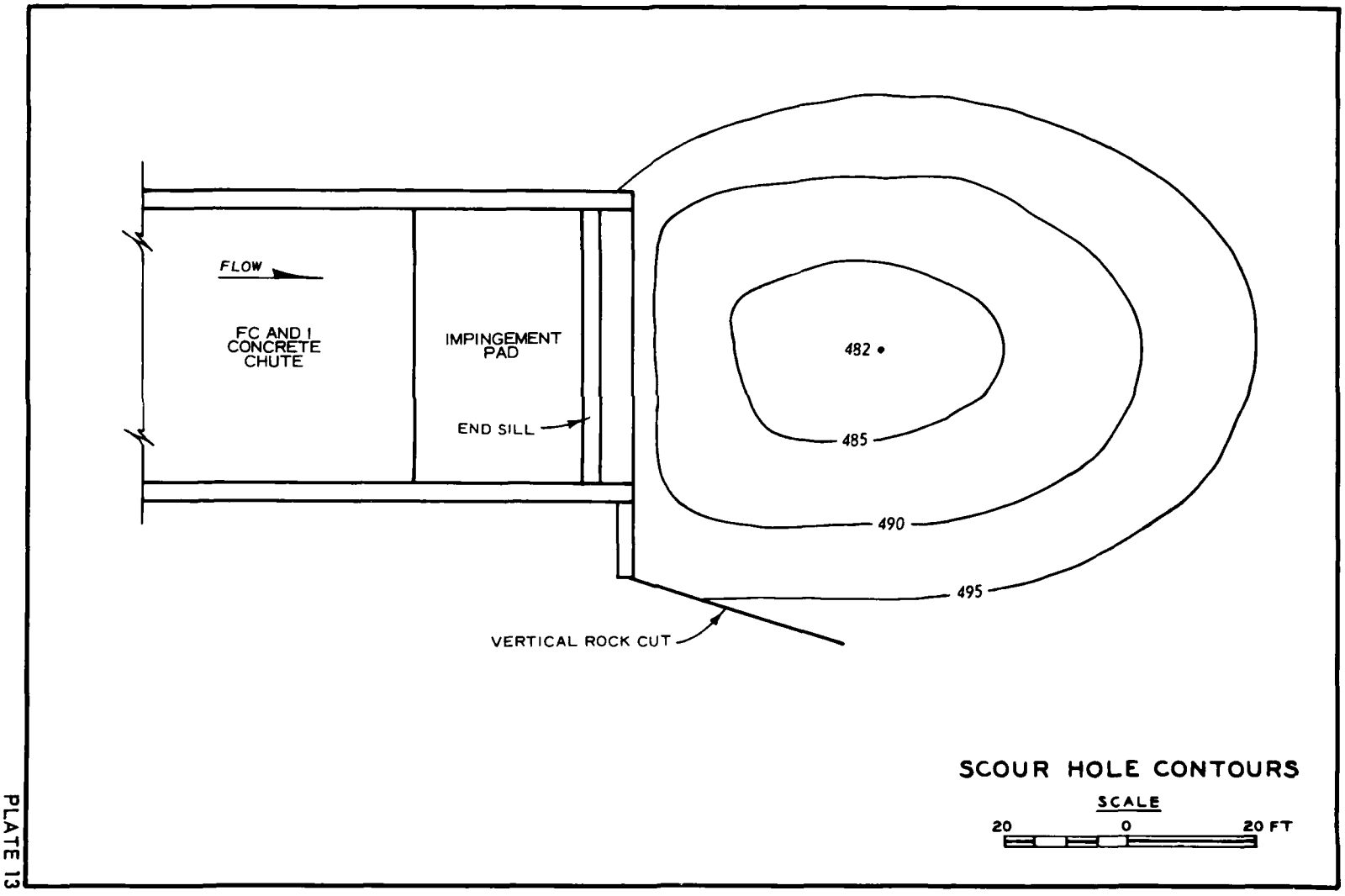
FLOW
FC AND I CONCRETE CHUTE
IMPINGEMENT PAD
END SILL
482
485
490
495
VERTICAL ROCK CUT
SCOUR HOLE CONTOURS
SCALE
20 0 20 FT

PLATE 13

PLATE 14

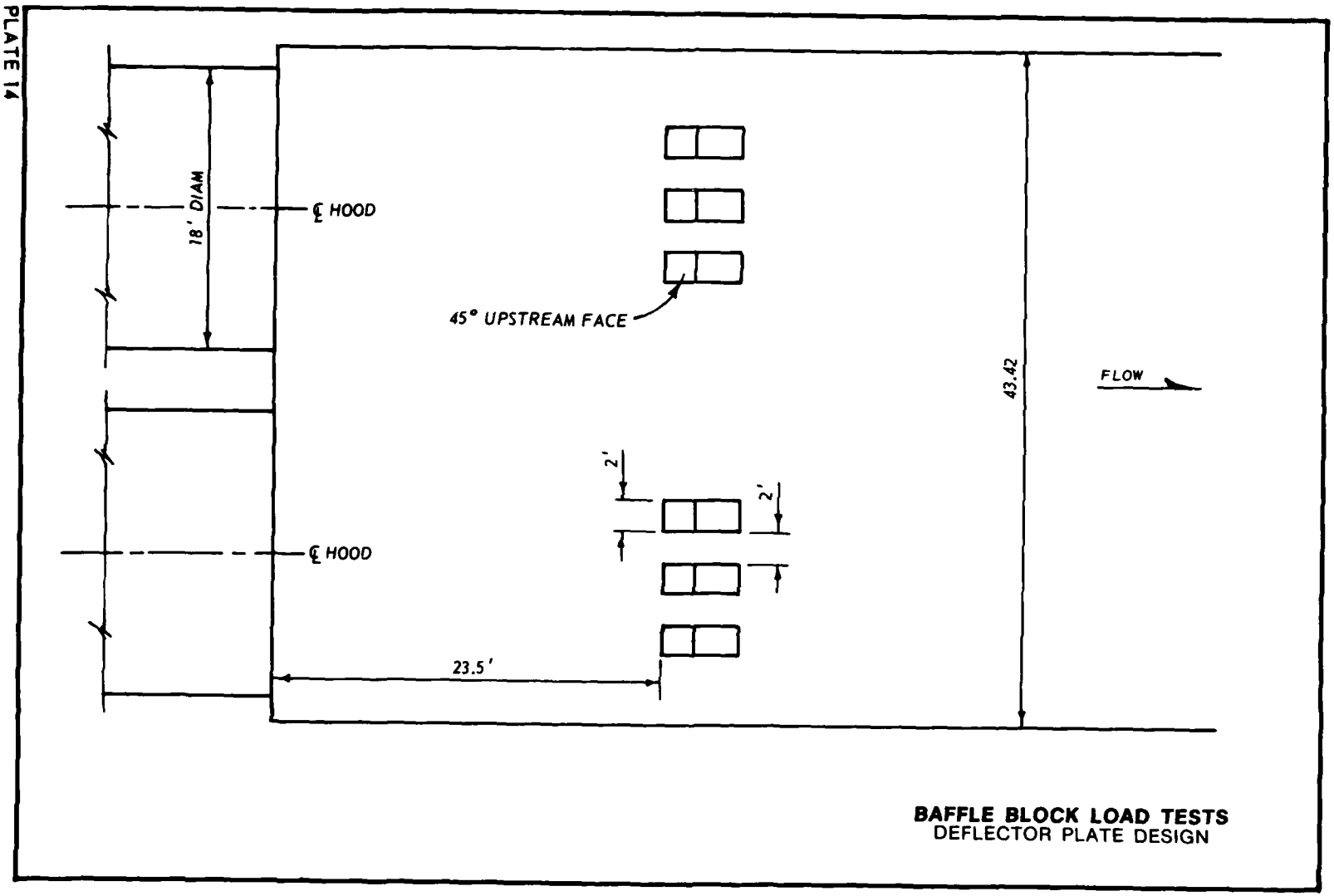

BAFFLE BLOCK LOAD TESTS
DEFLECTOR PLATE DESIGN

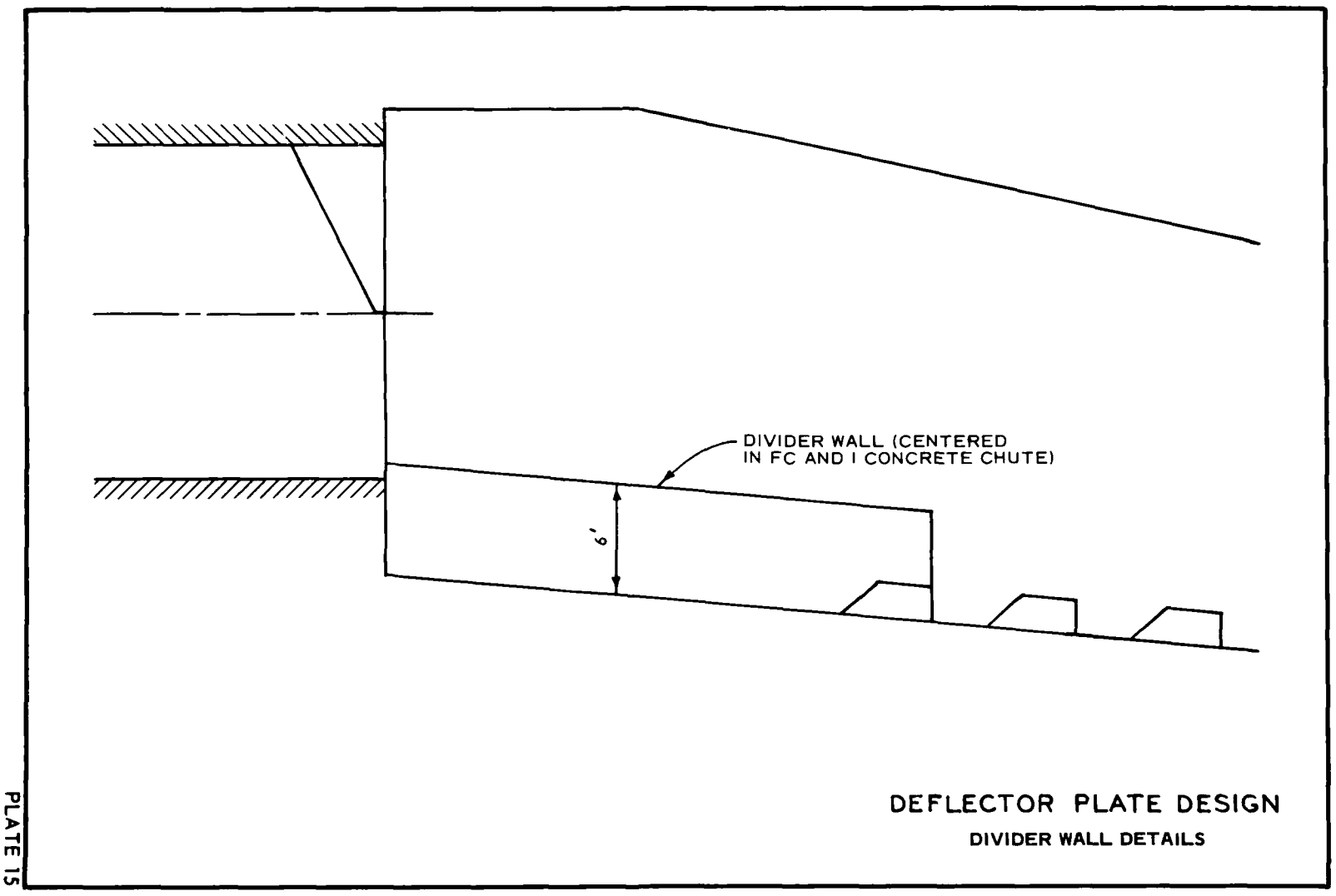

PLATE 15

DEFLECTOR PLATE DESIGN

DIVIDER WALL DETAILS

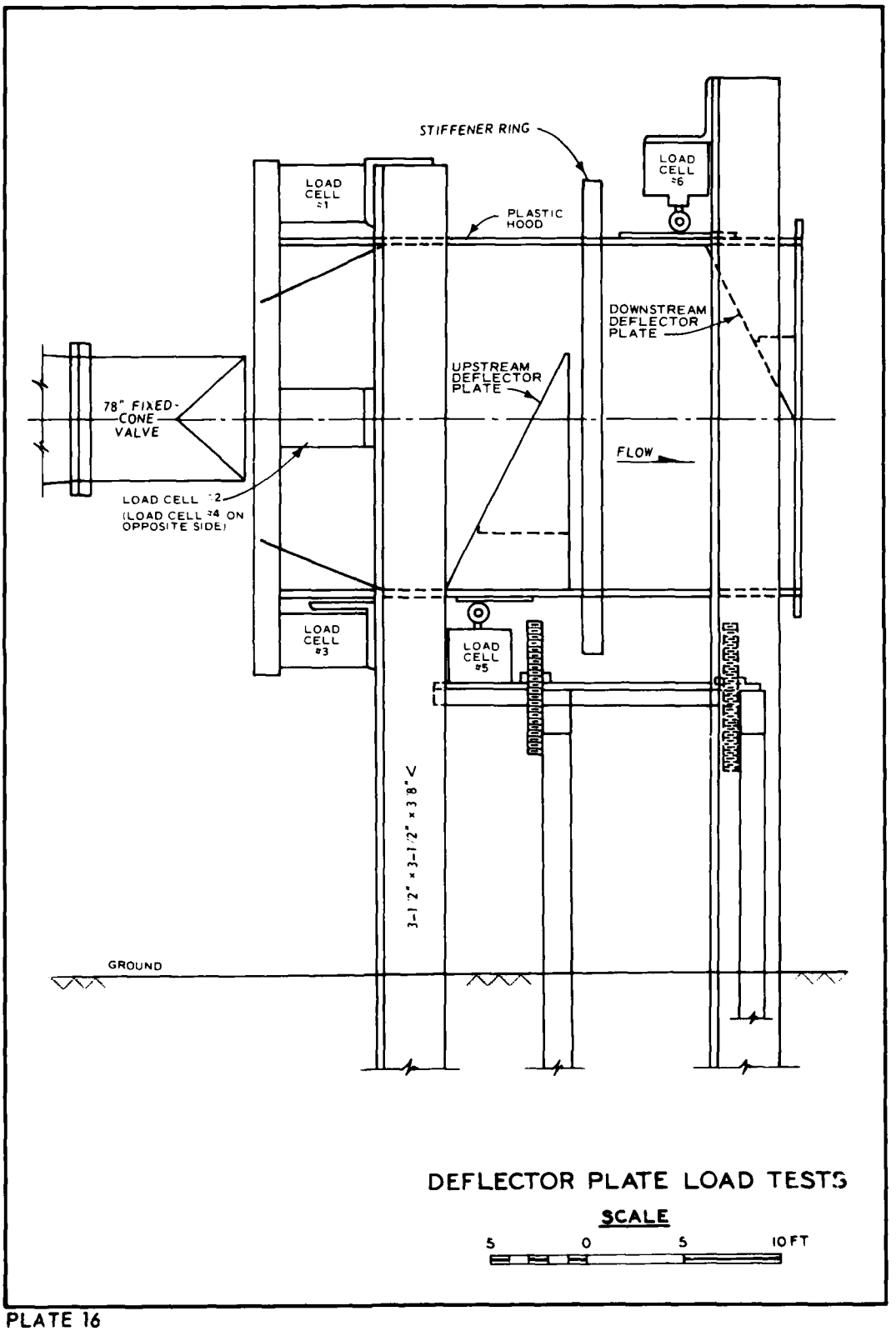
STIFFENER RING
LOAD CELL #6
LOAD CELL #1
PLASTIC HOOD
DOWNSTREAM DEFLECTOR PLATE
UPSTREAM DEFLECTOR PLATE
78" FIXED-CONE VALVE
FLOW
LOAD CELL #2
(LOAD CELL #4 ON OPPOSITE SIDE)
LOAD CELL #3
LOAD CELL #5
3-1'2" x 3-1/2" x 3'8" V
GROUND
DEFLECTOR PLATE LOAD TESTS
SCALE
5 0 5 10 FT

PLATE 16

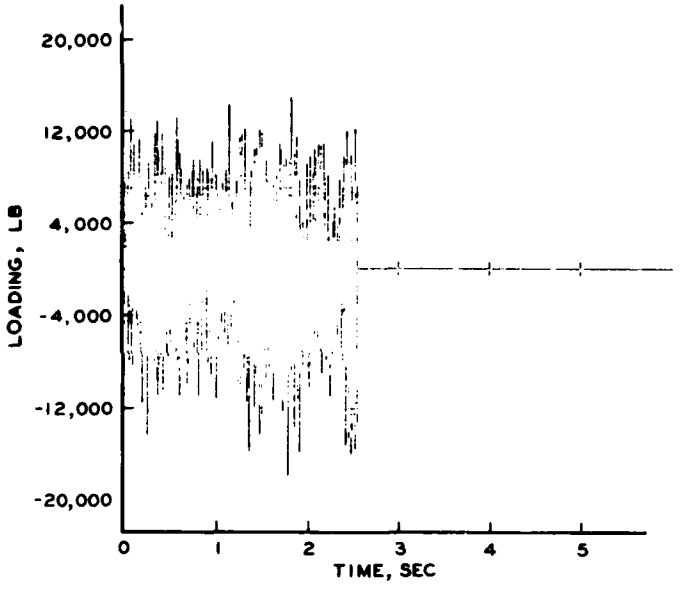

TIME-HISTORY

MEAN LOADING = -11,906 LB

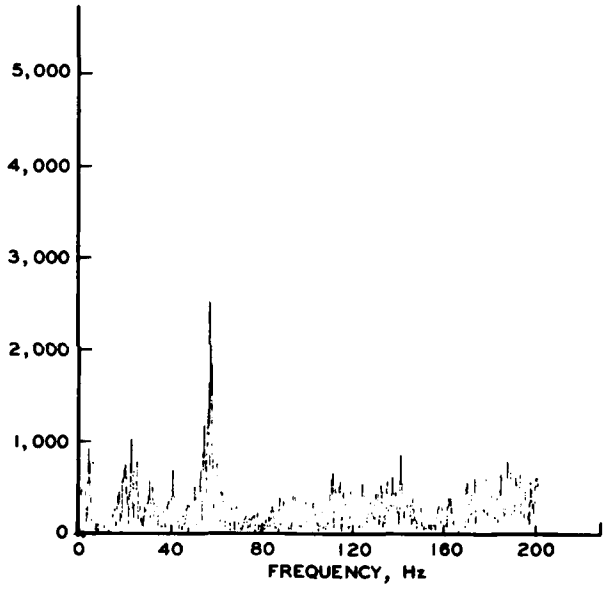

AMPLITUDE SPECTRUM

POOL EL 1088
SLEEVE TRAVEL . . . 28.1 IN.

LOAD CELLS 1-4: (-) LOAD UPSTREAM
(+) LOAD DOWNSTREAM
LOAD CELLS 5-6: (+) LOAD UPWARD
(-) LOAD DOWNWARD

DEFLECTOR PLATE DESIGN
LOADING WITHOUT DEFLECTOR PLATES
LOAD CELL 1

PLATE 17

PLATE 18

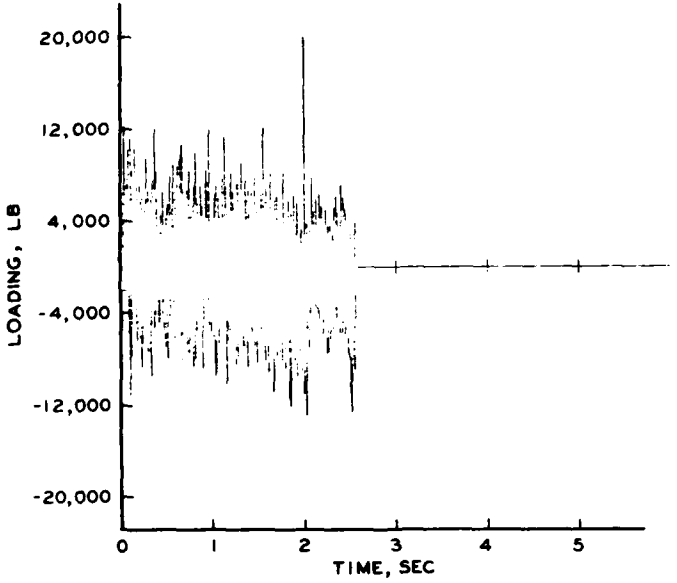

TIME-HISTORY

MEAN LOADING = -18,009 LB

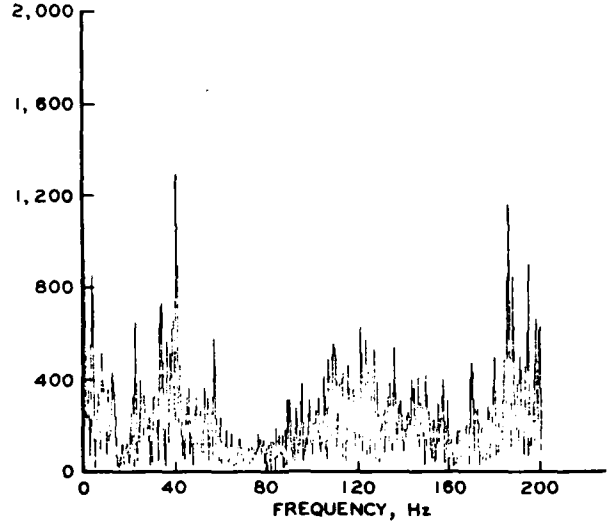

AMPLITUDE SPECTRUM

POOL EL 1088
SLEEVE TRAVEL . . . 28.1 IN.
LOAD CELLS 1-4: (-) LOAD UPSTREAM
(+) LOAD DOWNSTREAM
LOAD CELLS 5-6: (+) LOAD UPWARD
(-) LOAD DOWNWARD

DEFLECTOR PLATE DESIGN
LOADING WITHOUT DEFLECTOR PLATES
LOAD CELL 2

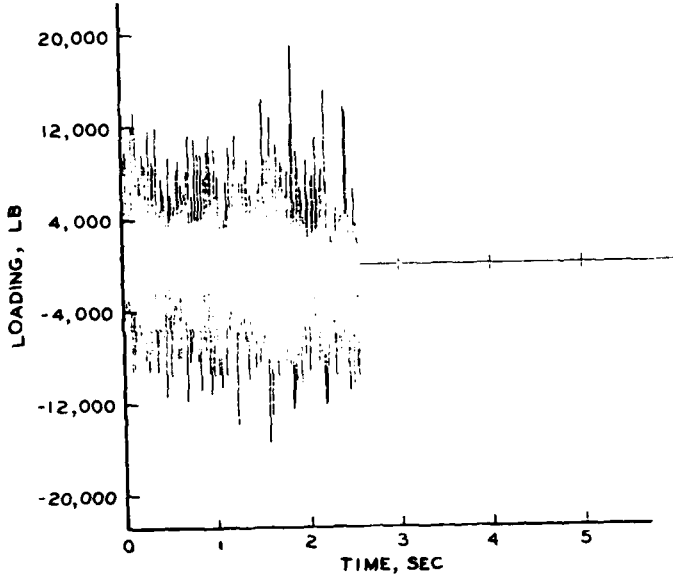

TIME-HISTORY

MEAN LOADING = -15,509 LB

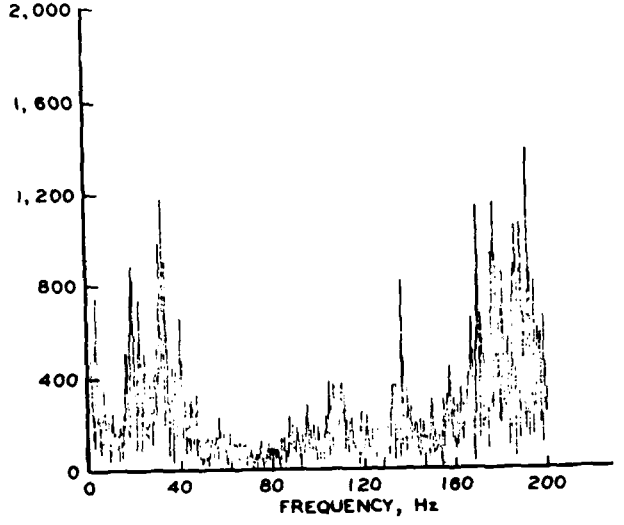

AMPLITUDE SPECTRUM

POOL EL 1088
SLEEVE TRAVEL . . . 28.1 IN.
LOAD CELLS 1-4: (-) LOAD UPSTREAM
(+) LOAD DOWNSTREAM
LOAD CELLS 5-6: (+) LOAD UPWARD
(-) LOAD DOWNWARD

DEFLECTOR PLATE DESIGN
LOADING WITHOUT DEFLECTOR PLATES
LOAD CELL 3

PLATE 19

PLATE 20

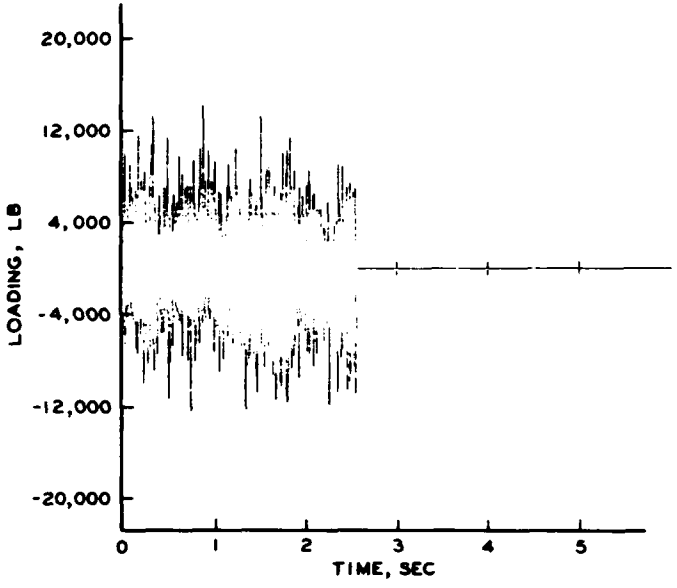

TIME-HISTORY

MEAN LOADING = -10,965 LB

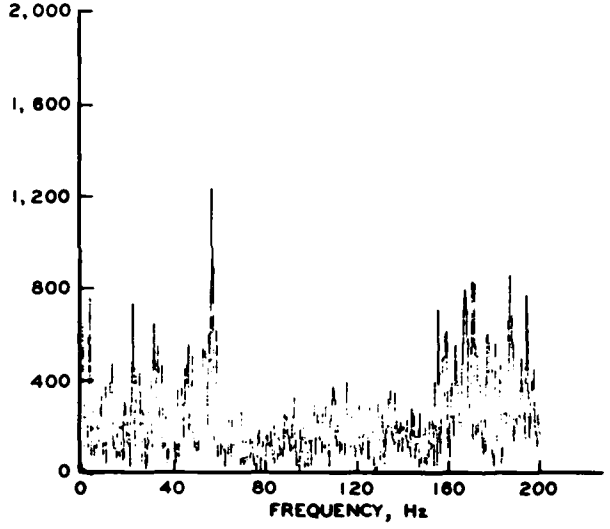

AMPLITUDE SPECTRUM

POOL EL 1088
SLEEVE TRAVEL . . . 28.1 IN.

LOAD CELLS 1-4: (-) LOAD UPSTREAM
(+) LOAD DOWNSTREAM
LOAD CELLS 5-6: (+) LOAD UPWARD
(-) LOAD DOWNWARD

DEFLECTOR PLATE DESIGN
LOADING WITHOUT DEFLECTOR PLATES
LOAD CELL 4

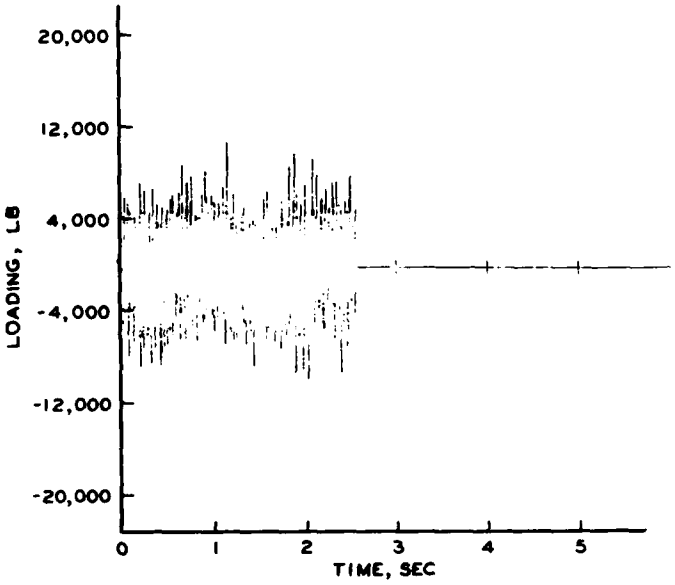

TIME-HISTORY

MEAN LOADING = 7,672 LB

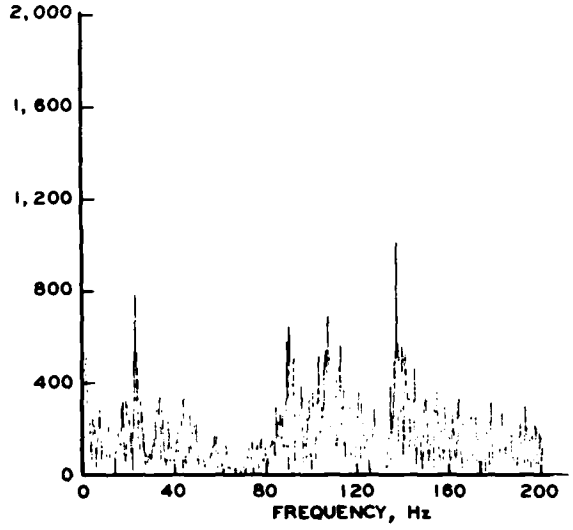

AMPLITUDE SPECTRUM

POOL EL 1088
SLEEVE TRAVEL . . . 28.1 IN.

LOAD CELLS 1-4: (-) LOAD UPSTREAM
(+) LOAD DOWNSTREAM
LOAD CELLS 5-6: (+) LOAD UPWARD
(-) LOAD DOWNWARD

DEFLECTOR PLATE DESIGN
LOADING WITHOUT DEFLECTOR PLATES
LOAD CELL 5

PLATE 21

PLATE 22

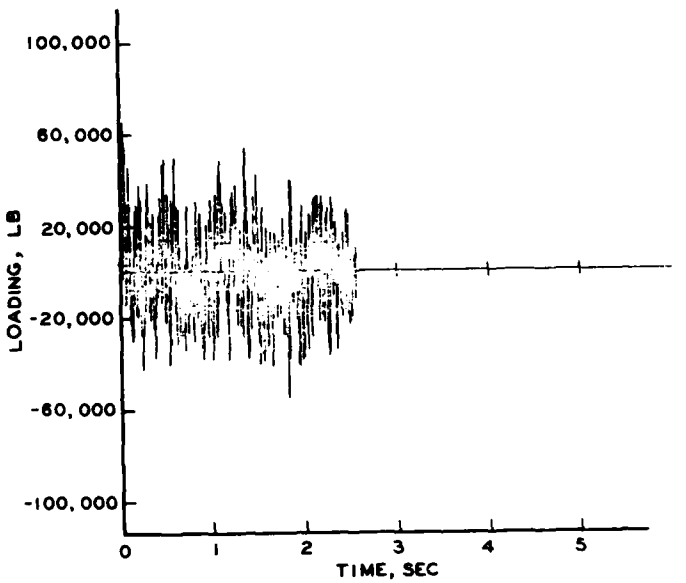

TIME-HISTORY

MEAN LOADING = -80,300 LB

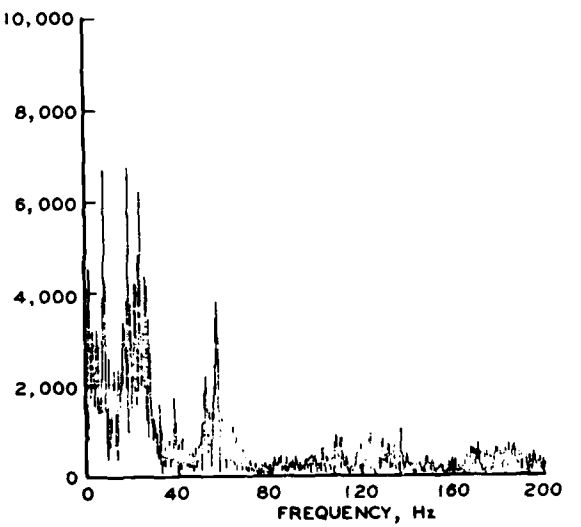

AMPLITUDE SPECTRUM

POOL EL 1088
SLEEVE TRAVEL . . . 28.1 IN.
LOAD CELLS 1-4: (-) LOAD UPSTREAM
(+) LOAD DOWNSTREAM
LOAD CELLS 5-6: (+) LOAD UPWARD
(-) LOAD DOWNWARD

DEFLECTOR PLATE DESIGN
LOADING WITH UPSTREAM DEFLECTOR PLATE
LOAD CELL 1

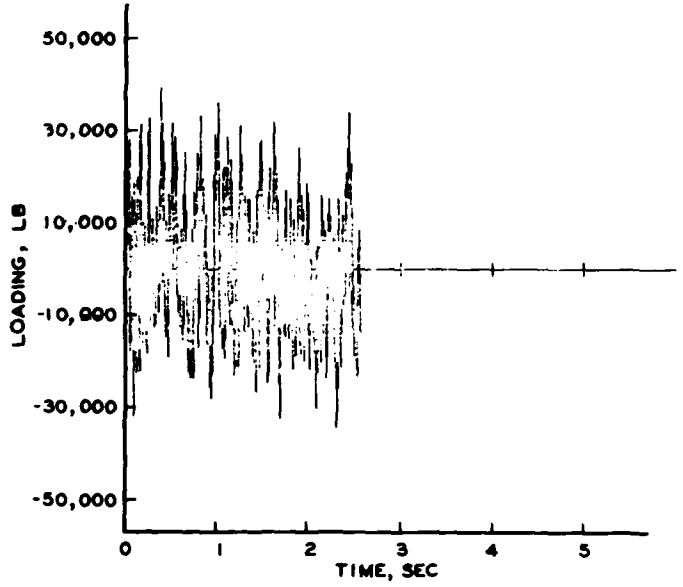

TIME-HISTORY

MEAN LOADING = 102,361 LB

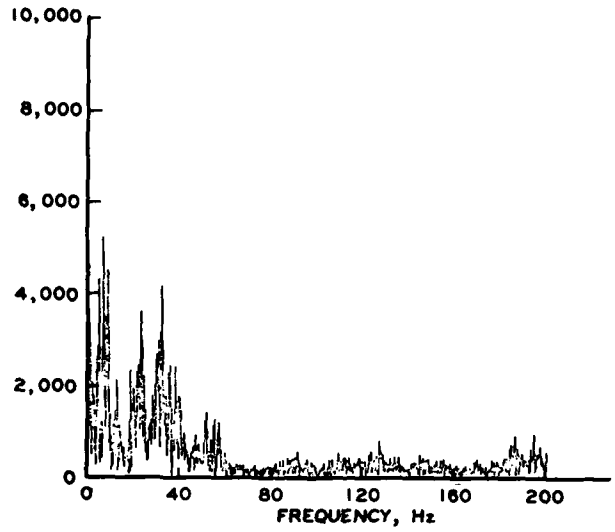

AMPLITUDE SPECTRUM

POOL EL 1088
SLEEVE TRAVEL . . . 28.1 IN.
LOAD CELLS 1-4: (-) LOAD UPSTREAM
(+) LOAD DOWNSTREAM
LOAD CELLS 5-6: (+) LOAD UPWARD
(-) LOAD DOWNWARD

DEFLECTOR PLATE DESIGN
LOADING WITH UPSTREAM DEFLECTOR PLATE
LOAD CELL 2

PLATE 23

PLATE 24

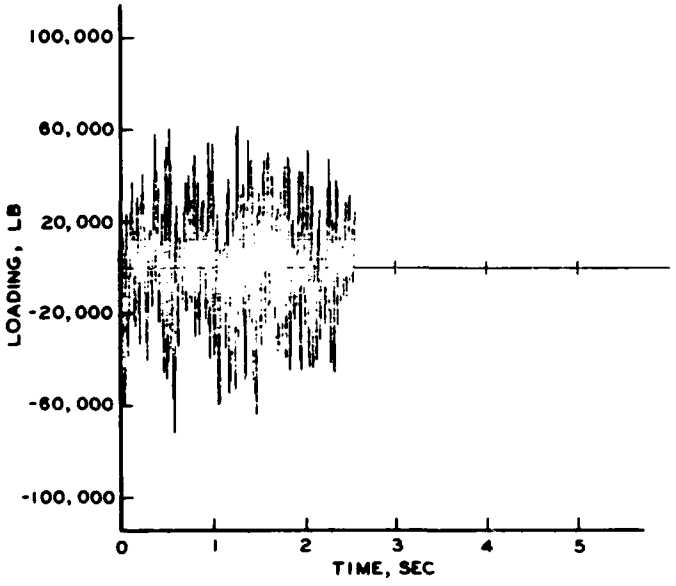

TIME-HISTORY

MEAN LOADING = 226,973 LB

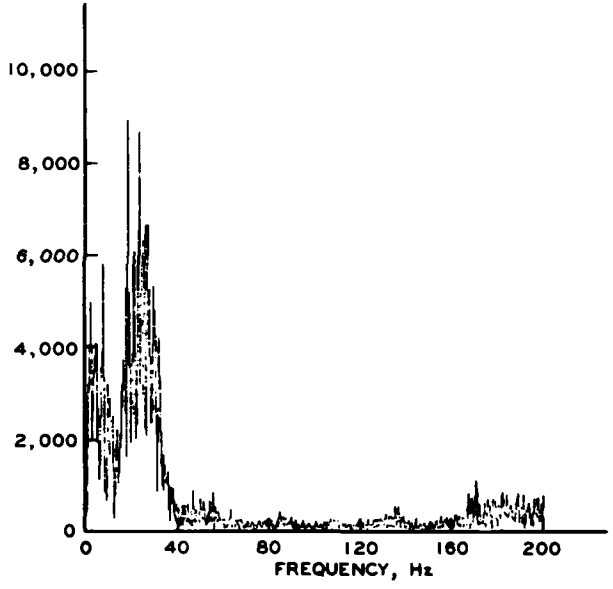

AMPLITUDE SPECTRUM

POOL EL 1088
SLEEVE TRAVEL . . . 28.1 IN.

LOAD CELLS 1-4: (-) LOAD UPSTREAM
(+) LOAD DOWNSTREAM
LOAD CELLS 5-6: (+) LOAD UPWARD
(-) LOAD DOWNWARD

DEFLECTOR PLATE DESIGN
LOADING WITH UPSTREAM DEFLECTOR PLATE
LOAD CELL 3

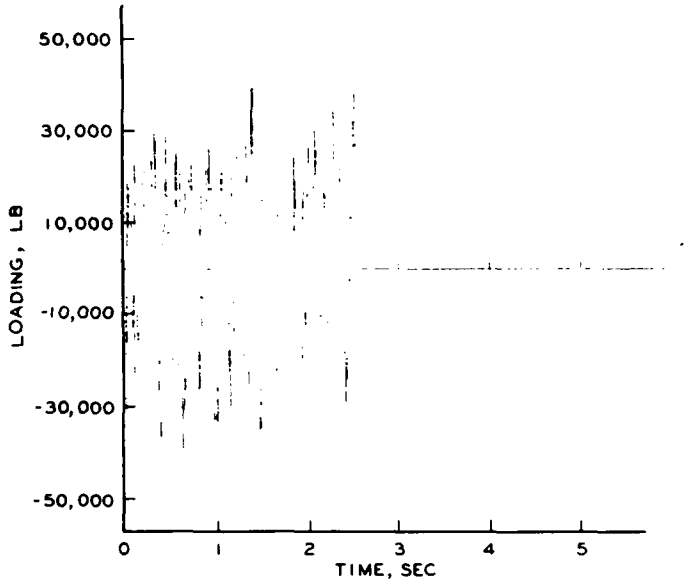

TIME-HISTORY

MEAN LOADING = 120,074 LB

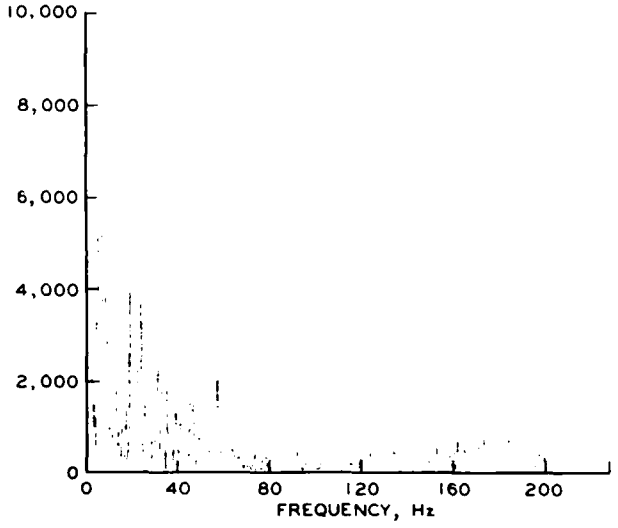

AMPLITUDE SPECTRUM

POOL EL 1088
SLEEVE TRAVEL . . . 28.1 IN.

LOAD CELLS 1-4: (-) LOAD UPSTREAM
(+) LOAD DOWNSTREAM
LOAD CELLS 5-6: (+) LOAD UPWARD
(-) LOAD DOWNWARD

DEFLECTOR PLATE DESIGN
LOADING WITH UPSTREAM DEFLECTOR PLATE
LOAD CELL 4

PLATE 25

PLATE 26

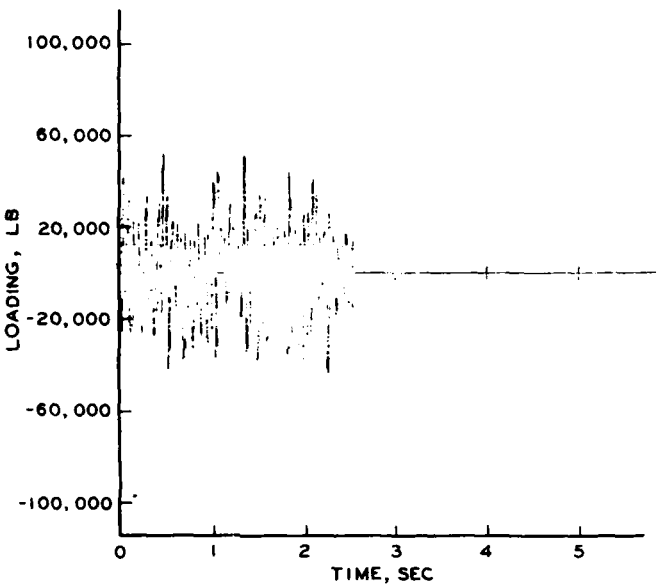

TIME-HISTORY

MEAN LOADING = -60,403 LB

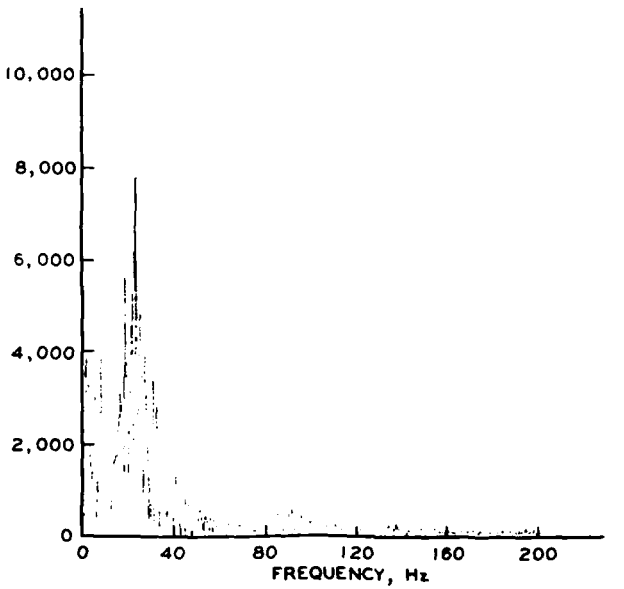

AMPLITUDE SPECTRUM

POOL EL 1088
SLEEVE TRAVEL . . . 28.1 IN.

LOAD CELLS 1-4: (-) LOAD UPSTREAM
(+) LOAD DOWNSTREAM
LOAD CELLS 5-6: (+) LOAD UPWARD
(-) LOAD DOWNWARD

DEFLECTOR PLATE DESIGN
LOADING WITH UPSTREAM DEFLECTOR PLATE
LOAD CELL 5

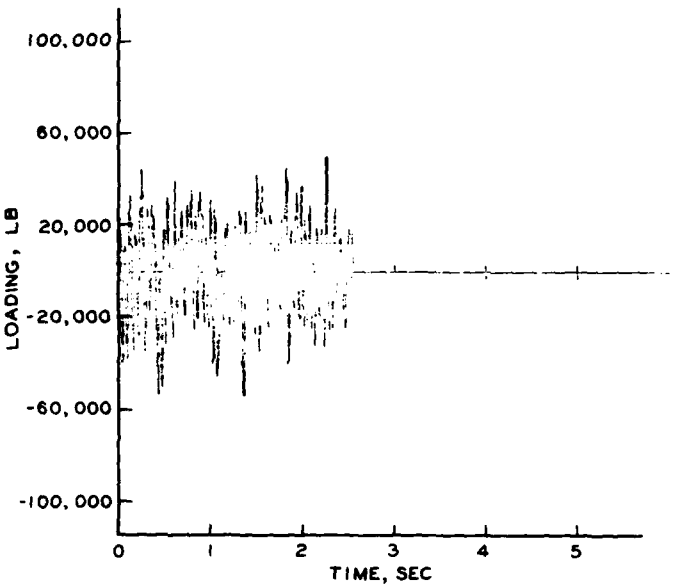

TIME-HISTORY

MEAN LOADING = 156,525 LB

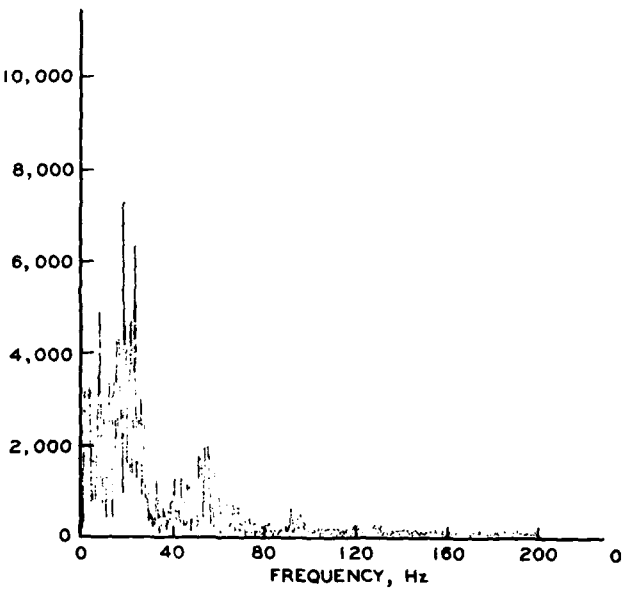

AMPLITUDE SPECTRUM

POOL EL 1088
SLEEVE TRAVEL . . . 28.1 IN.
LOAD CELLS 1-4: (-) LOAD UPSTREAM
(+) LOAD DOWNSTREAM
LOAD CELLS 5-6: (+) LOAD UPWARD
(-) LOAD DOWNWARD

DEFLECTOR PLATE DESIGN
LOADING WITH UPSTREAM DEFLECTOR PLATE
LOAD CELL 6

PLATE 27

PLATE 28

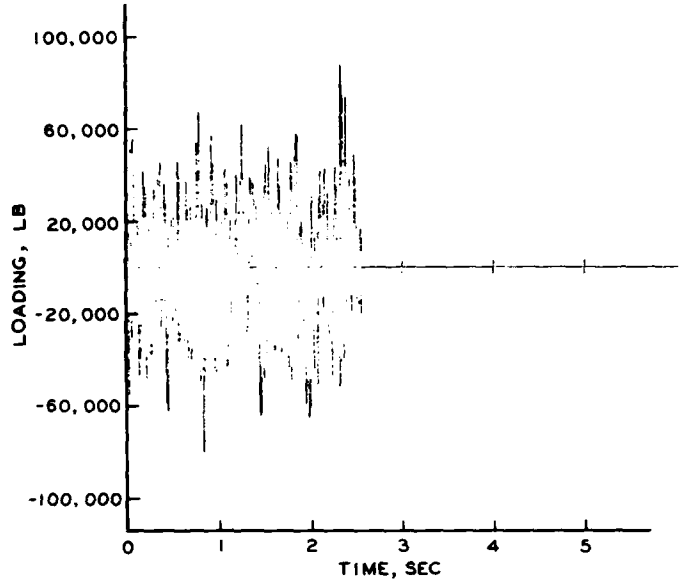

TIME-HISTORY

MEAN LOADING = -22,768 LB

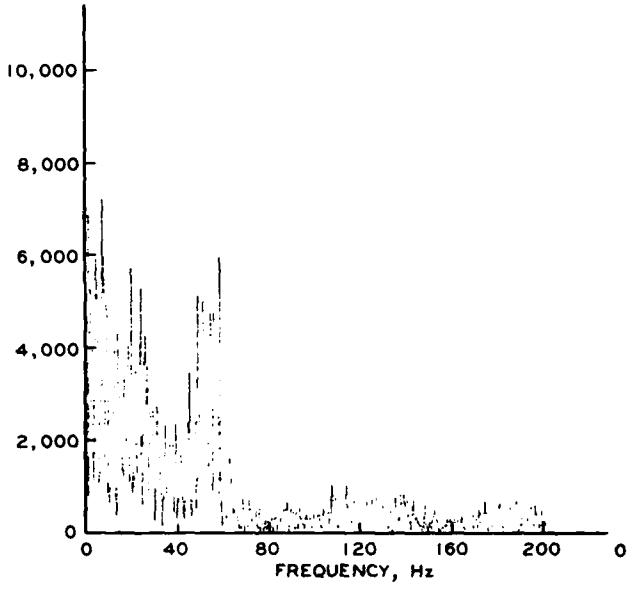

AMPLITUDE SPECTRUM

POOL EL 1088
SLEEVE TRAVEL . . . 28.1 IN.
LOAD CELLS 1-4: (-) LOAD UPSTREAM
(+) LOAD DOWNSTREAM
LOAD CELLS 5-6: (+) LOAD UPWARD
(-) LOAD DOWNWARD

DEFLECTOR PLATE DESIGN
LOADING WITH BOTH DEFLECTOR PLATES
LOAD CELL 1

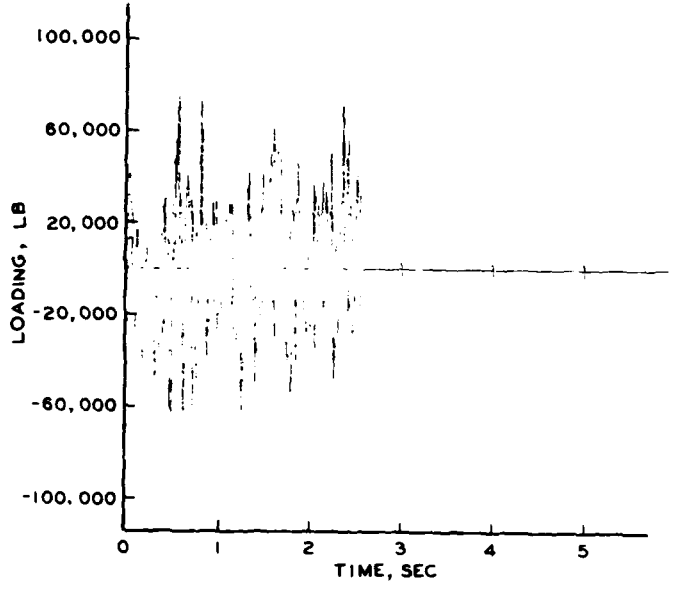

TIME-HISTORY

MEAN LOADING = 140,345 LB

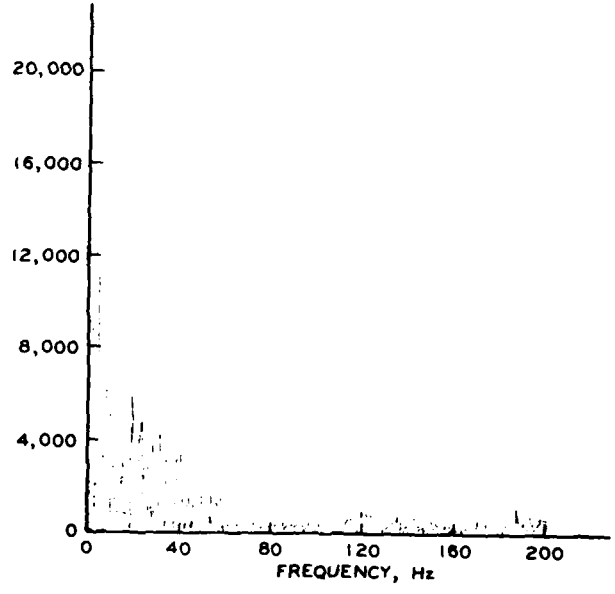

AMPLITUDE SPECTRUM

POOL EL 1088
SLEEVE TRAVEL . . . 28.1 IN.
LOAD CELLS 1-4: (-) LOAD UPSTREAM
(+) LOAD DOWNSTREAM
LOAD CELLS 5-6: (+) LOAD UPWARD
(-) LOAD INWARD

DEFLECTOR PLATE DESIGN
LOADING WITH BOTH DEFLECTOR PLATES
LOAD CELL 2

PLATE 29

PLATE 30

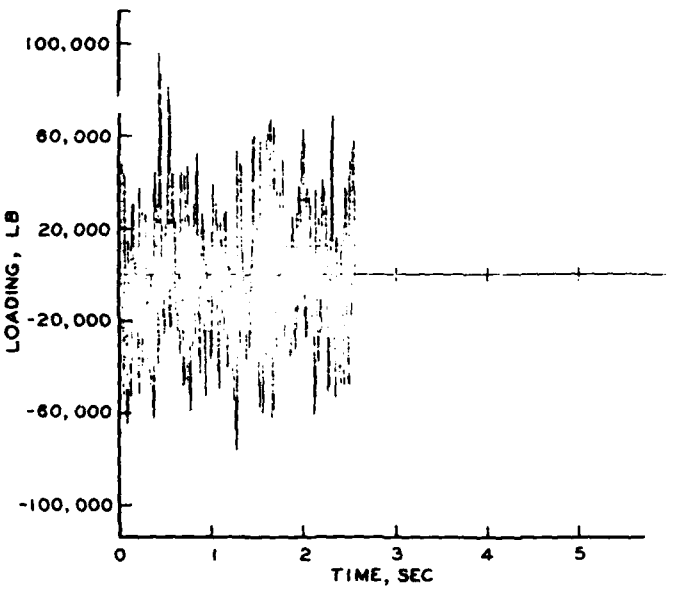

TIME-HISTORY

MEAN LOADING = 242,738 LB

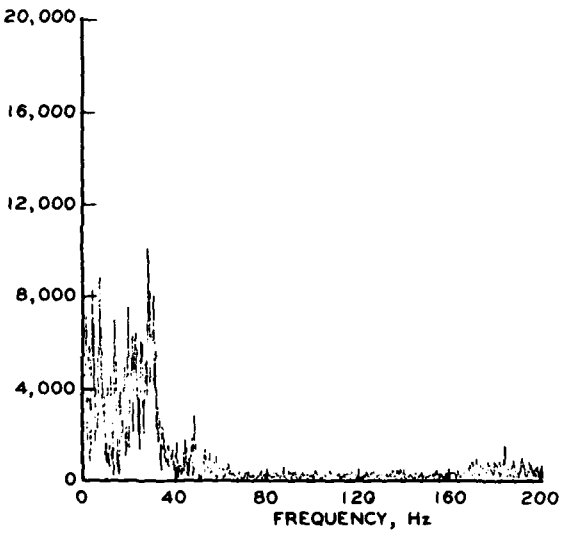

AMPLITUDE SPECTRUM

POOL EL 1088
SLEEVE TRAVEL . . . 28.1 IN.
LOAD CELLS 1-4: (-) LOAD UPSTREAM
(+) LOAD DOWNSTREAM
LOAD CELLS 5-6: (+) LOAD UPWARD
(-) LOAD DOWNWARD

DEFLECTOR PLATE DESIGN
LOADING WITH BOTH DEFLECTOR PLATES
LOAD CELL 3

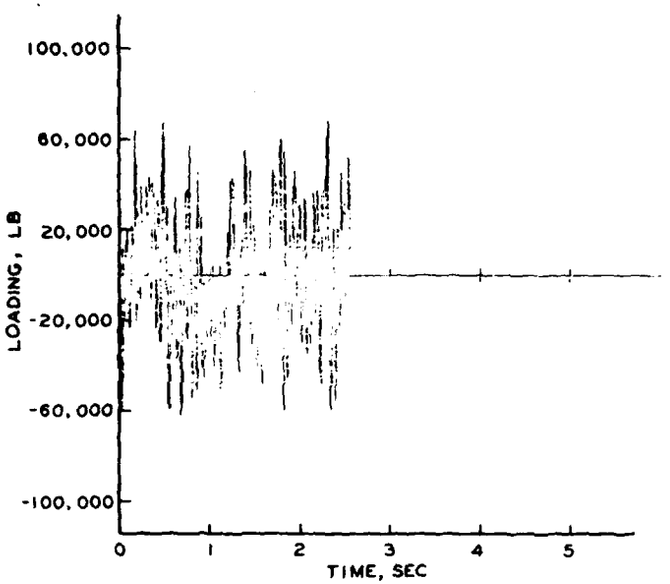

TIME-HISTORY

MEAN LOADING = 147,061 LB

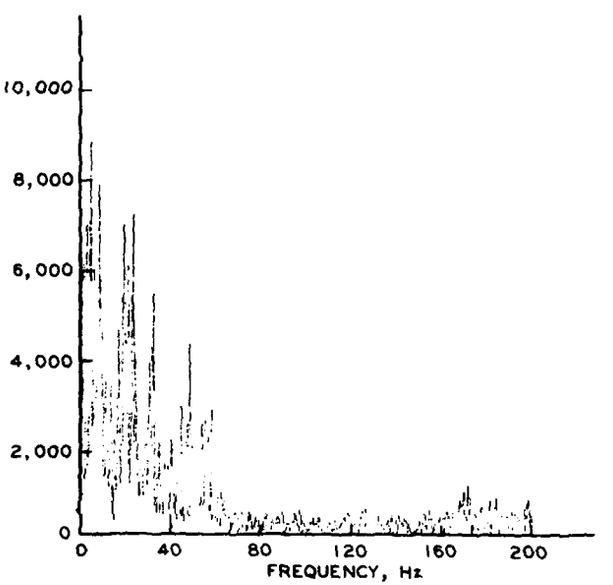

AMPLITUDE SPECTRUM

POOL EL 1088
SLEEVE TRAVEL . . . 28.1 IN.

LOAD CELLS 1-4: (-) LOAD UPSTREAM
(+) LOAD DOWNSTREAM
LOAD CELLS 5-6: (+) LOAD UPWARD
(-) LOAD DOWNWARD

DEFLECTOR PLATE DESIGN
LOADING WITH BOTH DEFLECTOR PLATES
LOAD CELL 4

PLATE 31

PLATE 32

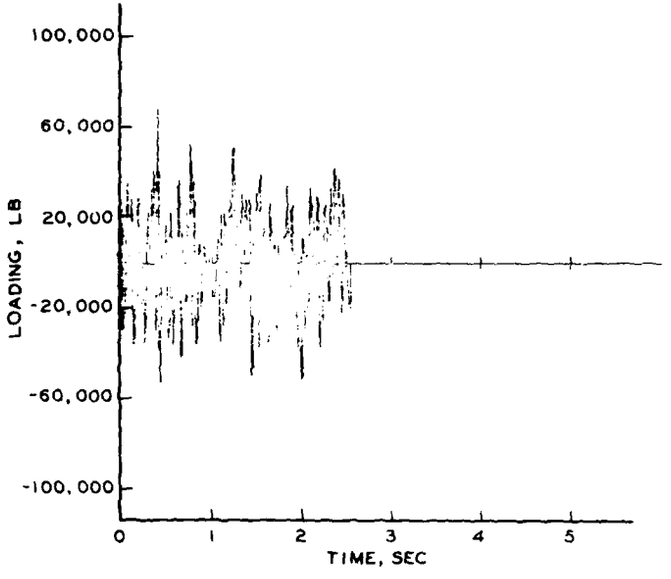

TIME-HISTORY

MEAN LOADING = -37,250 LB

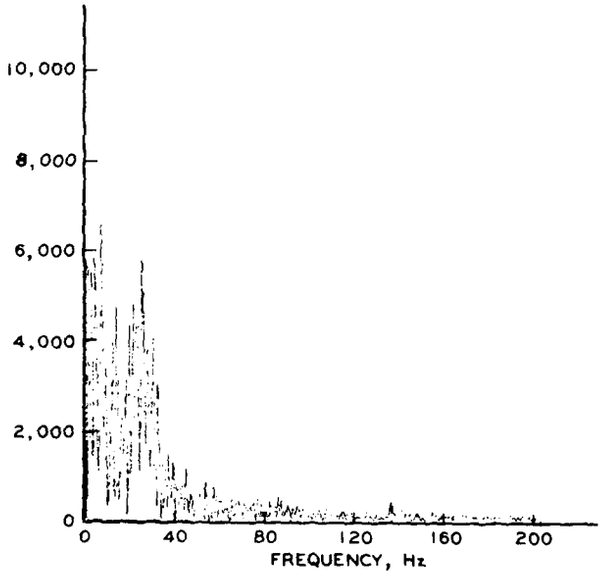

AMPLITUDE SPECTRUM

POOL EL 1088
SLEEVE TRAVEL . . . 28.1 IN.

LOAD CELLS 1-4: (-) LOAD UPSTREAM
(+) LOAD DOWNSTREAM
LOAD CELLS 5-6: (+) LOAD UPWARD
(-) LOAD DOWNWARD

DEFLECTOR PLATE DESIGN
LOADING WITH BOTH DEFLECTOR PLATES
LOAD CELL 5

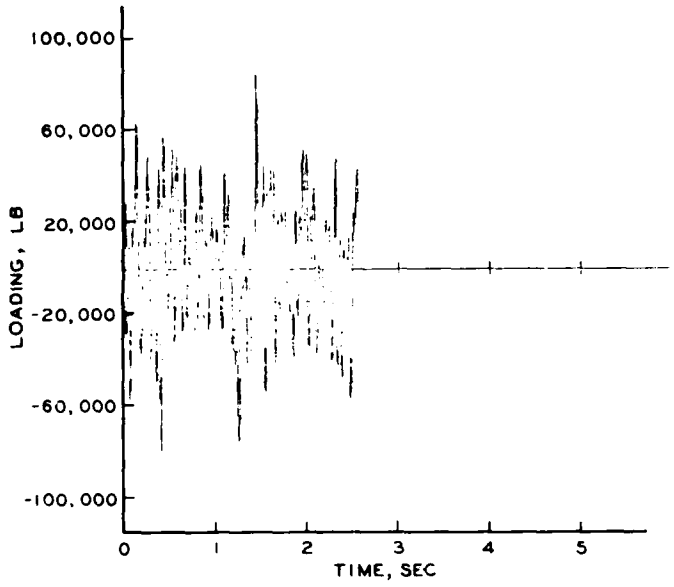

TIME-HISTORY

MEAN LOADING = 152,074 LB

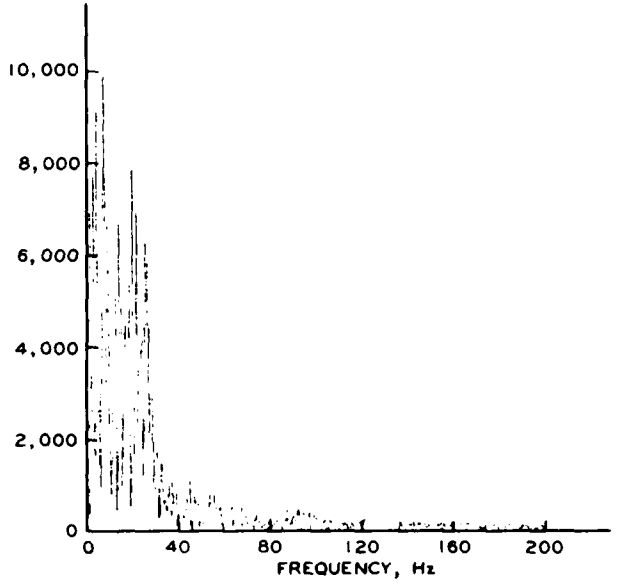

AMPLITUDE SPECTRUM

POOL EL 1088
SLEEVE TRAVEL . . . 28.1 IN.

LOAD CELLS 1-4: (-) LOAD UPSTREAM
(+) LOAD DOWNSTREAM
LOAD CELLS 5-6: (+) LOAD UPWARD
(-) LOAD DOWNWARD

DEFLECTOR PLATE DESIGN
LOADING WITH BOTH DEFLECTOR PLATES
LOAD CELL 6

PLATE 33

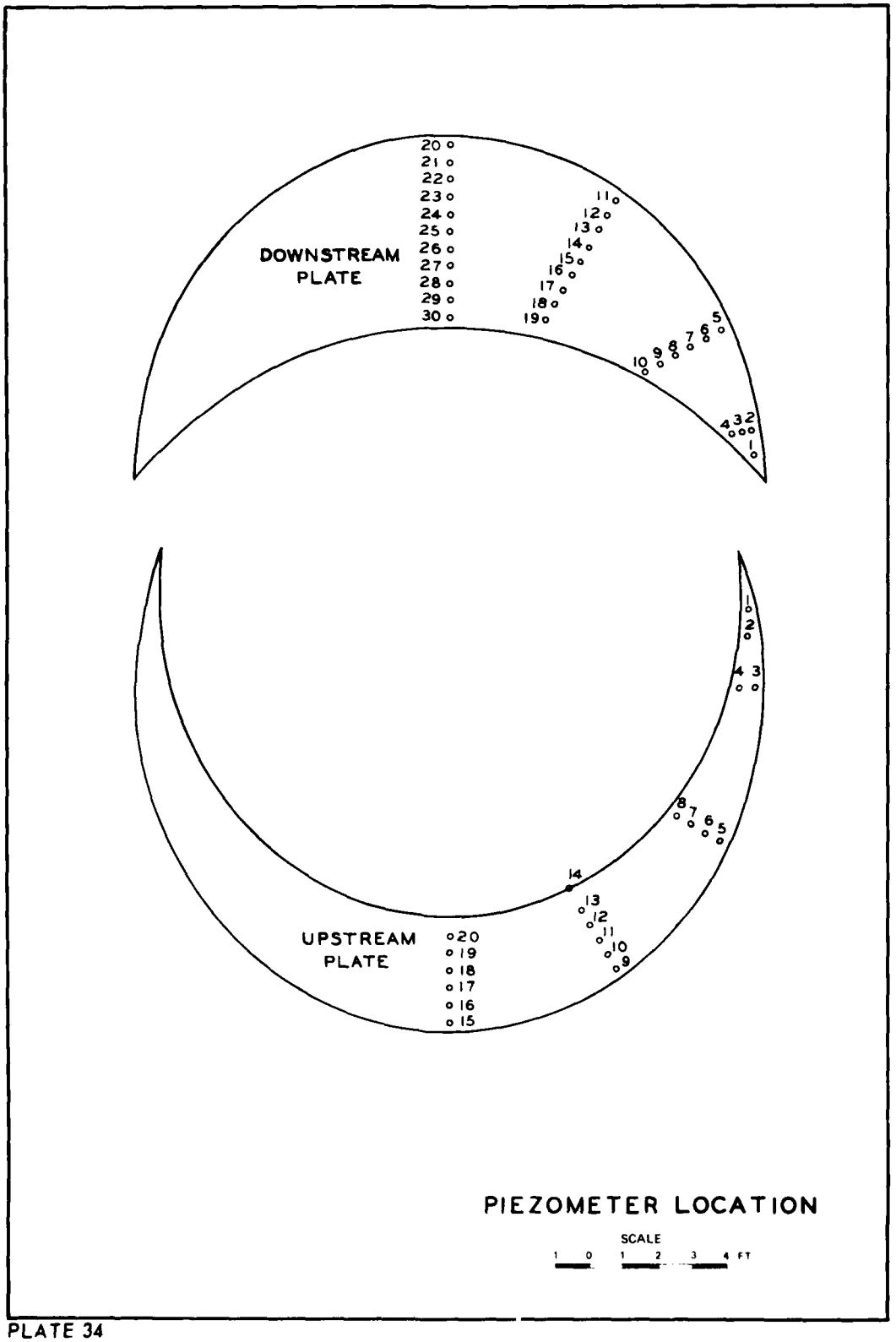
DOWNSTREAM PLATE
20
21
22
23
24
25
26
27
28
29
30
11
12
13
14
15
16
17
18
19
5
6
7
8
9
10
4
3
2
1
UPSTREAM PLATE
20
19
18
17
16
15
1
2
4
3
8
7
6
5
14
13
12
11
10
9
PIEZOMETER LOCATION
SCALE
1 0 1 2 3 4 FT

PLATE 34

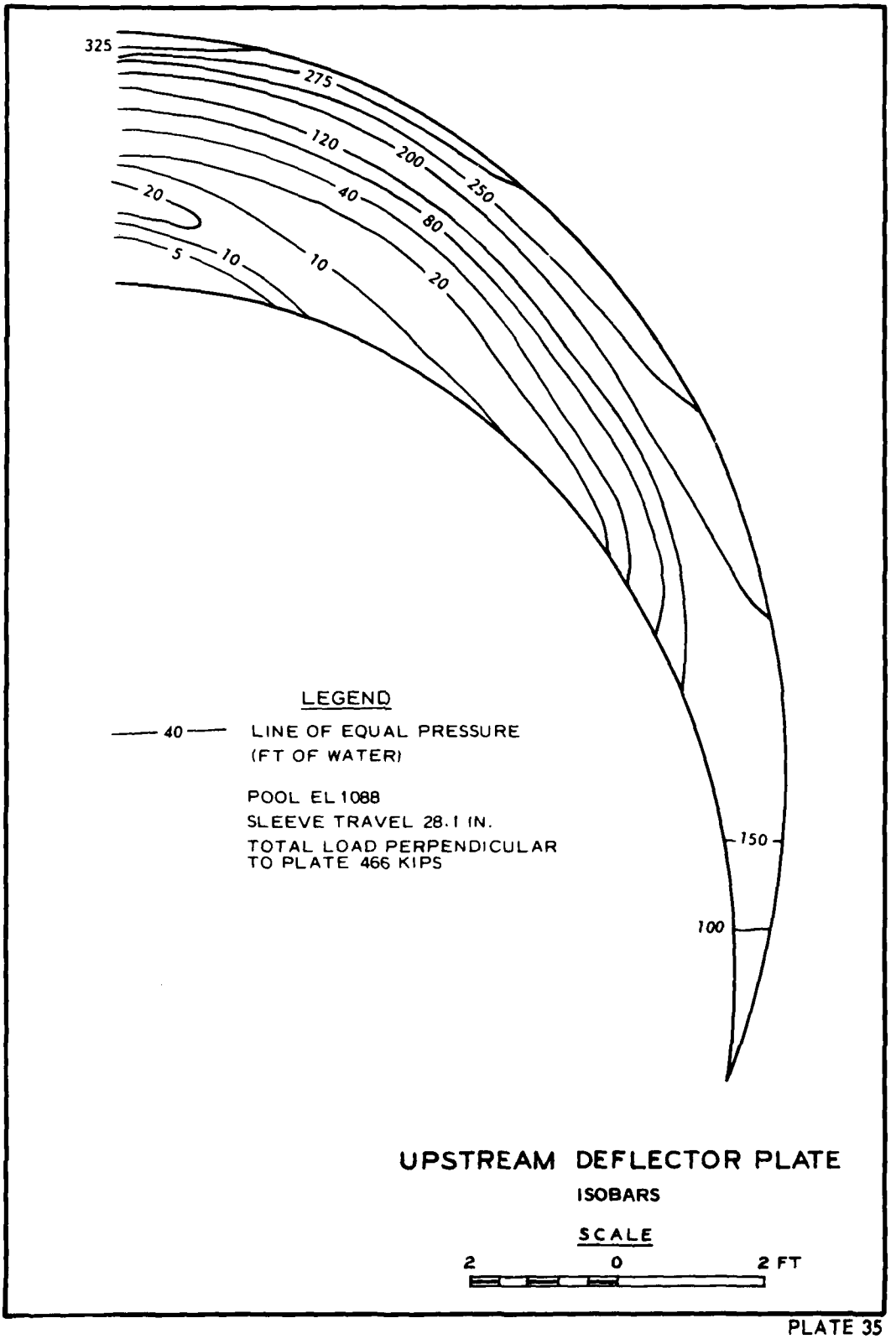
325
275
120
200
250
20
40
80
5
10
10
20
150
100
LEGEND
40
LINE OF EQUAL PRESSURE
(FT OF WATER)
POOL EL 1088
SLEEVE TRAVEL 28.1 IN.
TOTAL LOAD PERPENDICULAR
TO PLATE 466 KIPS
UPSTREAM DEFLECTOR PLATE
ISOBARS
SCALE
2
0
2 FT

PLATE 35

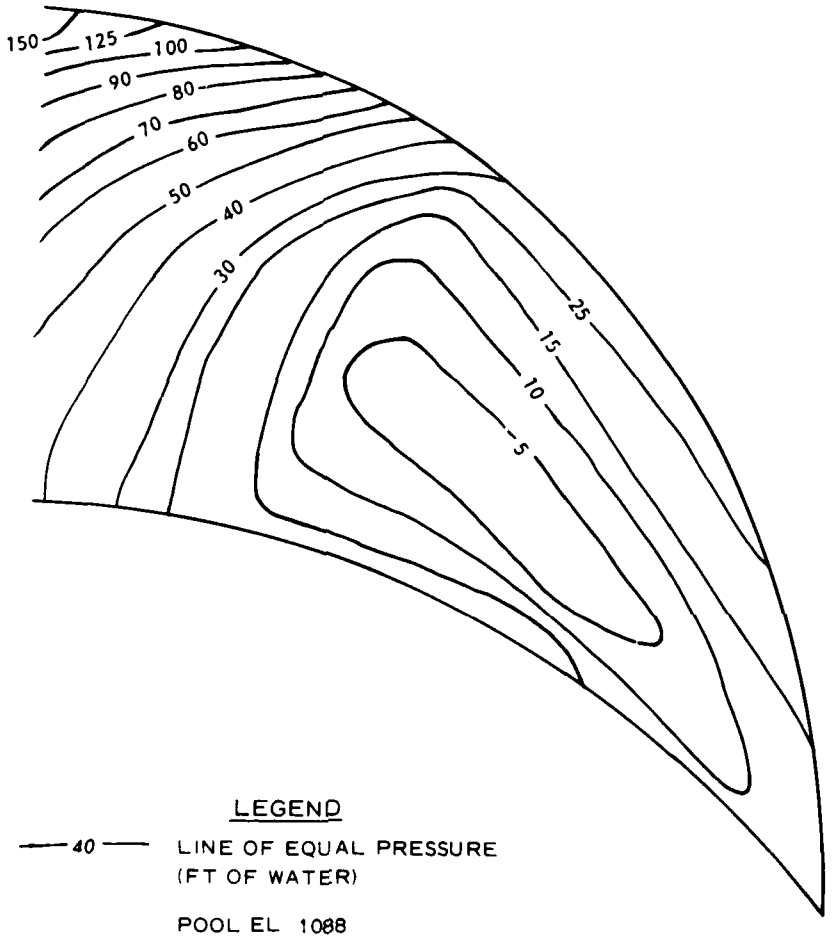

LEGEND

—— 40 —— LINE OF EQUAL PRESSURE (FT OF WATER)

POOL EL 1088

SLEEVE TRAVEL 28.1 IN.

TOTAL LOAD PERPENDICULAR TO PLATE 150 KIPS

DOWNSTREAM DEFLECTOR PLATE

ISOBARS

SCALE

2 0 2 FT

PLATE 36

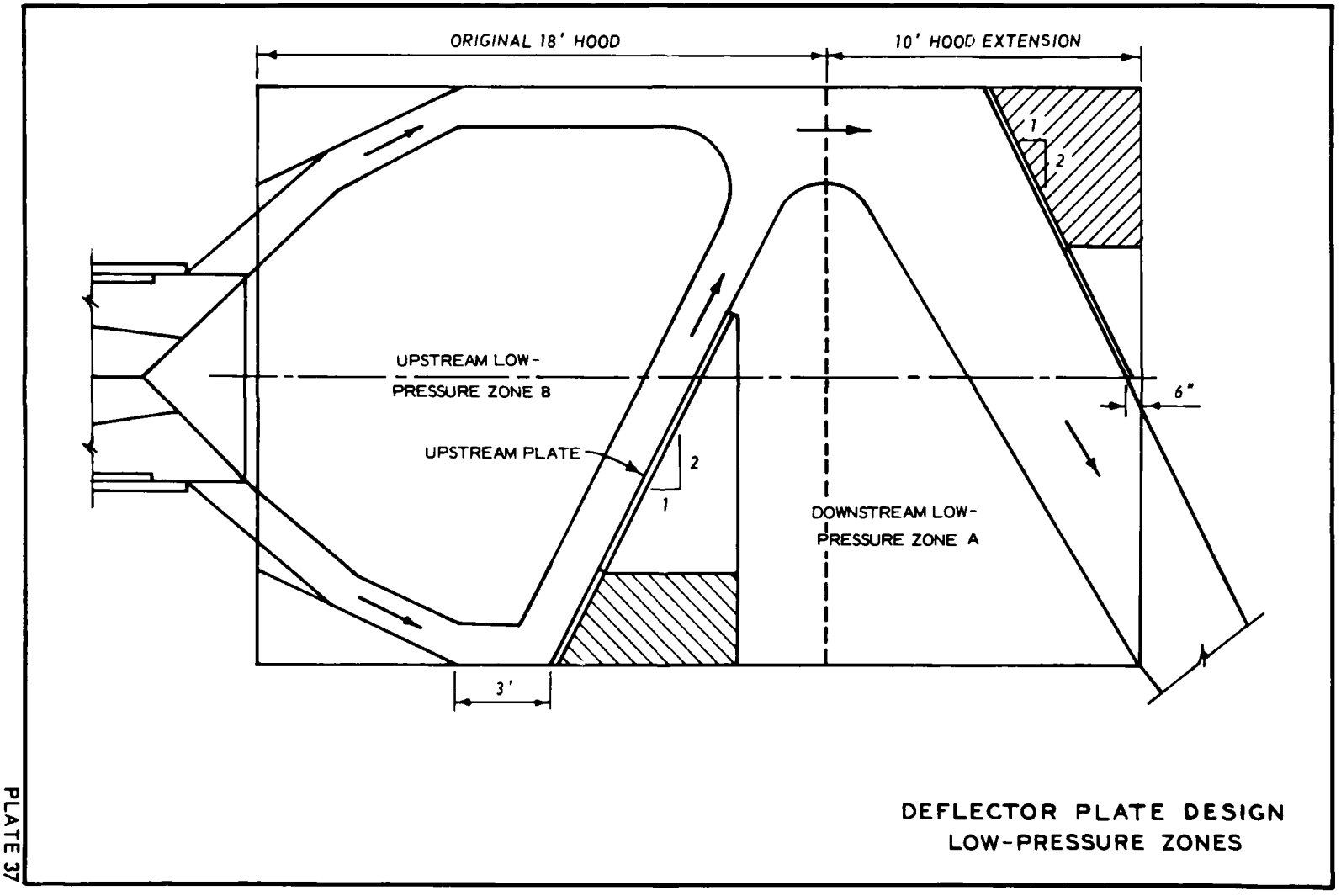

DEFLECTOR PLATE DESIGN
LOW-PRESSURE ZONES

PLATE 37

PLATE 38

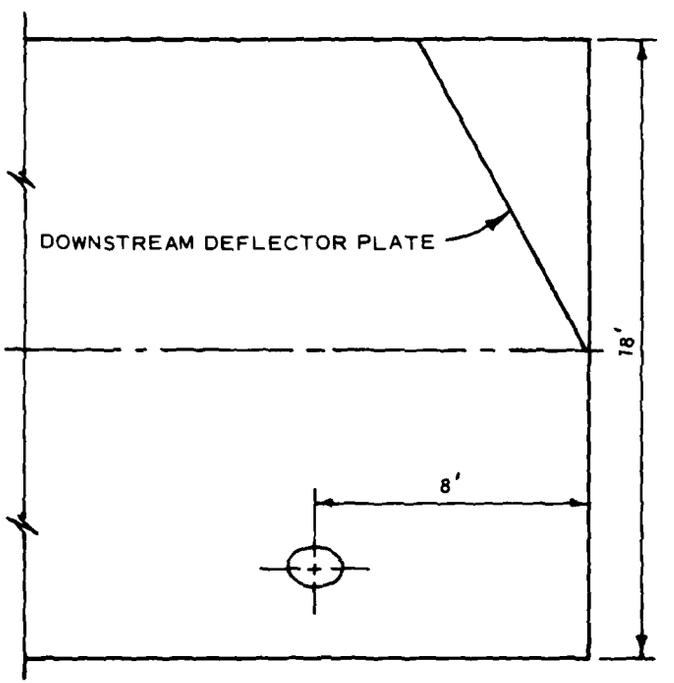

SIDE VIEW

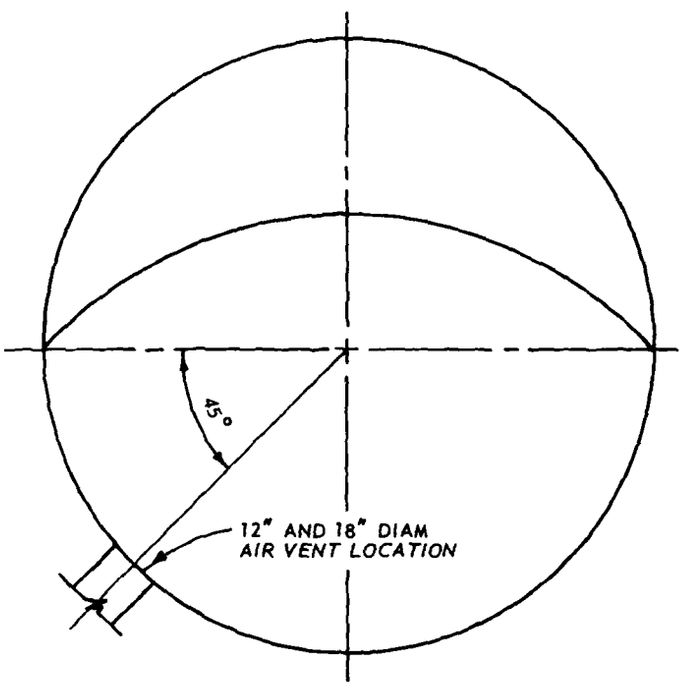

END VIEW

DEFLECTOR PLATE DESIGN

AIR VENT DETAILS

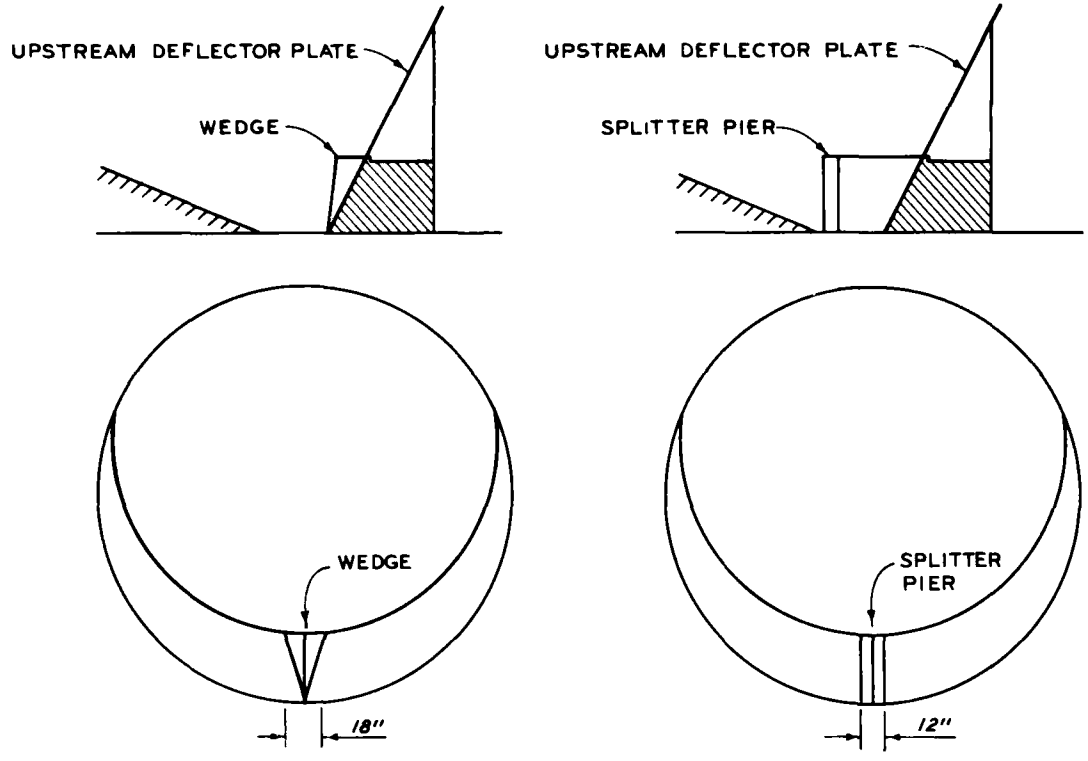

PLATE 39

DEFLECTOR PLATE DESIGN

WEDGE AND SPLITTER PIER DETAILS

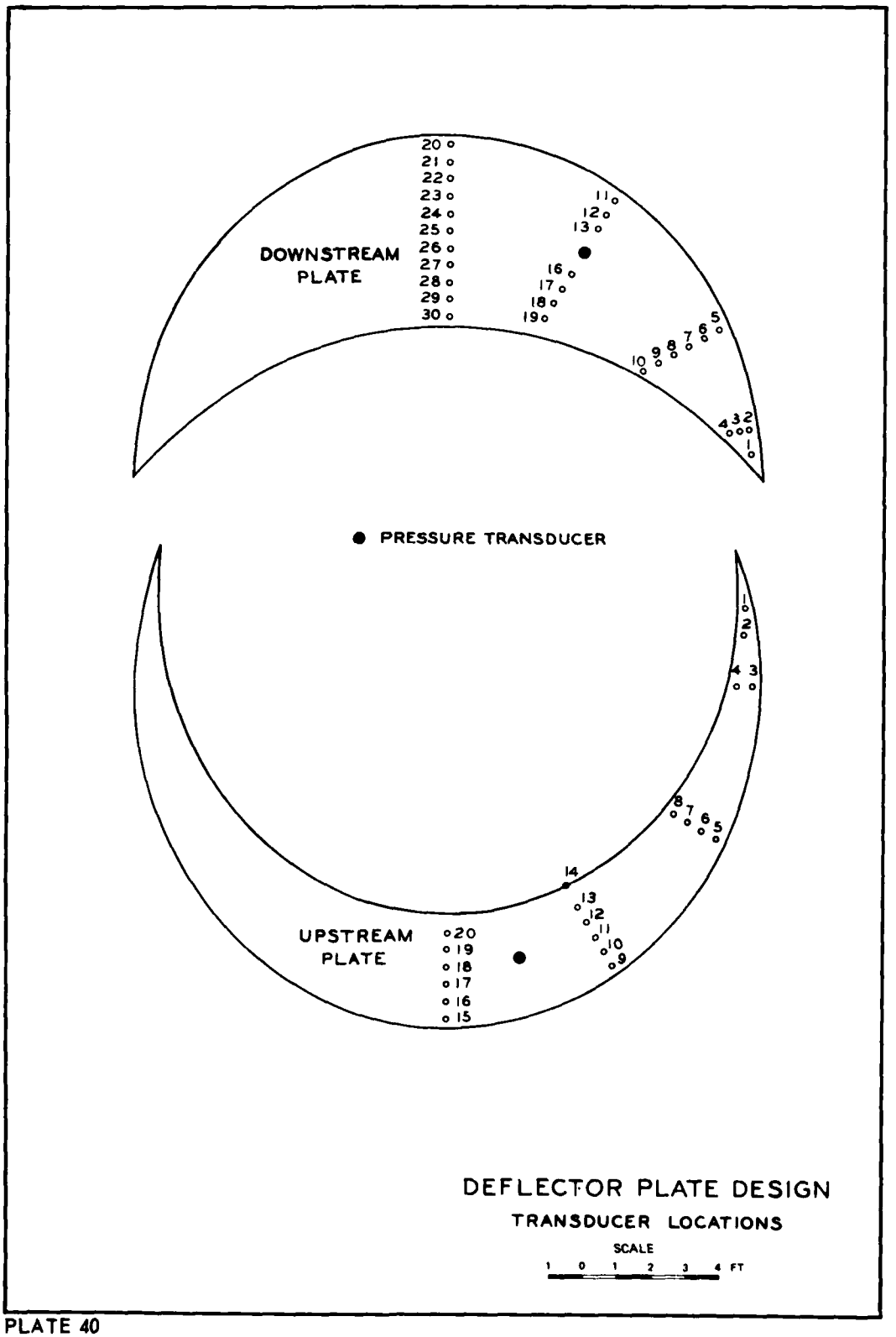
DOWNSTREAM PLATE
20
21
22
23
24
25
26
27
28
29
30
11
12
13
16
17
18
19
10
9
8
7
6
5
4
3
2
1
PRESSURE TRANSDUCER
1
2
4
3
8
7
6
5
14
13
12
11
10
9
UPSTREAM PLATE
20
19
18
17
16
15
DEFLECTOR PLATE DESIGN
TRANSDUCER LOCATIONS
SCALE
1 0 1 2 3 4 FT

PLATE 40

In accordance with letter from DAEN-RDC, DAEN-ASI dated 22 July 1977, Subject: Facsimile Catalog Cards for Laboratory Technical Publications, a facsimile catalog card in Library of Congress MARC format is reproduced below.

Maynord, Stephen T.
Flood control and irrigation outlet works and tailrace channel for New Melones Dam, Stanislaus River, California : Hydraulic model investigation / by Stephen T. Maynord (Hydraulics Laboratory, U.S. Army Engineer Waterways Experiment Station). -- Vicksburg, Miss. : The Station ; Springfield, Va. : available from NTIS, 1981.
31, [15] p., 40 p. of plates : ill. ; 27 cm. -- (Technical report / U.S. Army Engineer Waterways Experiment Station ; HL-81-6)
Cover title.
"September 1981."
"Prepared for U.S. Army Engineer District, Sacramento."
Final report.

1. Flood control. 2. Hydraulic models. 3. Hydraulic turbines. 4. New Melones Dam (Calif.) I.United States. Army. Corps of Engineers. Office of the Chief of Engineers. II. U.S. Army Engineer Waterways Experiment

Maynord, Stephen T.
Flood control and irrigation outlet works : ... 1981.
(Card 2)

Station. Hydraulics Laboratory. III. Title IV. Series: Technical report (U.S. Army Engineer Waterways Experiment Station) ; HL-81-6.
TA7.W34 no.HL-81-6


DAT
FILM